ENERGY MANAGEMENT IN PLUG-IN HYBRID ELECTRIC VEHICLE PENETRATED NETWORKS

A DISSERTATION SUBMITTED TO

THE GRADUATE SCHOOL OF ENGINEERING AND SCIENCE

OF BILKENT UNIVERSITY

IN PARTIAL FULFILLMENT OF THE REQUIREMENTS FOR

THE DEGREE OF

DOCTOR OF PHILOSOPHY

IN

INDUSTRIAL ENGINEERING

By

Okan Arslan

April 2016

ENERGY MANAGEMENT IN PLUG-IN HYBRID ELECTRIC VEHICLE PENETRATED NETWORKS

By Okan Arslan

April 2016

We certify that we have read this dissertation and that in our opinion it is fully adequate, in scope and in quality, as a dissertation for the degree of Doctor of Philosophy.

Oya Karaşan (Advisor)

Selim Aktürk

Meral Azizoğlu

Alper Şen

Hakan Gültekin

Approved for the Graduate School of Engineering and Science:

Levent Onural
Director of the Graduate School

ABSTRACT

ENERGY MANAGEMENT IN PLUG-IN HYBRID ELECTRIC VEHICLE PENETRATED NETWORKS

Okan Arslan
Ph.D. in Industrial Engineering
Advisor: Oya Karaşan
April 2016

With the introduction of electric vehicles (EVs) and plug-in hybrid electric vehicles (PHEVs) into the transportation system, a new line of research has emerged in the literature that reconsiders existing problems from the electrified transportation point of view. In this context, our objective is to understand the challenges that arise with the emergence of PHEV technology through a series of essays.

Due to their ability to use electricity and gasoline as sources of energy with different cost structures and limitations, PHEVs stand as both a challenge and an opportunity for the existing transportation systems. They provide transportation cost reductions by utilizing less gasoline, which in turn contribute to the environmental benefits. In this context, we addressed a practically important problem: 'finding the minimum cost path for PHEVs'. We formally present this problem, show that it is NP-Complete and propose exact and heuristic solution techniques. Using these techniques, we investigate impacts of battery characteristics, driver preferences and road network features on travel costs of a PHEV for long-distance trips. Through this analysis, the location of charging stations is identified as one of the critical factors affecting the costs. In this regard, we introduce another practically important problem: 'Hybrid charging station location'. Different than existing approaches to the charging station location problems, we also consider PHEVs when locating stations. We propose a Benders Decomposition algorithm as an exact solution methodology, and accelerate the implementation by generating nondominated cuts. Finally, we analyze the cost and emission impacts of PHEV penetration into electricity networks with widespread adoption of distributed energy resources.

Approaching PHEVs from a long-distance point of view, we introduced new problems and solution approaches to the literature. Our results show that by establishing an adequate level of the intercity charging station infrastructure, well-studied benefits of electrified transportation in urban regions can be extended to long-distance trips.

Keywords: Plug-in hybrid electric vehicles, energy management, charging station location, virtual power plant, Benders decomposition, dynamic programming.

ÖZET

ELEKTRİKLİ HİBRİT ARAÇLARIN BULUNDUĞU AĞLARDA ENERJİ YÖNETİMİ

Okan Arslan
Endüstri Mühendisliği, Doktora
Tez Danışmanı: Oya Karaşan
Nisan 2016

Elektrikli Araçların (EA) ve Hibrit Elektrikli Araçların (HEA) ulaştırma sistemine duhûlü ile birlikte, literatürde bulunan mevcut ulaştırma problemlerini elektrikli araç bakış açısı ile yeniden değerlendiren bir araştırma çizgisi ortaya çıktı. Bu kapsamda amacımız bir dizi makale vasıtasıyla HEA teknolojisinin ortaya çıkışı ile birlikte vücut bulan zorlukları anlamaktır.

Farklı maliyet yapıları ve kısıtları olan elektrik ve benzin enerji kaynağını kullanabildiğinden ötürü, HEA'lar mevcut ulaştırma sistemleri için hem zorluklar hem de fırsatlar sunuyor. Daha az benzin kullanarak ulaştırma maliyetlerini azaltan HEA'lar, aynı zamanda dolaylı olarak doğaya fayda sağlıyor. Bu kapsamda, pratik olarak önem arz eden "HEA'lar için en ucuz yolun bulunması" problemine değiniyoruz. Formal olarak problemi tanıtıyor, NP-Tam kümesine ait olduğunu gösteriyor ve tam ve sezgisel çözüm teknikleri öneriyoruz. Bu teknikleri kullanarak, batarya karakteristikleri, sürücü tercihleri ve yol ağı özelliklerinin uzun mesafe yolculuklarında HEA ulaştırma maliyetleri üzerindeki etkilerini inceliyoruz. Bu analiz ile, şarj istasyonlarının konumlarının maliyetleri etkileyen önemli bir faktör olduğunu tespit ediyoruz. Bu kapsamda, bir diğer pratik olarak önemli problem olan "Hibrit şarj istasyonu konumlandırması" problemini tanımlıyoruz. Şarj istasyonu yerleştirme problemine mevcut yaklaşımlardan farklı olarak, istasyonları konumlandırırken aynı zamanda HEA'ları da dikkate alıyoruz. Tam çözüm tekniği olarak Benders Ayrıştırma Algoritması öneriyor ve domine edilmemiş kesiler üreterek uygulamayı hızlandırıyoruz. Son olarak, HEA'ların yaygın bir şekile dağıtık enerji kaynaklarının kullanıldığı elektrik ağlarına dahil olmaları ile oluşan maliyet ve emisyon etkilerini inceliyoruz.

HEA'lara uzun mesafe bakış açısı ile yaklaşarak, literatüre yeni problemler ve çözüm teknikleri tanıtıyoruz. Sonuçlarımız göstermektedir ki, yeterli seviyede şehirlerarası şarj istasyonu altyapısının kurulması ile, elektrikli ulaştırmanın iyi değerlendirilmiş olan şehir içi faydaları, uzun mesafeli yolculuklar için de geçerli olacaktır.

Anahtar sözcükler: Hibrit elektrikli araçlar, enerji yönetimi, şarj istasyonu yerleştirmesi, sanal elektrik santrali, Benders ayrışımı, dinamik programlama.

Aileme...

Acknowledgement

I would like to express my special appreciation and thanks to my advisor Professor Oya Karaşan, you have been a tremendous mentor for me. I would like to thank you for encouraging me in every endeavor to help me grow as a researcher. Your advice has always been invaluable for me and being your student has been the best thing that could ever happen at Bilkent.

I would like to thank my Doctoral Supervisory Committee members, Assoc.Prof. Alper Şen and Assoc.Prof. Hakan Gültekin for taking their time off from their busy schedule every now and then to read and comment on several aspects of my thesis work. Your valuable comments and suggestions have contributed to this work significantly. I also owe a big thank-you to Prof. Selim Aktürk as both our department chair and my Dissertation Committee member and to Prof. Meral Azizoğlu for serving as my Dissertation Committee member.

I express my sincere gratitude to The Scientific and Technological Research Council of Turkey (TÜBİTAK) for financially supporting me with grant 2211, and this thesis work as part of the research grant 214M211.

I would like to thank to my colleagues at the Scientific Decision Support Branch of the Turkish Air Force for enduring my absence during this long endeavor. I especially want to thank Ahmet Kandakoğlu who has been a great friend to me and with whom I shared a lot during the last 7 years.

It was a dream for me to study at Bilkent, and I would like to thank each and every faculty member and staff of the Industrial Engineering Department for providing this valuable opportunity for me. Special thanks to you Prof. Hande Yaman, Prof. Bahar Yetiş Kara, Prof. Mustafa C. Pinar, Prof. Ülkü Gürler, late Prof. Barbaros Tansel and Assoc.Prof. Osman Oğuz for providing a high-quality education for us.

I would love to thank each of my peers in the department. Thank you for sharing good-times at Bilkent Burak Pac, Can Taylan Sarı, Ece Zeliha Demirci, Esra Koca, Gizem Özbaygın, Hatice Çalık, Kamyar Kargar, Meltem Peker, Nihal Berktaş, Okan Dükkancı and Ramez Kian. Particularly, I would like to thank Başak Yazar for having me as a colleague in her research. During my life at Bilkent, I have always seen Vedat Bayram and Türker Tanergüçlü as my foregoers. Thank you for being a great support to me. And Barış, your friendship has been invaluable for me throughout this experience. Spending time with you has always helped me cope with hard moments. I sincerely wish our brotherhood will last ever.

I am indebted to my parents: mom and dad. You have gone through lots of hardships to raise me as a person. Words cannot express my gratitude to you. I also express my deepest appreciation to my sister, sister-in-law, and father-in-law for their invaluable support.

God has given us a gift in 2014. Our baby-girl Asya has brought joy and happiness to our family. Her existence makes it all worthwhile. Finally, my wife, my life. You have given me the power and the will to complete yet another challenge. Leave alone this dissertation - or anything for that matter - *I* would be incomplete without you.

Contents

List of Figures

List of Tables

Chapter 1

Introduction

Volatile gasoline prices, security concerns associated with oil and increasing environmental consciousness have fostered cheaper and greener transportation through the emergence of several new transportation technologies. One such technology, the electric transportation, is an emerging challenge for the transportation sector and an opportunity in logistics operations from the environmental and cost perspectives. Electric vehicles (EVs) and their variants such as hybrid electric vehicles (HEVs) or Plug-in Hybrid Electric Vehicles (PHEVs) appeal to more customers worldwide and a proliferation of these vehicles has been observed on the roads [1].

An EV has an electricity motor and uses its battery as the only source of energy. An HEV has both an electricity motor and a regular internal combustion engine (ICE), benefiting from the electricity to increase the efficiency and reduce the gasoline usage. Another technology that combines the advantages of EVs and conventional vehicles (CVs) is the PHEV. It has an electric motor and an ICE as its power sources. Different from an HEV, a PHEV can be plugged-in be charge. It provides reduction in both transportation costs and greenhouse gas emissions with respect to a comparable CV [2]. It has the capabilities of an EV such as charging from a regular power outlet and the convenience of a gasoline powered

CV such as long-distance trips. PHEVs operate in either charge depleting (CD) mode or charge sustaining (CS) mode. On CD mode, the electric motor generates the required power and the PHEV uses its batteries as the energy supply. Once a minimum state-of-charge is reached, the PHEV switches to CS mode, and the power that propels the vehicle is mainly generated by the ICE using gasoline as the energy source. Thus, the difference between an EV and a PHEV is the CS mode drive flexibility of the latter [3–8]. PHEVs can be refueled at regular gasoline stations similar to CVs, or can be charged en-route in charging stations similar to EVs [9]. As such, with its unique capabilities, PHEV technology stands as a major milestone on the road to 'electrification of the automobile' [10].

Several parties benefit from the introduction of PHEVs into the transportation sector. This new technology results in various new opportunities; with increasing gasoline prices, drivers are more drawn to electric-drive transportation. From the individual drivers' perspective, they are an efficient way of reducing the transportation costs. A reduction in gasoline usage is also a benefit for oil-importing governments because it implies less foreign dependency and governments are encouraging fuel provider fleets to implement petroleum-reduction measures [11]. Using electricity as an energy source also significantly reduces greenhouse gas (GHG) emissions [12–14]. In addition, investment opportunities emerge with the introduction of PHEVs into the transportation system; vehicle manufacturers and infrastructure investors alike may benefit from this new technology. New fast charging station facilities are being established to provide more charging opportunities. The transportation sector is undergoing a profound transformation. Our objective in this dissertation is to understand the impacts of PHEV penetration into the transportation system, identify possible problems and propose solution approaches. In this context, we concentrate on the long-distance travel of PHEVs. There are three major problems that are inter-related. Initially, we address the problem of finding the least cost path for PHEVs in long-distance trips. Then, we investigate the impacts of battery, driver and road characteristics on the travel costs of PHEVs in these trips. The third problem we deal with is the optimal location of charging stations in intercity road network. In a different context, we also investigate the cost and emission impacts of virtual power plant (VPP) formation in PHEV-penetrated electricity networks. With increasing interest in alternative energy resources and technologies, widespread utilization of distributed energy resources (DERs) are anticipated in the near future. As an aggregation unit, the VPP is introduced for load management and resource scheduling. As part of our dissertation, we also develop an energy management model for VPPs and analyze the cost and emission impacts of VPP formation and PHEV penetration into electricity network.

1.1 Motivation

Identification of the minimum cost path problem for PHEVs (MCPP-PHEV) is a fundamental problem for long-distance PHEV trips that possibly require several refueling/charging stops. As one of the initial steps of renewable energy revolution in transportation, benefits and shortcomings of PHEVs for the urban (short distance) trips are well appreciated and investigated. However, as we review in the related literature below, the long-distance use of PHEVs is not well studied. From the economic and environmental perspectives, long-distance travel is certainly an important subject when the potential benefits of these vehicles are considered, and focusing solely on the short range usage would fail to achieve a complete treatment of the topic. According to the National Household Travel Survey by the U.S. Department of Transportation [15], the trips by personally owned vehicles that are longer than 50 miles added up to 575 billion miles in the U.S. in 2009. The role of the long-distance trips is even more prominent in the logistics. This work is aimed to be a first attempt to study the long-distance PHEV trips that require several refueling/charging stops.

MCPP-PHEV is a practically important problem for a broad audience. The first and the foremost subjects of interest are the personal PHEV drivers. A recent study by Turrentine and Kurani [16] reports that personal vehicle drivers lack the basic building blocks of knowledge related to transportation costs. When it comes to PHEVs, the cost components get much more complicated compared to single energy source vehicles, and decision-support models are needed both for the routing and refueling/charging decisions. In this respect, this study offers personal PHEV drivers the possibility of understanding the PHEV economics more clearly. Furthermore, navigation devices might implement the methodologies in this study to offer a valuable decision support tool for the PHEV drivers.

The second major interest group is the logistics firms with a green logistics perspective. Alternative fuel vehicles, and PHEVs in particular, are primarily used by individuals for personal transportation purposes. Nevertheless, a PHEV, with its comparatively long driving-range with respect to an EV, is a promising alternative to be used in logistics. There are different studies directed towards exploring the possible usage of EVs and PHEVs in the future transportation fleets [17–20]. U.S. Department of Energy [21] also prepared a handbook for fleet managers on the guidelines of incorporating EVs and PHEVs into their fleets. Navigant Research [22] estimates that fleet purchases of EVs and PHEVs will be more than 291,000 in 2020 worldwide. Production of light, medium and heavy-duty PHEV trucks by several companies [23–28] is a strong indication of the expected proliferation of PHEVs in logistics fleets highlighting the practical significance of the problem investigated in this study.

Thirdly, MCPP-PHEV is also an interesting problem for the governments and infrastructure investors. With economic, security and environmental motivations, governments take an active role in promoting EV and PHEV usage. They provide several incentives and subsidize investments in the infrastructure such as charging stations. Moreover, new incentives started to emerge targeting specifically the business use of PHEVs [29–31]. Investigating the long-distance transportation costs of PHEVs, MCPP-PHEV is a significant tool for the governments to better direct their incentive programs and for businesses to assess the opportunities and risks regarding their investment decisions. In summary, MCPP-PHEV is an interesting problem for:

- Personal PHEV drivers who want to learn about the travel costs,
- Firms which want to offer navigation systems tailored for PHEV drivers,
- PHEV truck/van fleets that want to minimize the transportation costs,
- Policy makers from both the auto industries and the governments that decide on the infrastructure establishment incentives,
- Policy makers that decide on the subsidy schemes for PHEVs.

With its electric motor and charging capability, a PHEV offers unique opportunities to decrease the travel costs and GHG emissions. However, various parameters, such as battery characteristics, availability of charging stations and driver preferences affect the magnitude of these improvements. This motivates the analyses carried out to understand the impacts of these parameters for long-distance travel costs of PHEVs.

Along with the optimal-path finding problem lies another critical problem: finding the optimal siting of charging stations. As the EVs are infamous for their rather limited range, their increasing numbers naturally raise the problem of insufficient charging stations. Lack of enough infrastructure has been identified as one of the barriers for the adoption of alternative fuel vehicles [32–36]. However, hybrid vehicles are not embedded into location decisions. Since they also use the same set of charging stations in long-distance trips, their effect need to be taken into account as well.

Finally, a PHEV's battery can also be seen as an energy source from the electricity network's point of view. In other words, PHEVs are also regarded as DERs due to their ability to provide energy for the grid. Mass penetration of PHEVs into the electricity grid and widespread utilization of DERs such as microturbines, fuel cells, photovoltaic systems and wind systems complicate the energy resource scheduling problem, and aggregating several different generation units further compounds this challenge. With these changes, energy scheduling is another emerging subject in the literature.

1.2 Literature Review

Green transportation is an emerging research topic that has made its debut in the literature in recent years. There are different studies taking into account the green perspective in transportation problems such as pollution-routing problem [37–42], green vehicle routing problem [43–46], optimal routing problems [44, 47–49], green supply chains [50–53] and location optimization of alternative fuel stations [54–60]. The main common objective of these studies is to establish the environmental and cost impacts of alternative fuel vehicles (EVs in particular) from the logistics perspective. In this respect, Pelletier et al. [61] cover possible research perspectives for the goods distribution with electrified transportation.

On the PHEV side, several articles deal with PHEV-related subjects, including, but not limited to, range requirement analyses [62, 63], PHEV impacts on the electricity network [64–72], battery capacity analyses [73–75], environmental impacts [76–78], market analyses [79–82], demand analyses [83–86] and charging infrastructure [87, 88]. Limiting our literature survey to the problems that we deal with in this study, the following four sections introduce the optimal path search literature, PHEV economics literature, charging station location literature and the virtual power plant literature with the given order.

1.2.1 Finding the Optimal Path for a PHEV

In the first part of this research effort, we approach PHEVs from a routing perspective and investigate their travel costs. A driver of a vehicle may prefer to minimize total travel distance, total travel time or total travel cost of a trip, and these problems can basically be modeled as variants of the shortest path problem. In terms of cost, there are various studies that separately investigate the minimum cost path problem for CVs (MCPP-CV) and for EVs (MCPP-EV) as we review below, and polynomial time algorithms are proposed for both problems. We formally present the minimum cost path problem for PHEVs (MCPP-PHEV) and its solution methodologies.

Several articles address the MCPP-CV in the literature [89–100]. Mixed Integer Programming (MIP) formulations, heuristic techniques and linear-time algorithms with dynamic programming approach are proposed as solution methodologies for both fixed and non-fixed path assumptions. [101] provides interesting complexity results about several variants of MCPP-CV. On the EV side, the problem of energy efficient routing of EVs has been addressed in the literature by considering limited cruising range and regenerative breaking capabilities of EVs [102–104] and polynomial time algorithms have been developed. These problems only consider routing in a network without charging facilities. [105] and [106] further include battery charging stations in their models and propose heuristic techniques as solution methodologies. Note that assuming the electricity as a commodity similar to gasoline, the algorithms mentioned above for MCPP-CV can also be used as solution methodologies for MCPP-EV. Routing in a network with battery switching stations is also considered in the literature [107]. Even though it is presented in a different context, Laporte and Pascoal [108] present a methodology that can also be customized to solve the MCPP-EV problem in a network with battery switching stations. In the existing MCPP-EV studies, battery degradation costs are not considered. Furthermore, all the aforementioned studies consider a single energy source, either gasoline or electricity. Thus, their solution methodologies cannot be directly used for the solution of MCPP-PHEV.

An important problem related to the minimum cost path problems is the shortest weight-constrained path problem (SWCPP) which is known to be NP-complete [109, 110]. In SWCPP, there are typically two independent measures such as cost and time associated with a path (e.g. 111, 112). It can efficiently be solved by a shortest path algorithm (i.e. polynomial-time solution algorithms exist) if one of the measures is disregarded or the two measures are consistent.

1.2.2 PHEV Economics in Long-distance Trips

Table 1.1: Recent literature related to PHEV economics

Authors	Subject	Driving Data Source
Özdemir and Hartmann [113]	Impacts of electricity range and gasoline price levels on the PHEV economics	Mobilität in Deutschland
Lunz et al. [114]	The influence of PHEV charging strategies on charging and battery degradation cost	European Energy Exchange (EEX)
Neubauer et al. [115]	The impacts of driving pattern, electricity range, energy management and charge strategies on PHEV economics	The Puget Sound Regional Council's 2007 Traffic Choices Study
Karabasoglu and Michalek [116]	PHEV life-cycle cost and emission benefits for varying ranges and driving conditions	2009 National Household Travel Survey (NHTS)
Peterson and Michalek [117]	The cost-effectiveness of PHEV battery capacity and charging infrastructure investment	2009 NHTS
Shiau et al. [118]	The impacts of charging patterns on PHEV economics	Simulations

A summary of recent studies in the literature related to the economics of PHEVs is presented in Table 1.1. In particular, Özdemir and Hartmann [113] put forward that battery prices have a significant effect on PHEV economics. The authors analyze how the PHEV electricity range and gasoline price levels affect PHEV economics. The driving data for their study is obtained from Mobilität in Deutschland. Predicting future use, the authors estimate the driving ranges and battery sizes for varying oil prices and report the estimated mobility costs and GHG emissions per vehicle kilometer for the year 2030. They conclude that battery prices have a significant effect on PHEV economics and that an electric-drive range of 12 to 32 kilometers is the optimum value. In a different study, Lunz et al. [114] investigate the influence of PHEV charging strategies on charging and battery degradation cost by taking into account the interaction of a distribution grid with PHEV batteries. Driving data is obtained from the European Energy Exchange (EEX). Several researchers identify driving patterns as a significant factor in PHEV economics and analyze their impacts. In this respect, Neubauer et al. [115] investigate the impacts of driving pattern, electricity range, energy management and charge strategies utilizing the Battery Ownership Model developed by the U.S. National Renewable Energy Laboratory (NREL). Driving data is obtained from the Puget Sound Regional Council's 2007 Traffic Choices Study. The authors show that the key parameters affecting PHEV economics are driving patterns. Neubauer et al. [119] conduct a similar study for EVs. Karabasoglu and Michalek [116] investigate PHEV life-cycle cost and emission benefits for varying ranges and driving conditions, utilizing the Powertrain Systems Analysis Toolkit (PSAT) developed by Argonne National Laboratory. Trip data for their study is obtained from the 2009 National Household Travel Survey (NHTS) conducted by the U.S. Department of Transportation. The authors argue that fuel economy labels make an optimistic estimate on the mileage per gallon and customers typically observe lower fuel economies in reality. They report that driving conditions have a significant impact on PHEV economics and environmental benefits, and conclude that under urban driving conditions, plug-in vehicles cut GHGs up to 60% and costs up to 20%. Along these lines, another interesting article is presented by Shiau et al. [118], who investigate the impacts of charging patterns on PHEV economics. The authors consider PHEV charging frequencies and investigate the results with respect to how often the vehicles must stop in order to charge their batteries. They argue that the best battery capacity choice for PHEVs depends on this charging frequency and PHEV economics depend largely on charging patterns of the driver. In a different article, Peterson and Michalek [117] study the cost-effectiveness of PHEV battery capacity and charging infrastructure investment for reducing U.S. gasoline consumption. The authors obtain driving pattern data from the 2009 NHTS and utilize the Department of Energy's Greenhouse Gases, Regulated Emissions, and Energy Use in Transportation (GREET) model. In their study, they analyze three types of charging infrastructure: home charging only, home and work charging and all stops charging. The authors conclude that increased PHEV battery capacity results in higher gasoline savings than charging infrastructure.

Most the aforementioned articles assume exogenous data corresponding to trips originally traveled by CVs. Some also consider driving data that were actually traveled by a limited number of PHEVs in experimental surveys. They carry out analyses by generalizing these results. Davies and Kurani [120] report that these assumptions may not reflect the real world and must be cautiously made. This finding has a significant bearing on the point of origin of the current study.

1.2.3 Charging Station Location in Intercity Road Network

As the EVs are infamous for their rather limited range, their increasing numbers naturally raise the problem of insufficient charging stations. Lack of enough infrastructure has been identified as one of the barriers for the adoption of alternative fuel vehicles in a more general setting [32–36]. In this respect, the refueling station location problem has been touted in the recent literature. There are two mainstream approaches in AFV refueling station location: maximum-coverage and set-covering. The cover-maximization approach for refueling station problem has been considered by Kuby and Lim [34] with the flow refueling location problem

(FRLP). The objective of the FRLP is to locate p stations in order to maximize the flow volume that can be refueled respecting the range limitations of the vehicles. A demand is assumed to be the vehicle flow driving on the shortest path between an origin and destination (OD) pair on a roundtrip. Satisfying a demand, or in other words, refueling a flow requires locating stations at a subset of the nodes on the path such that the vehicles never run out of fuel. Kuby and Lim [34] pregenerate minimal feasible combinations of facilities to be able to refuel a path, and then build a mixed integer linear programming (MILP) problem to solve the FRLP. There are applications of the problem in the literature [121, 122] and different extensions to the original problem are considered such as capacitated stations [123], driver deviations from the shortest paths [124, 125] and locating stations on arcs [126]. Different than other studies on FRLM, Kuby et al. [121] consider maximizing the vehicle-miles-traveled (VMT) on alternative fuel rather than maximizing the flow volume. The authors use FRLM for the location decisions of hydrogen stations in Florida, and build a decision support system to investigate strategies for setting up an initial refueling infrastructure in the metropolitan Orlando and statewide. Since the pregeneration phase of the method by Kuby and Lim [34] requires extensive memory and time, several solution enhancements have been proposed [127–131]. In particular, MirHassani and Ebrazi [130] present an innovative graph transformation and Capar et al. [131] propose a novel modeling logic for the FRLP problem, depending on the notion of arc-coverage, both of which increase the solution efficiency of the FRLP drastically. In the set-covering approach to the refueling station location problem, the objective is to minimize the number of stations while covering every possible demand in the network [55, 60, 130, 132].

FRLM and flow covering problems in general have recently been referred to as viable solution techniques and used to locate charging stations [55, 133–137]. Chung and Kwon [133] extended FRLM to model the multi-period charging station location problem, and a case study for Korean Expressways is carried out. The authors proposed a model based on the network transformation by MirHassani and Ebrazi [130] and two heuristics to solve their model. Jochem et al. [134]

investigated the optimal fast charging station locations in the German autobahn with a focus on the states Baden-Württemberg and Bavaria. They applied the formulation proposed by Capar et al. [131]. Hosseini and MirHassani [135] investigated the refueling station location problem for AFVs under uncertainty and used a modified version of their previous solution technique in MirHassani and Ebrazi [130] to solve it. They also indicate that their model can also be used for electric vehicles by using Level 3 fast charging technology. Wang and Lin [55] proposed a flow-based set covering model for optimally locating refueling stations, such as battery exchange or hydrogen refueling stations. Later, Wang and Lin [136] generalized the same formulation with the characteristics of maximum covering and set covering to locate multiple types of charging stations. Along with the ideas behind all these applications of flow based models to the charging station location problem, Nie and Ghamami [138] identified Level 3 fast charging as necessary to achieve a reasonable level of service in intercity charging station location. A similar result is also attained in Lin and Greene [139] using the National Household Travel Survey. Therefore, similar to aforementioned studies, we assume that the charging stations to be located provide Level 3 service. There are also applications with a flow based set covering formulation to locate slow charging stations for electric scooters [137].

In this study, our objective is to embed the PHEVs into the charging station location problem. All of the aforementioned studies related to refueling or charging station location consider single-type-fueled vehicles. However, using dual sources of energy, PHEVs utilize electricity as well as gasoline for transportation and they have comparable sales numbers with respect to EVs. According to Center for Sustainable Energy [140], 66,813 EV rebates and 48,733 PHEV rebates have been claimed in California State only between March 2010 and August 2015. Similar to the approach by Kuby et al. [121], we maximize the VMT on electricity which minimizes the total cost of transportation under the existing cost structure between electricity and gasoline. Even though maximizing the AFV numbers in long-distance trips brings environmental benefits, maximizing VMT brings along additional value from an environmental point of view; and in essence, it is also equivalent to minimizing the effects of greenhouse gases. With our approach to the charging station location problem, the cost and environmental benefits of charging station location are fully exploited by considering VMT and additionally taking the PHEVs into account.

1.2.4 Virtual Power Plant Formation in PHEV Penetrated Networks

Several electricity suppliers and DERs can be brought together to satisfy the demand load. The VPP, a newly introduced aggregation unit, is responsible for load management and resource scheduling. It obtains energy from the DERs, and contracts with the consumers in order to supply energy to their PHEVs and residential loads. To this end, it creates economies of scale in a whole new way [141]. VPPs minimize the total cost while ensuring that the energy generated by the DERs is efficiently used. They have no large-scale infrastructure requirements and can interact with the smallest DERs with higher efficiencies and more flexibility [142]. This new technology is usually referred to as the 'Internet of energy' [141]. Some real-world examples of VPPs are presented by Nikonowicz and Milewski [143].

The terms VPP and microgrid are usually used interchangeably with a slight difference that the microgrid can be 'islanded' from the grid whereas the VPP must be connected to the grid [141]. The aggregator centrally controls energy distribution to a set of consumers with time-elastic (TE) and time-inelastic (TIE) loads. The latter, such as refrigeration or heating, must be satisfied as soon as demanded, whereas the former, such as PHEVs, can be scheduled as desired during the connection period. For instance, the PHEV owner connects the vehicle to the electricity grid after returning from work in the evening and needs the battery fully charged by morning. If needed, the aggregator can discharge energy from the PHEV at any time during the night as long as the battery has reached its demanded level by morning.

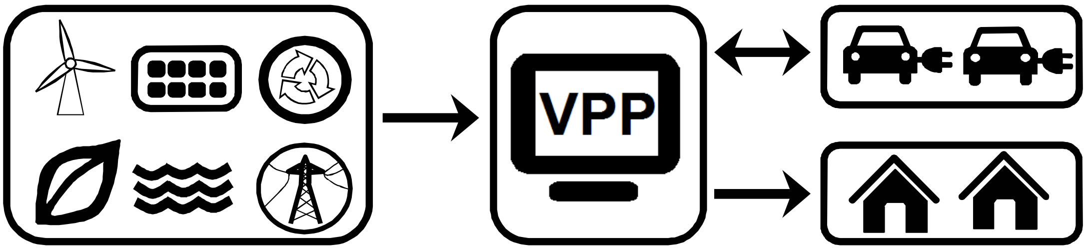

Figure 1.1: Energy scheduling process

Figure 1.1 depicts VPP energy scheduling process. The electricity suppliers and DERs are referred to as energy providers (EPs) within the context of this study. Energy transfers between EPs, VPP, the PHEVs and houses, i.e., TIE loads, are depicted by the arrows.

The problem of microgrid energy scheduling for a forecast load with the objective of cost minimization is addressed from several different aspects in the recent literature [144–160]. Aside from the microgrid energy scheduling literature, different papers address the energy scheduling problem in PHEV-penetrated networks [161–168]. Future trends of PHEVs [169–173] and emission impacts [174–176] are also considered. Even though an energy management methodology and/or market analysis models are presented, the common drawback is that the cost and emission impacts are not explicitly put forward. Sioshansi and Denholm [177] analyze the value of PHEVs as grid resources and model the charge scheduling of PHEV batteries. This is a unit commitment model of the Electricity Reliability Council of Texas (ERCOT) electric power system, formulated as a Mixed Integer Linear Program (MILP). The objective of the model is to minimize the total system cost, which consists of conventional generator costs and PHEV operation costs. The study considers the cost and emission impacts in the grid domain, but DERs and VPP are not considered in this study. A later study by Sioshansi [178] uses the same model and includes another model to make driving and charging decisions for the PHEV owner. Combining the two, the paper examines the incentives for individual drivers with different electricity tariffs. However, the ability to use PHEV batteries as storage is not included in the model. Sousa et al. [179] address the problem of energy scheduling from the VPP perspective, also considering technical constraints such as bus voltage magnitude and angle limits. The authors schedule PHEV battery charging and discharging by aggregating PHEVs into units of ten. The objective function of the model is defined to be cost minimization, but the charging price for PHEVs is added to the objective function with a negative coefficient. Therefore, the model actually minimizes the cost less the income, which implies profit maximization. Due to this representation, the objective function actually drives the solution to schedule PHEV charging at time intervals with higher costs. The presented objective value is always positive in this study because the income from TIE loads is not included in the objective function.

1.3 Contributions

We initially introduce a practically important and theoretically challenging problem: finding the minimum cost path for PHEVs in a network with refueling and charging stations, considering electricity and gasoline as sources of energy with different cost structures and limitations. We show that this problem is NP-complete even though its electric vehicle and conventional vehicle special cases are polynomially solvable. We propose three solution techniques: (1) a mixed integer quadratically constrained program that incorporates non-fuel costs such as vehicle depreciation, battery degradation and stopping, (2) a dynamic programming based heuristic and (3) a shortest path heuristic. Our study is the first that addresses the battery degradation in the MCPP context. We conduct extensive computational experiments using both real world road network data and artificially generated road networks of various sizes. Practical applications of the problem in transportation and logistics, considering specifically the long-distance trips, are discussed in detail.

Next, we analyze long-distance travel costs of PHEVs in terms of real-world dynamics on three groups of independent factors: battery characteristics, often-overlooked driver preferences and road network features and compare the results with hybrid electric and conventional vehicles. We investigate the interactions of these factors, and rank the contribution of each level of these factors to the total cost. This analysis provides critical managerial insights which are extremely relevant in shaping future investment decisions about PHEVs and their infrastructure. In particular, our findings show that increasing the number of charging stations may not be enough to overcome the range anxiety of the drivers. In addition to the charging infrastructure availability, a driver's stopping tolerance arises as another critical factor affecting the transportation costs. Ultimately, our findings lead to critical information for policy makers, governments and investors who would like to fully exploit the opportunities offered by the game changing PHEV technology.

We then introduce the hybrid charging station location problem (HCSLP) as a generalization of the flow refueling location problem by Kuby and Lim [34]. To our knowledge, this is the first study to consider the PHEVs in intercity charging station location decisions. Our objective is to maximize the vehicle-miles-traveled (VMT) using electricity and thereby minimize the total cost of transportation under the existing cost structure between electricity and gasoline. This is also indirectly equivalent to maximizing the environmental benefits. We also address the topic of multi-class vehicles with different ranges in our formulations. For the exact solution of this practically important and theoretically challenging problem, we present an arc-cover model. To enhance the solution process, we propose a Benders Decomposition algorithm. We construct subproblem solutions in closed form expressions to accelerate the algorithm. Furthermore, three different cut generation schemes are proposed: singlecut, multicut and Pareto-optimal cut. Using the special structure of the subproblem and its dual, we construct these three types of cuts as closed form expressions without having to solve any LPs. The computational gains with the Pareto-optimal cut generation scheme are significant and the efficiency of the decomposition algorithm is increased by orders of magnitude.

The results of the computational studies show that the proposed algorithm both accelerates the solution process and effectively handles instances of realistic size.

Finally, we investigate the cost and emission impacts of VPP formation in PHEV-penetrated networks. We propose a new model that minimizes the total cost from the VPP viewpoint and we present an integer linear representation of the model. We conduct a sensitivity analysis on the battery price, the gasoline price, DER price and capacities, and present extensive insightful results.

In the following chapter, we start off by introducing the minimum cost path problem for PHEVs. Using the solution methodology, we analyze long-distance travel costs of PHEVs in Chapter 3. The Hybrid Charging Station Problem and its solution techniques are introduced in Chapter 4. The VPP Formation in PHEV-penetrated networks and its impacts on cost and emissions are investigated in Chapter 5. Finally, we conclude our study in Chapter 6.

Chapter 2

Minimum Cost Path for Plug-in Hybrid Electric Vehicles[1]

2.1 Problem Definition

We provide the basic definitions and assumptions necessary for the formalization of MCPP-PHEV. Consider a directed transportation graph $G = (N, A)$ and a PHEV traveling from an origin node $s \in N$ to a destination node $t \in N$. Refueling and/or charging stations are located at some of the nodes of the graph and pricing may vary between nodes. Therefore, a PHEV can reduce its travel costs by a proper choice of refueling and/or charging stations.

Proposition 1. *If a PHEV does not refuel or charge its battery when traveling from node $i \in N$ to node $j \in N$, then the minimum cost path is the shortest path between nodes i and j.*

[1]An extended version of this chapter is authored by Okan Arslan, Barış Yıldız and Oya Ekin Karaşan and is published in Transportation Research Part E: Logistics and Transportation Review, 80:123 141, 2015 [48].

The proof of Proposition 1 is straightforward. Next, we introduce a graph transformation which will be useful for the solution methodologies. A similar construction in a completely different application setting is provided in [180–182].

Definition 1. *Given a weighted graph $G = (N, A)$: let $\widehat{N} = \{s, t\} \cup \{i \in N :$ i has a charging and/or refueling station$\}$ and $\widehat{A} = \{(i, j) : i, j \in \widehat{N}$ and j is reachable from i if a PHEV at node i with a full tank of gasoline and fully charged battery can reach node j along a shortest path in $G\}$. Arc $(i, j) \in \widehat{A}$ has a distance equal to the shortest path distance, say $d^\star_{ij}$, from i to j in G. The graph $\widehat{G} = (\widehat{N}, \widehat{A})$ is called the **meta-network** of G.*

Proposition 1 implies that an optimal solution of a MCPP on a given graph can also be obtained by solving the same MCPP instance on its meta-network. Now, consider nodes B, C and D in graph G in Figure 2.1. Only node C has a refueling station. The meta-network $\widehat{G}$ is also shown in the same figure. Observe that the arc from s to t is redundant and corresponds to traveling on the path $s \to C \to t$. Since the shortest path from s to t contains a node with a refueling station in the original graph G, arc (s, t) can be omitted.

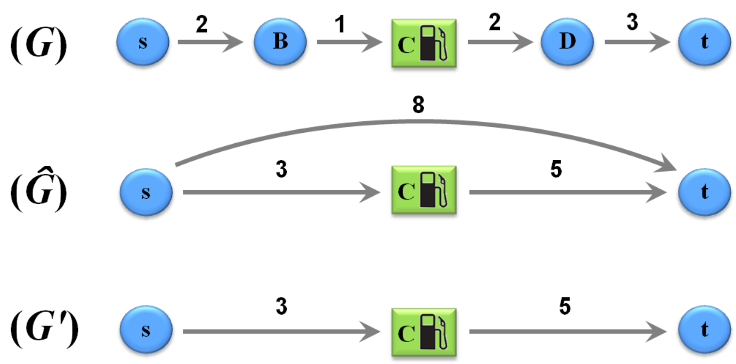

Figure 2.1: Graph transformation for MCPP-PHEV

Meta-networks can be very dense due to the combined CD and CS mode ranges. The size of the graph is a burden on the solution efficiency, and thus it is useful to omit the redundant arcs in the meta-network. We refer to the graph formed by the omission of redundant arcs as the **reduced meta-network** denoted by G' in Figure 2.1. In particular, the arcs that are present in the reduced meta-network G' correspond to shortest paths in the original graph G that contain no intermediate nodes with refueling or charging stations.

Definition 2. *A vehicle instance (vehicle) is a vector with 6 entries:* $\langle \overline{P}, \underline{P}, \overline{G}, \underline{G}, \varepsilon, \rho \rangle$ *where* $\overline{P}$ *and* $\underline{P}$ *are the battery maximum and minimum energy capacities, respectively (kWh),* $\overline{G}$ *and* $\underline{G}$ *are the maximum and minimum tank capacities, respectively (gallons),* ε *is the average electricity usage (kWh/mile) and* ρ *is the average gasoline usage (gallon/mile).*

Definition 3. *A network instance (network) is a 7-tuple:* $\langle N, A, s^e, s^g, c^e, c^g, d \rangle$ *where* N, A *are the sets of nodes and arcs,* $s^e : N \to \{0, 1\}$ *and* $s^g : N \to \{0, 1\}$ *are functions indicating whether a charging or refueling station is located at a node, respectively,* $c^e : N \to \mathbb{R}^+$ *is the electricity price function (¢/kWh),* $c^g : N \to \mathbb{R}^+$ *is the gasoline price function (¢/gallon) and* $d : A \to \mathbb{R}^+$ *is the length function (miles).*

Definition 4. *The Minimum Cost Path Problem for PHEV (MCPP-PHEV) is defined as finding a path for a vehicle* V *from a departure node* s *to a destination node* t *in a network, and deciding on how much to refuel and where to charge its battery on the path. More formally, the decision version of the problem is:*

INSTANCE: $\langle V, X, s, t, P_s, G_s, P_t, G_t \rangle$ *where* V *is a vehicle instance,* X *is a network instance, nodes* s *and* t *are departure and destination nodes,* P_s *and* G_s *are the initial electricity and gasoline storages at node* s, P_t *and* G_t *are the minimum final electricity and gasoline storage requirements at node* t*, respectively, and a positive number* C.

QUESTION: Is there a path from s *to* t *in network* X *that can be traveled by vehicle* V *with initial electricity and gasoline levels of* P_s *and* G_s *and final electricity and gasoline levels of at least* P_t *and* G_t *for a cost less than or equal to* C*?*

The solution of the MCPP-PHEV is a triplet $\langle \vartheta, e^+, g^+ \rangle$ where ϑ is the incidence vector of the optimal path, e^+ and g^+ are vectors of size $|N|$ representing the electricity and gasoline purchases that are transferred to PHEV at each node, respectively.

2.1.1 NP-Completeness

Consider the shortest weight-constrained path problem (SWCPP) for directed graphs which is known to be NP-Complete [183]:

INSTANCE: A directed graph $G = (N, A)$ with length $l_{ij} \in \mathbb{Z}^+$ and weight $w_{ij} \in \mathbb{Z}^+$ for each $(i, j) \in A$, specified nodes $s, t \in N$ and positive integers K and W.

QUESTION: Is there a path in G from s to t with total length K or less and total weight W or less?

First, note that multiplying both W and w_{ij} $\forall(i, j) \in A$ by a positive constant ϕ does not change the solution in SWCPP, and the question in the original instance has a YES answer if and only if the modified instance has a YES answer.

Theorem 1. *The MCPP-PHEV is NP-complete.*

Proof. Observe that the MCPP-PHEV is in NP: given a solution and a value C, one can verify in polynomial time if the solution is feasible and the associated cost is at most C. Given an instance $\langle G, l, w, s, t, K, W \rangle$ to SWCPP, let $l^{min} = \min_{(i,j)\in A} l_{ij}$, $l^{max} = \max_{(i,j)\in A} l_{ij}$, $w^{max} = \max_{(i,j)\in A} w_{ij}$, $\phi = \dfrac{l^{min}}{2 \times l^{max} \times w^{max}} > 0$, $\hat{W} = \phi \times W$ and $\hat{w_{ij}} = \phi \times w_{ij}$ $\forall(i, j) \in A$. Now, consider an equivalent SWCPP instance $\langle G, l, \hat{w}, s, t, K, \hat{W} \rangle$.

We now transform this SWCPP instance into an MCPP-PHEV instance by the following polynomial time transformation: we add a node, say node ij, on each arc

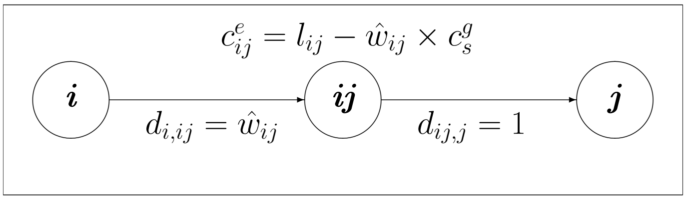

Figure 2.2: Graph transformation to show NP-Completeness

$(i, j) \in A$ as shown in Figure 2.2. Let N' be the set of newly added nodes, A_1 be the set of arcs from node i to node ij, $\forall (i, j) \in A$ with distance equal to $\hat{w}_{ij}$ and A_2 be the set of arcs from node ij to node j, $\forall (i, j) \in A$ with distance equal to 1 mile. The graph is then transformed into $G' = (N \cup N', A_1 \cup A_2)$. In the transformed graph, no gasoline or charging station is located at node $i \in N/\{s\}$. We locate only a refueling station at the source node and the cost of gasoline at this node is $c^g_s = l^{max}$. We also locate a charging station, but no refueling station, at every node $ij \in N'$ and the cost of electricity at node ij is $c^e_{ij} = l_{ij} - \hat{w}_{ij} \times c^g_s = l_{ij} - \phi \times w_{ij} \times l^{max}$. Replacing ϕ, we get $c^g_s > c^e_{ij} > 0$ for all nodes $ij \in N'$ so that traveling on electricity is always preferable to traveling on gasoline. Let X be this transformed network. Let V be the vehicle $\langle 1, 0, \hat{W}, 0, 1, 1 \rangle$. That is, PHEV V has 1 mile of CD mode range and $\hat{W}$ miles of CS mode range.

Consider the MCPP-PHEV instance $\langle V, X, s, t, 0, 0, 0, 0 \rangle$, i.e. a PHEV V travels from node s to node t in network X with zero initial and final gasoline and electricity levels. Let K be the associated cost input. In Figure 2.2, V at node i with minimum electricity level needs to spend $\hat{w}_{ij}$ units of gasoline in order to arrive at node ij. Since electricity is preferable to gasoline, it charges its battery fully at node ij and travels to node j on the CD mode. At node j, its battery depletes and it starts running on CS mode again. The cost of electricity at node ij and the distance between nodes ij and j are such that the total cost of traversing this arc is $l_{ij} - \hat{w}_{ij} \times c^g_s$ cents. Observe that the vehicle needs to buy the required level of gasoline at the source node at a cost of $\hat{w}_{ij} \times c^g_s$ in order to travel from node i to node j.

Now, it is easy to observe that V has a path from node s to t with cost at most K if and only if the SWCPP has a path from s to t with length at most K and weight at most $\hat{W}$. □

2.1.2 Extensions

In order to model real world more closely, non-fuel costs such as vehicle depreciation and/or stopping costs need to be taken into account [94]. To this end, we extend the MCPP-PHEV from three aspects and refer to this problem as the Extended MCPP-PHEV (E-MCPP-PHEV). The first extension is ***vehicle depreciation cost***. A PHEV incurs electricity and gasoline costs while traveling. Furthermore, it loses its value with increasing mileage. Therefore, it incurs a vehicle depreciation cost for every mile traveled. Unless depreciation cost is included in the objective function, an optimal path might get much longer than the shortest path which cannot be tolerated even for the most cost averse driver. Therefore, we indirectly avoid long trip distances by including the depreciation cost in the model. In a sense, the depreciation cost can be considered as the cost of tolerating longer distances, and high depreciation costs would force the E-MCPP-PHEV solutions to follow the shortest path.

Another cost component of a vehicle trip is the ***stopping cost***. This cost component can be a measure of the tolerance for stops on the route. That is, for high enough stopping costs, the optimal solution would be the one with the least number of stops. Note that by including the stopping cost, we avoid excessive number of stops on the optimal path which is not tolerable even for the most cost averse driver.

The battery of a PHEV has a limited lifespan, and its life shortens at each cycle. Thus, apart from the electricity purchase cost, PHEV owners also incur **battery**

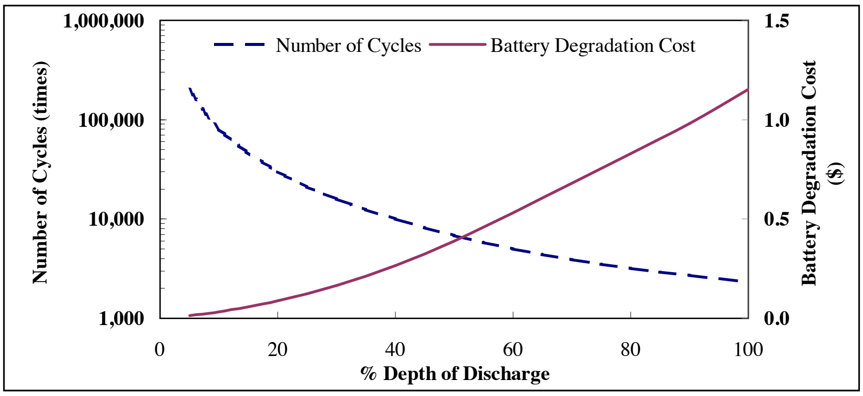

Figure 2.3: Cycle life of PHEV batteries as a function of DoD

degradation cost for each battery charge/discharge cycle. The number of cycles is a nonlinear function of depth of discharge (DoD) as reported by [184] and [185]. A sample cycle life function is presented in Figure 2.3 by dashed lines. The more the battery is discharged, the less the number of cycles is. For instance, consider a battery worth \$2650 being discharged to 40% DoD throughout its lifetime. The expected number of cycles at this DoD is approximately 10000. Therefore each discharging costs the PHEV owner 26.5 ¢ (\$2650 $\times$ 1/10000). A sample degradation cost function for a \$2650 battery is presented in Figure 2.3. In our study, we assume that a cycle is completed each time a battery is charged at a station and a PHEV owner incurs a battery degradation cost depending on the DoD level upon arrival to a charging station. We determine this cost by evaluating a quadratic function of DoD. To the best of our knowledge, [177] are the first to include battery degradation cost in their energy management model.

Within this context, the cost components of a PHEV trip are the gasoline cost, the electricity cost, the battery degradation cost, the vehicle depreciation cost and the stopping cost. For simplicity in representing an E-MCPP-PHEV instance, we use the MCPP-PHEV instance representation and assume that all cost components are embedded in the corresponding network instance.

2.2 Solution Techniques

In this section, we provide a mathematical formulation for the E-MCPP-PHEV. Then we present a dynamic programming approximation heuristic along with its extension and a shortest path heuristic.

2.2.1 E-MCPP-PHEV Mathematical Model

The parameters and variables to be used in the formulation of the E-MCPP-PHEV are presented below. We assume that the parameters are known with certainty, and the routing decisions are based on the known pricing of electricity and gasoline at every node of the network.

- *Parameters*

N, A	:	Sets of nodes and arcs
s, t	:	Source and destination nodes
s_i^e, s_i^g	:	1 if there is an electricity or refueling station, respectively, at node i, and 0 otherwise
$\overline{P}, \underline{P}$	:	Battery maximum and minimum energy capacities, respectively (kWh)
$\overline{G}, \underline{G}$	:	Maximum and minimum tank capacities, respectively (gallons)
P_s, P_t	:	Initial and final energy stored in battery of the PHEV (kWh), respectively
G_s, G_t	:	Initial and final gasoline stored in tank of the PHEV (gallons), respectively
ε	:	Average electricity usage of the PHEV (kWh/mile)
ρ	:	Average gasoline usage of the PHEV (gallon/mile)
d_{ij}	:	Length of arc (i, j) (miles)
c_i^e	:	Price of electricity at node i (¢/kWh)
c_i^g	:	Price of gasoline at node i (¢/gallon)

c_i^{st} : Stopping cost at node i (¢)
c^{dep} : Depreciation cost of traveling for a mile (¢/miles)

• *Variables*

$e_i^{\alpha}, e_i^{\beta}$: Charge level at node i at arrival and departure, respectively (kWh)
e_i^{+} : Net electric energy change at node i (kWh)
$g_i^{\alpha}, g_i^{\beta}$: Gasoline level at node i at arrival and departure, respectively (gallons)
g_i^{+} : Gasoline transferred to the PHEV at node i (gallons)
ϑ_{ij} : 1 if arc (i, j) is on the minimum cost path, 0 otherwise
v_i : 1 if the PHEV charges battery at node i, and 0 otherwise
u_i : 1 if the PHEV refuels and/or charges battery at node i, and 0 otherwise
δ_i : Depth of Discharge (DoD) at node i at arrival
$c^{bat}(\delta_i)$: Degradation cost of the PHEV battery at node i
We assume the expected battery replacement cost as a quadratic function of DoD δ, i.e., $c^{bat}(\delta) = a \times \delta^2 + b \times \delta$ where a and b are coefficients for a given battery type
d_{ij}^{cd}, d_{ij}^{cs} : Travel distance in charge-depleting (CD) and charge-sustaining (CS) mode while traveling on arc (i, j), respectively (miles)

The formulation is as follows:

$$\text{minimize} \sum_{i\in N} c_i^e \times e_i^+ + \sum_{i\in N} c_i^g \times g_i^+ + \sum_{i\in N} c^{bat}(\delta_i) + \sum_{(i,j)\in A} d_{ij} \times c^{dep} \times \vartheta_{ij} + \sum_{i\in N} c_i^{st} \times u_i \tag{2.1}$$

subject to

$$\sum_{j:(i,j)\in A} \vartheta_{ij} - \sum_{j:(j,i)\in A} \vartheta_{ji} = \begin{cases} 1, & i = s \\ -1, & i = t \\ 0, & \forall i \in N/\{s,t\} \end{cases} \tag{2.2}$$

$$e_i^{\beta} = e_i^{\alpha} + s_i^e \times e_i^+ \qquad \forall i \in N \tag{2.3}$$

$$M \times (\vartheta_{ij} - 1) \le e_j^{\alpha} - e_i^{\beta} + \varepsilon \times d_{ij}^{cd} \le M \times (1 - \vartheta_{ij}) \qquad \forall (i,j) \in A \tag{2.4}$$

$$\underline{P} \le e_i^{\alpha} \le \overline{P} \qquad \forall i \in N \qquad (2.5)$$

$$\underline{P} \le e_i^{\beta} \le \overline{P} \qquad \forall i \in N \qquad (2.6)$$

$$e_i^{+} \le v_i \times \overline{P} \qquad \forall i \in N \qquad (2.7)$$

$$v_i \le u_i \qquad \forall i \in N \qquad (2.8)$$

$$e_s^{\alpha} = P_s \qquad (2.9)$$

$$e_t^{\alpha} \ge P_t \qquad (2.10)$$

$$\delta_i = \frac{e_i^{+}}{\overline{P}} \qquad \forall i \in N \qquad (2.11)$$

$$c^{bat}(\delta_i) \ge a \times (\delta_i)^2 + b \times \delta_i - M \times (1 - v_i) \qquad \forall i \in N \qquad (2.12)$$

$$g_i^{\beta} = g_i^{\alpha} + s_i^{g} \times g_i^{+} \qquad \forall i \in N \qquad (2.13)$$

$$M \times (\vartheta_{ij} - 1) \le g_j^{\alpha} - g_i^{\beta} + \rho \times d_{ij}^{cs} \le M \times (1 - \vartheta_{ij}) \qquad \forall (i,j) \in A \qquad (2.14)$$

$$\underline{G} \le g_i^{\alpha} \le \overline{G} \qquad \forall i \in N \qquad (2.15)$$

$$\underline{G} \le g_i^{\beta} \le \overline{G} \qquad \forall i \in N \qquad (2.16)$$

$$g_i^{+} \le u_i \times \overline{G} \qquad \forall i \in N \qquad (2.17)$$

$$g_s^{\alpha} = G_s \qquad (2.18)$$

$$g_t^{\alpha} \ge G_t \qquad (2.19)$$

$$d_{ij}^{cs} + d_{ij}^{cd} = d_{ij} \qquad \forall (i,j) \in A \qquad (2.20)$$

$$\vartheta_{ij}, v_k, u_k \in \{0,1\};\ d_{ij}^{cd}, d_{ij}^{cs}, e_k^{\alpha}, e_k^{\beta}, e_k^{+}, g_k^{\alpha}, g_k^{\beta}, g_k^{+}, \delta_k^{\alpha}, c_k^{bat} \ge 0 \qquad \forall k \in N, \forall (i,j) \in A \qquad (2.21)$$

The objective function minimizes the cost of traveling. The cost components are the cost of obtaining electricity and gasoline, the battery degradation cost, the depreciation cost and the stopping cost. Constraints (2.2) enforce the solution to be a path from s to t. Constraints (2.3) are the electricity balance equations for nodes. The level of electricity upon leaving node i equals the entering electricity level plus the electricity obtained at node i. Similarly, Constraints (2.4) are the electricity balance equations for those arcs that are on the path. For the non-path arcs, the constraints are relaxed with appropriate big-M values. Constraints (2.5)-(2.6) set the upper and lower bounds for the electricity level when entering or leaving a node. Constraints (2.7) assign binary v_i variable a value of 1 if battery is charged at node i. Constraints (2.8) require that u_i is set to 1 if v_i equals 1 and therefore a stopping cost is incurred in the objective function if the PHEV stops to charge its battery. Constraints (2.9)-(2.10) set the electricity level at nodes s and t, respectively. Constraints (2.11) assign proper depth of discharge values and Constraints (2.12) calculate the battery degradation for each node if battery is charged. Constraints (2.13)-(2.19) are the counterparts of constraints (2.3)-(2.9) for the gasoline case. Constraints (2.20) ensure that the sum of the distances on CS and CD modes is equal to the arc length if the arc is on the path. Constraints (2.21) are the domain requirements.

Observe that one can easily extract the following information from the outputs of the model: the path to travel from node s to node t, how many miles to travel on CD and CS modes on each arc, where to stop to refuel or charge battery, and how much to refuel at each refueling stop.

The following lemma presents a valid inequality for the E-MCPP-PHEV formulation.

Lemma 1. $\Big(\sum_{i\in N} e_i^+ + P_s - P_t\Big)/\varepsilon + \Big(\sum_{i\in N} g_i^+ + G_s - G_t\Big)/\rho \geq \sum_{(i,j)\in A} \vartheta_{ij} \times d_{ij}$ *is a valid inequality to (2.2)-(2.21).*

Proof. The inequality simply states that we need to have enough electricity and gasoline to travel the trip distance. □

Computational studies show that the above cut is very effective in improving the relaxation bound.

2.2.2 Handling Non-simple Paths in the Model

A *directed path* is an alternating sequence of nodes $(n_0, n_1, n_2, ..., n_k)$ with $(n_i, n_{i+1}) \in A$, $\forall i = 0, \ldots, k-1$. A directed path is a *non-simple path* if it repeats nodes and *simple path* otherwise. Non-simple paths can occur in transportation networks and as solutions to the E-MCPP-PHEV. The presented MIQCP formulation constructs a simple path in the input network $G = (N, A)$. The input network can be the original transportation network, the meta-network or the reduced meta network, depending on how the non-simple paths are handled. By choosing G as the meta-network or as the reduced meta-network of the input transportation network, a wide group of non-simple paths as potential solutions can be handled by this formulation. All non-simple path occurrences, including extremely rare ones, can be taken into account by duplicating the nodes in G and taking its meta-network at the expense of computational inefficiency. In this part, we demonstrate examples of non-simple paths that might appear as the optimal solutions of the E-MCPP-PHEV problem and present methods to handle these non-simple paths by the mathematical model.

First, note that all of the non-simple paths can be handled by duplicating every node in the graph G (as many times as the drivers are willing to revisit the same node in the same trip or as the number of nodes in the worst case). But this implies a much larger graph size and brings along computational burden. Thus, we first present ways to handle those cases by modifying the input graph for the MIQCP model before resorting to the costly node duplication.

Problem Instance

- We consider the vehicle Instance $V = \langle \overline{P} = 1, \underline{P} = 0, \overline{G} = 9, \underline{G} = 0, \varepsilon = 1, \rho = 1 \rangle$. Thus the gasoline range of a PHEV is 9 miles and the electricity range is 1 mile.
- To illustrate different cases, we use a different network instance for each of

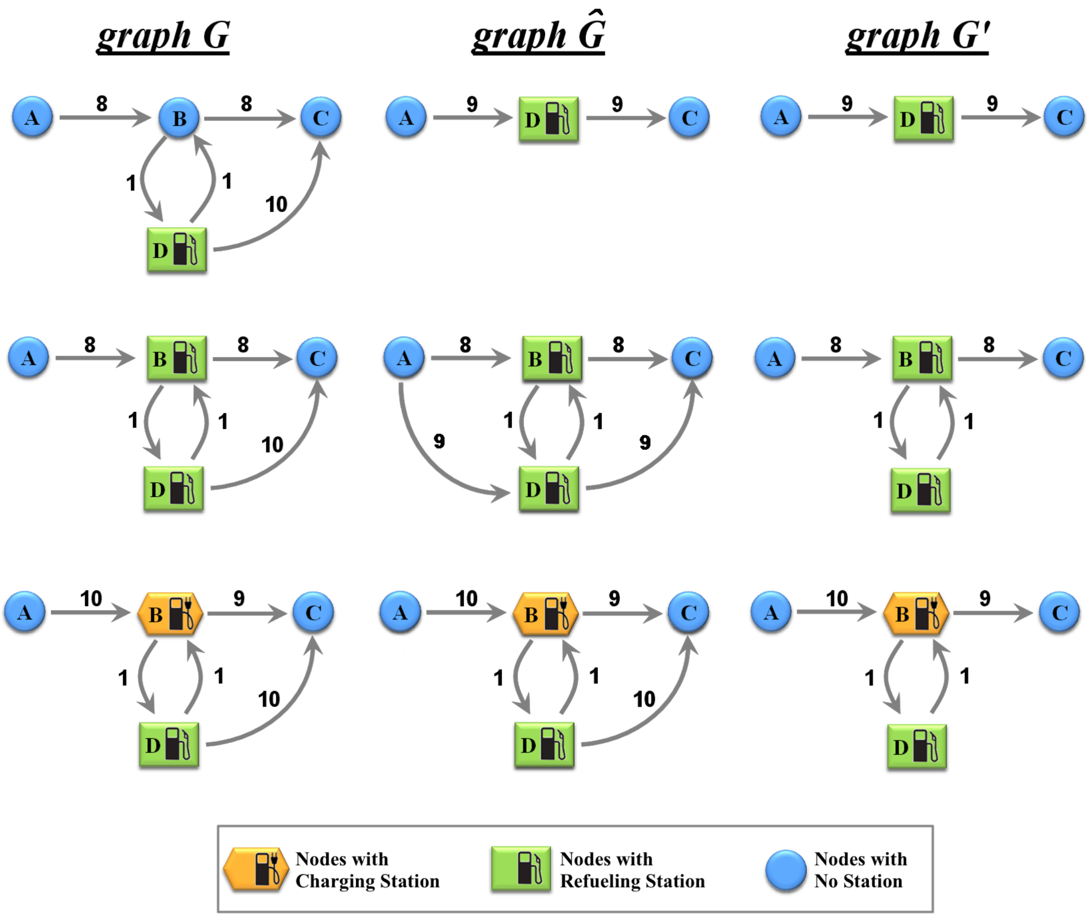

Figure 2.4: Non-simple path examples

the three examples (Figure 2.4). In all three networks, nodes A, B and C are points on the highway.

- The problem instance is given as $\langle V, X, A, C, 1, 9, 0, 0\rangle$ where X is the input network instance. For the sake of simplicity, we also assume that battery degradation, vehicle depreciation and stopping costs are all zero.

Case-1: Detour from the highway to refuel

We can think of nodes A, B and C as points on the highway, and D is a refueling station just one mile away from the highway. Node B is deleted in the meta-network or reduced meta-network since it does not have a station. The optimal non-simple path from A to C in G is $A \rightarrow B \rightarrow D \rightarrow B \rightarrow C$ and can be attained by using the reduced meta-network G' as input to the MIQCP formulation.

Case-2: Detour from the highway to refuel in a cheaper station

The middle figure illustrates a detour from the highway. But this time, there is a refueling station on the highway (possibly with a more expensive gasoline price) at which the PHEV can detour and go to node D in order to refuel. In this case, MIQCP formulation can handle the optimal non-simple path $A \rightarrow B \rightarrow D \rightarrow B \rightarrow C$ by using meta-network $\hat{G}$ as the input graph. Indeed, simple path $A \rightarrow D \rightarrow C$ in $\hat{G}$ will correspond to this solution.

Case-3: Refuel twice in the same station

Now, consider the bottom figure. This time, node B has a charging station and node D has a refueling station. Observe that there is only one feasible solution for this problem: $A \rightarrow B \rightarrow D \rightarrow B \rightarrow C$. The PHEV charges battery at node B, travels to node D to refuel. Then it necessarily returns back to node B and charges its battery again in order to be able to reach to node C. In this example, the optimal path is a non-simple path in all three graph types and thus, MIQCP formulation can only handle such non-simple paths by a node duplication.

Note that this particular instance can be generalized so that more than two visits to the same node, and hence more than one duplication of the node set, is necessary. Note also that this is a rather rare occurrence. The emergence of such non-simple paths is not only due to price differences, but also to range limitations as well. In the example, node B is reachable from node A, but node D is not. Considering the combined gasoline and electric range of existing PHEVs, this example is not very representative of the real network instances under our scope.

2.2.3 Discrete Approximation Dynamic Programming Heuristic

In this section, we introduce a dynamic programming based heuristic algorithm referred to as DH. We first define a set of states associated with electricity and gasoline levels at nodes. Then, we present Bellman's equations [186] that should be satisfied by minimum cost path lengths in order to facilitate the dynamic programming solution methodology. Lastly, we present a graph transformation by which the solution of these equations can be computed efficiently (i.e. in polynomial time) by solving a shortest path problem on the transformed graph.

Definition 5. *A state is a triplet $\langle i, \sigma, \lambda \rangle$ which represents the arrival at a node $i \in N$ with $\sigma \in [\underline{P}, \overline{P}]$ kWh electricity charge and $\lambda \in [\underline{G}, \overline{G}]$ gallons of gasoline. We will use the notation $\omega_i^{\sigma,\lambda}$ to refer to a state and replace this notation with ω or ω_i when the context does not require specific values of i, σ and λ to be discerned.*

Given an E-MCPP-PHEV instance $\langle V, X, s, t, P_s, G_s, P_t, G_t \rangle$, a solution $\langle \vartheta, e^+, g^+ \rangle$ contains a path from s to t which can be extracted from the vector ϑ. With the specific energy (e^+) and gasoline (g^+) purchases at the nodes, the distances to be covered in CD and CS modes on this path can easily be extracted. Together with P_s and G_s, the vectors ϑ, e^+ and g^+ induce the levels of state-of-charge and gasoline at arrival to the nodes on the solution path. So, for every solution of the E-MCPP-PHEV, there is a unique sequence of states that represents this solution. Note that in general, the E-MCPP-PHEV has an uncountable number of feasible solutions. Since each of these solutions maps uniquely to a sequence of *states*, the state space is also uncountable. However, this uncountable state space can be approximated with a finite one which is the main idea behind the DH.

Let $\xi, \tau \in \mathbb{N}$ be the discretization parameters for the state space. Consider two sets $\Sigma = \{\sigma_0, \sigma_1, \ldots, \sigma_\xi\}$ and $\Lambda = \{\lambda_0, \lambda_1, \ldots, \lambda_\tau\}$ where $\sigma_0 = \underline{P}, \lambda_0 = \underline{G}$, $\sigma_k = \sigma_0 + k \times \frac{\overline{P} - \underline{P}}{\xi} \quad \forall k \in \{1, 2, \ldots, \xi\}$ and $\lambda_l = \lambda_0 + l \times \frac{\overline{G} - \underline{G}}{\tau} \quad \forall l \in \{1, 2, \ldots, \tau\}$.

Every σ_i represents the interval of electricity levels $[\sigma_i, \sigma_{i+1}] \quad \forall i \in \{0, 1, \ldots, \xi - 1\}$ and σ_ξ represents the fully charged battery. The representation for each λ is similar.

For a given E-MCPP-PHEV instance $\langle V, X, s, t, P_s, G_s, P_t, G_t \rangle$, ξ and τ values, we define the *discrete state space* Ω as:

$$\Omega = \{(\omega_i^{\sigma,\lambda} | i \in N - \{s, t\}, \sigma \in \Sigma, \lambda \in \Lambda\} \cup \{\omega_s^{P_s,G_s}, \omega_t^{P_t,G_t}\} \tag{2.22}$$

Observe that the cardinality of the *discrete state space* Ω is bounded by $n \times (\xi + 1) \times (\tau + 1)$ where n is the number of nodes in X, and is finite. Algorithm DH uses Ω and incurs an approximation error on representing the amount of electricity charge and gasoline left with the PHEV arriving at a node. Obviously this approximation error can be reduced arbitrarily by choosing ξ and τ large enough.

Definition 6. *$\pi : \Omega \to \mathbb{R}$ is called the value function and $\pi(\omega_i^{\sigma,\lambda})$ is defined to be the optimal solution value of the E-MCPP-PHEV instance $\langle V, X, s, i, P_s, G_s, \sigma, \lambda \rangle$.*

The minimum cost transition function $f : \Omega \times \Omega \to \mathbb{R}^+$ takes two states $\omega_i^{\sigma,\lambda}, \omega_j^{\bar{\sigma},\bar{\lambda}}$ as its arguments and returns the minimum cost of the transition from node i starting with σ kWh charge and λ gallons of gasoline to node j ending with at least $\bar{\sigma}$ kWh charge and $\bar{\lambda}$ gallons of gasoline. When calculating $f(\omega_i^{\sigma,\lambda}, \omega_j^{\bar{\sigma},\bar{\lambda}})$, we only consider how much to refuel and charge at node i. Four cases as detailed below should be considered. A feasibility condition is stated for each case. The cost value is as presented if the feasibility condition is met, and is not finite otherwise. Let $d^\star$ represent the shortest path lengths.

- Case 1: No battery charging and no refueling.

  Feasibility Condition: The existing electricity charge and gasoline are enough to travel from node i to node j while satisfying the end-state conditions, i.e.,

$$\sigma \geq \bar{\sigma}, \lambda \geq \bar{\lambda} \text{ and } \frac{(\sigma - \bar{\sigma})}{\varepsilon} + \frac{(\lambda - \bar{\lambda})}{\rho} \geq d_{ij}^\star.$$

Total Cost: The only cost component to be incurred is the depreciation cost. Thus, $f_1(\omega_i^{\sigma,\lambda}, \omega_j^{\bar{\sigma},\bar{\lambda}}) = c^{dep} \times d_{ij}^{\star}$.

- Case 2: Refueling but no battery charging.

  Feasibility Condition: The existing electricity charge and full tank of gasoline are enough to travel from node i to node j while satisfying the end-state conditions, i.e.,

  $$s_i^g = 1, \sigma \geq \bar{\sigma} \text{ and } \frac{(\sigma - \bar{\sigma})}{\varepsilon} + \frac{(\overline{G} - \bar{\lambda})}{\rho} \geq d_{ij}^{\star}.$$

  Total Cost: The minimum cost transition requires to use $(\sigma - \bar{\sigma})$ electricity charge first. Thus $d_{ij}^{cd} = \min\{d_{ij}^{\star}, \frac{(\sigma-\bar{\sigma})}{\varepsilon}\}$ and $d_{ij}^{cs} = d_{ij}^{\star} - d_{ij}^{cd}$. On the other hand, we need to purchase enough gasoline at node i to cover the travel distance and retain $\bar{\lambda}$ gallons of gasoline at node j, i.e., $g_i^+ = (d_{ij}^{cs} \times \rho + \bar{\lambda} - \lambda)^+$ gallons of gasoline should be purchased at node i. Note that, by the feasibility condition, we make sure that the purchased gasoline is between the limits, i.e. $0 \leq g_i^+ \leq \overline{G} - \lambda$. Since the battery is not charged, only the gasoline cost, vehicle depreciation cost and stopping cost are included in the total cost function which is $f_2(\omega_i^{\sigma,\lambda}, \omega_j^{\bar{\sigma},\bar{\lambda}}) = c_i^g \times g_i^+ + c^{dep} \times d_{ij}^{\star} + c_i^{st}$.

- Case 3: Battery charging but no refueling.

  Feasibility Condition: A full battery charge and existing level of gasoline are jointly enough to travel from node i to node j while satisfying the end-state conditions, i.e.,

  $$s_i^e = 1, \lambda \geq \bar{\lambda} \text{ and } \frac{(\overline{P} - \bar{\sigma})}{\varepsilon} + \frac{(\lambda - \bar{\lambda})}{\rho} \geq d_{ij}^{\star}.$$

  Total Cost: With the analogous arguments presented for the previous case, we have $e_i^+ = (d_{ij}^{cd} \times \varepsilon + \bar{\sigma} - \sigma)^+$, where $d_{ij}^{cd} = d_{ij}^{\star} - d_{ij}^{cs}$ and $d_{ij}^{cs} = \min\{d_{ij}^{\star}, \frac{(\lambda-\bar{\lambda})}{\rho}\}$. We do not purchase gasoline in this case. The electricity cost, battery degradation cost, vehicle depreciation cost and stopping cost are included in the total cost. Thus the total cost is, $f_3(\omega_i^{\sigma,\lambda},\omega_j^{\bar{\sigma},\bar{\lambda}}) = c_i^e \times e_i^+ + c^{bat}(\frac{\overline{P}-\sigma}{\overline{P}}) + c^{dep} \times d_{ij}^{\star} + c_i^{st}$.

- Case 4: Both battery charging and refueling.

  Feasibility Condition: A full battery charge and a full tank of gasoline are enough to travel from node i to node j, while satisfying the end-state conditions, i.e.,

  $$s_i^e = 1, s_i^g = 1 \text{ and } \frac{(\overline{P}-\bar{\sigma})}{\varepsilon} + \frac{(\overline{G}-\bar{\lambda})}{\rho} \geq d_{ij}^{\star}.$$

  Total Cost: We define the *excess-distance* $\bar{d}_{ij} = (d_{ij}^{\star} - \frac{(\sigma-\bar{\sigma})^+}{\varepsilon} - \frac{(\lambda-\bar{\lambda})^+}{\rho})$ as the additional mileage that cannot be covered by the existing charge and fuel levels before charging or refueling at node i. Observe that depending on the cost of electricity and gasoline at node i, it is cheaper to drive on either CD or CS mode to cover $\bar{d}_{ij}$.

  - If CD mode is cheaper, i.e. $(c_i^e \times \varepsilon) < (c_i^g \times \rho)$, we check if a fully charged battery is enough to cover the required distance $\bar{d}_{ij}$, i.e. $(d_{ij}^{cd} + \bar{d}_{ij}) < \frac{\overline{P}-\bar{\sigma}}{\varepsilon}$. If so, we have $e_i^+ = \bar{d}_{ij} \times \varepsilon + (\bar{\sigma}-\sigma)^+$ and $g_i^+ = (\bar{\lambda}-\lambda)^+$. Otherwise, $e_i^+ = (\overline{P}-\sigma)$ and $g_i^+ = \big((d_{ij}^{\star} - \frac{\overline{P}-\bar{\sigma}}{\varepsilon}) \times \rho + \bar{\lambda} - \lambda\big)^+$.
  - If CS mode is cheaper, all the calculations to find e_i^+ and g_i^+ values are just symmetric to the ones presented above and here we skip the details for the sake of brevity.

  Once we find the electricity and gasoline amounts e_i^+, g_i^+, we can easily calculate the total cost $f_4(\omega_i^{\sigma,\lambda},\omega_j^{\bar{\sigma},\bar{\lambda}}) = c_i^e \times e_i^+ + c_i^g \times g_i^+ + c^{bat}(\frac{\overline{P}-\sigma}{\overline{P}}) + c^{dep} \times d_{ij}^{\star} + c_i^{st}$.

Considering all four cases, the minimum cost transition function is defined as:

$$f(\omega,\bar{\omega}) = \min_{i \in \{1,2,3,4\}} \{f_i(\omega,\bar{\omega})\} \tag{2.23}$$

The following Bellman's equations are based on the principle of optimality:

$$\pi(\omega_s^{P_s,G_s}) = 0 \tag{2.24}$$

$$\pi(\omega) = \min_{\bar{\omega}\in\Omega}\{\pi(\bar{\omega}) + f(\bar{\omega},\omega)\} \qquad \forall\omega\in\Omega \tag{2.25}$$

Definition 7. $\tilde{G} = (\Omega, \tilde{A})$ *is called the DH-Graph where the node set is the discrete state space* Ω*. The arc set* $\tilde{A}$ *includes an arc between states* ω_i *and* $\omega_j \in \Omega$ *with a cost of* $f(\omega_i, \omega_j)$ *if this cost is finite.*

Once the DH-Graph is obtained, solving the Bellman's equations, which is the core of the DH algorithm, reduces to solving the shortest path problem on $\tilde{G}$ from *state* $\omega_s^{P_s,G_s}$ to the *state* $\omega_t^{P_t,G_t}$. Observe that arcs on the shortest path contain the information where the PHEV stops for refueling/charging and how much electricity charge/gasoline to purchase at those stops. So obtaining the shortest path in $\tilde{G}$ is sufficient to obtain a solution for the E-MCPP-PHEV instance.

$\tilde{G}$ contains $|\Omega|$ nodes and the cardinality of the arc set $\tilde{A}$ is bounded by $|\Omega|^2$. Constant time calculation of the transition function f results in $O\big(|\Omega|^2\big)$ run time bound for the generation of the DH-Graph. Using Dijkstra's algorithm to find the shortest path in $\tilde{G}$, the overall run time complexity of DH becomes $O\big(|\Omega|^2\big)$.

2.2.4 Enhancing the DH Heuristic (DHE)

Due to the discrete approximation of the true levels of gasoline and electricity, DH might not always give the optimal solution in terms of refueling and battery charging amounts even if the optimal path is correctly identified. To that end, we provide the enhanced version of DH (DHE) in which we take into account the path that is given by the algorithm, but not the refueling and battery charging decisions. Instead, we consider the subgraph that consists of only the path nodes and the path arcs. Then, we solve the MCPP-PHEV model on this subgraph. Since the subgraph size is much smaller than the original graph, the solution times of the model formulation reduce drastically and we attain improved refueling and battery charging strategies.

2.2.5 Shortest Path Heuristic (SP)

Minimizing the operating cost on the shortest path is a commonly used solution technique to solve the minimum cost path problems in the literature. Since well known polynomial-time algorithms are available for finding shortest paths, such heuristics are also pervasive in industrial and commercial applications as well. In this context, we propose to solve MIQCP model considering the shortest path as the input graph and optimizing only the refueling and charging decisions.

2.3 Computational Study

To test the performances of the proposed solution methodologies and drive insights about the solutions, we conducted extensive numerical experiments using problem instances that represent various network structures and user behaviors. The experiments are carried out on a workstation with 2.66 GHz Xeon processor and 8 GB memory. We present the data and the results related to computational performances and several measures in the following parts. It is important to note that with several preliminary experimentations, we have observed that working with reduced meta-networks is satisfactory in capturing the non-simple paths that might arise in our instances and opted to using reduced meta-networks throughout our computational experiments.

2.3.1 Data

A 2013 Chevrolet Volt PHEV has the following specifications: 16.5 kWh battery capacity, 9.3 gallon tank capacity, 0.352 kWh per mile and 0.027 gallons per mile [187] usages. In order to avoid over-charging degradation, we assume 20% and 85% as the minimum and maximum battery charge levels respectively. Hence, the simulated vehicle has a hard bound of 14 kWh on capacity rather than 16.5 kWh. The battery cost of PHEV is assumed to be \$2650 and the cost function with respect to depth of discharge is $c^{dep}(\delta) = 79.517 \times \delta^2 + 37.854 \times \delta$, as presented in Figure 2.3. We also assume that the minimum tank capacity is zero and the depreciation cost is 1 ¢/mile. Five different stopping cost values are tested: 0, 50, 100, 200 and 500 ¢.

For the network instances, we consider square mesh shaped networks of node sizes 6x6, 7x7, 8x8, 9x9 and 10x10. We generate 10 instances of each size. Every node in a given network is connected with an arc to the next node on the right, left, top and bottom, if there is one. The source and destination nodes are the top left and bottom right nodes of the graph, respectively. The arc distances are random values uniformly distributed between 20 and 40 miles. This is to simulate the fact that real road networks distances between two points could be quite different from Euclidean distances in a plane due to elevation differences, geographical obstacles etc. A refueling station is located at every node and the gasoline prices are uniformly generated in \$3.5 and \$4.1 range. We assume that battery charging stations are located randomly at 0%, 25%, 50%, 75% and 100% of the total nodes and the electricity prices at charging stations change uniformly between 10 ¢ and 12 ¢. In total, we have 250 mesh shaped networks and 5 different stopping cost values, i.e. 1250 runs. For each set of parameters, we report the averages corresponding to 10 network instances.

It is clear that mesh networks cannot fully capture all the aspects of a real network. Our main motivation in using such networks is to be able to have an extensive problem set to conduct our numerical experiments. As a better approximation of the real world problem instances, we also consider California road network which will be elaborated in the following parts.

2.3.2 Performances of the Solution Techniques

We present the basic computational performance measures of the solution methodologies in Table 2.1. DH is solved with two different levels of approximation $\xi = \tau = 4$ and $\xi = \tau = 1$, which we refer to as DH4 and DH1, respectively. The percentage of the optimal solutions for DH4 (DH1) range in 46.8-54.0% (46.4-54.0%) for all instances, which is improved by the extended versions of the algorithms to around 89.6-96.8% (83.2-92.8%). An optimal path is found by DH4 (DH1) in around 84.4-94.8% (77.2-91.2%) of all the instances. Since a high percentage of the optimal solutions (ranging between 64.8-84.8%) coincide with the shortest paths, the SP heuristic also performs well in minimum cost path problems. DHE1 and SP have very similar run times and both can solve very large problem instances quite fast. However, emphasizing the merits of the proposed dynamic programming approximation, DHE1 performs at least as good as SP for the problem instances considered in this study.

We observe that the solution times for the MIQCP start getting prohibitive as the node number increases. Beyond 100 nodes, there exist problem instances with more than 60-minute solution times. On the other hand, observe that the average solution time of the DH1 is less than 0.028 seconds on all network sizes. In fact, the average runtime of DH1 for problem instances with 900 nodes is only 40.3 seconds which makes it the suitable solution technique for devices with limited computational capacity. However, since other solution techniques did not scale up to such dimensions, these results are not presented here.

One important fact to note is that the valid inequality greatly contributes to the solution times of the MIQCP. The average gap of the LP relaxation solution from the optimal solution with and without the cut is 24.89% and 90.02%, respectively. We also observe that optimal paths of DH4 (DH1) coincide with the shortest paths on the average 62.4-82.4% (58.0-81.2%) of the instances. On the average, the deviation from the shortest path changes in the range of 1.21-1.99% (2.34-5.55%) of the shortest path distance.

Table 2.1: Computational results

Node Number	Solution Technique	Opt. sol. found (%)	Avg opt. gap (%)	Opt. path found (%)	Is shortest path? (%)	Avg deviation from the shortest path (%)	CPU Seconds
6	MIQCP	100.0	0.000	100.0	79.2	0.364	1.828
	DH4	54.0	0.688	93.2	80.8	1.212	0.585
	DH1	54.0	1.410	90.4	78.8	2.344	0.004
	DHE4	95.2	0.009	93.2	80.8	1.212	1.532
	DHE1	92.0	0.031	90.4	78.8	2.344	0.928
	SP	79.2	0.424	79.2	100.0	0.000	0.858
7	MIQCP	100.0	0.000	100.0	84.8	0.382	2.947
	DH4	52.0	0.685	94.8	82.4	1.409	1.277
	DH1	52.0	1.499	91.2	81.2	3.030	0.005
	DHE4	96.8	0.004	94.8	82.4	1.409	2.327
	DHE1	92.8	0.044	91.2	81.2	3.030	1.060
	SP	84.8	0.399	84.8	100.0	0.000	1.002
8	MIQCP	100.0	0.000	100.0	69.6	0.350	8.696
	DH4	49.6	0.731	89.6	67.6	1.664	2.418
	DH1	49.6	1.539	84.0	64.0	5.044	0.010
	DHE4	92.8	0.027	89.6	67.6	1.664	3.581
	DHE1	86.8	0.058	84.0	64.0	5.044	1.173
	SP	69.6	0.562	69.6	100.0	0.000	1.030
9	MIQCP	100.0	0.000	100.0	75.2	0.337	33.105
	DH4	50.8	0.726	88.8	74.4	1.542	4.281
	DH1	50.4	1.627	82.8	70.8	3.593	0.017
	DHE4	91.6	0.030	88.8	74.4	1.542	5.579
	DHE1	87.2	0.069	82.8	70.8	3.593	1.325
	SP	75.2	0.404	75.2	100.0	0.000	1.196
10	MIQCP	100.0	0.000	100.0	64.8	0.473	184.848
	DH4	46.8	0.766	84.4	62.4	1.992	6.916
	DH1	46.4	1.683	77.2	58.0	5.554	0.028
	DHE4	89.6	0.023	84.4	62.4	1.992	8.284
	DHE1	83.2	0.058	77.2	58.0	5.554	1.359
	SP	64.8	0.646	64.8	100.0	0.000	1.231

2.3.3 California Road Network

In order to test the performances of the solution techniques in larger problems and validate the results that we obtained in the randomly generated mesh networks, we consider a real-world California road network [188]. After processing this network, we have 339 nodes and 1234 arcs as depicted in Figure 2.5. It is assumed that there is a refueling station located on every node, and the nodes on the highway also have charging stations. The gasoline prices and the electricity prices change uniformly in \$3.5 and \$4.1 range and 10 ¢ and 12 ¢ range, respectively. More waiting in the refueling/charging stations might significantly affect the driver tolerance for the stops hence change the stopping cost in our model. In order to take this factor into account and increase the realism of the problem instances we consider varying stopping costs for the California Road Network problem instances. Since larger cities inherently mean more time waiting to get a service, we associated stopping costs with population numbers. For the nodes with an urban population of 50,000 or less according to U.S. Census Bureau [189], the stopping cost is assumed to be 50 ¢. For those nodes with an urban population more than 50,000, the cost ranges between 50 ¢ and 500 ¢ in proportion with the population numbers. For these settings, we have obtained the minimum cost path and refueling/charging policies for each origin-destination pair between 10 randomly selected nodes as depicted in Figure 2.5.

The results of the average of 45 runs are presented in Table 2.2. For the MIQCP solutions, 27 of the 45 runs resulted in optimal solutions in 60-minute time limit. For the remaining 18 runs, the average optimality gap after 60 minutes was 19.69%. In the table, all the statistics are given with respect to the MIQCP results. This justifies the negative average gap of DHE4 solution.

Table 2.2: Computational results for California road network

Solution Technique	MIQCP sol. found (%)	Average gap (%)	MIQCP sol. path found (%)	Is shortest path? (%)	Avg deviation from the shortest path (%)	Solution Time (sec)
MIQCP	100.0	0.000	100.0	77.8	1.537	1684.612
DH4	13.3	1.672	97.8	80.0	1.517	289.142
DH1	13.3	2.314	82.2	77.8	14.858	0.867
DHE4	95.6	-0.010	97.8	80.0	1.517	291.179
DHE1	82.2	0.026	82.2	77.8	14.858	2.628
SP	77.8	0.272	77.8	100.0	0.000	1.684

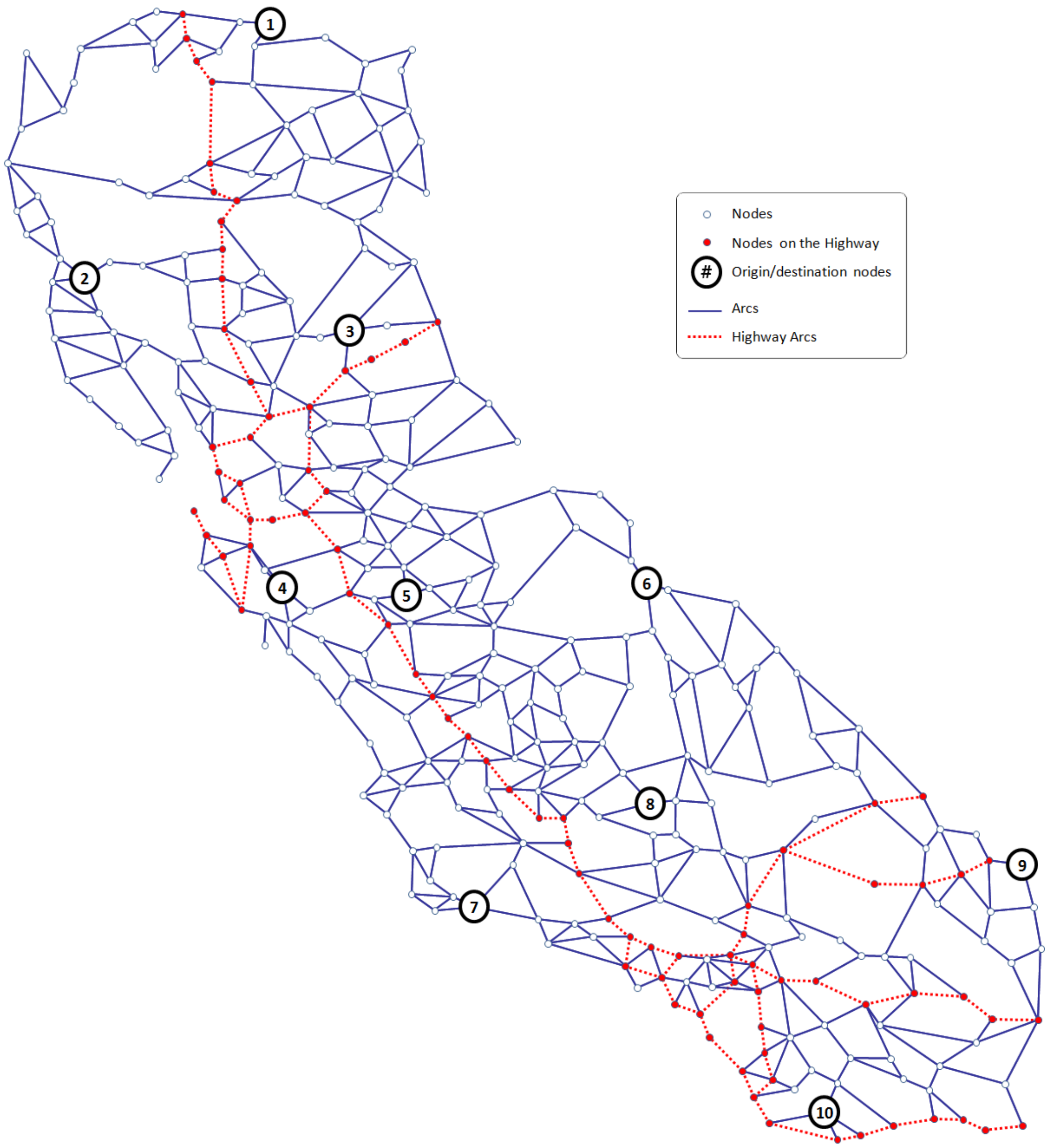

Figure 2.5: California network with 339 nodes and 1234 arcs

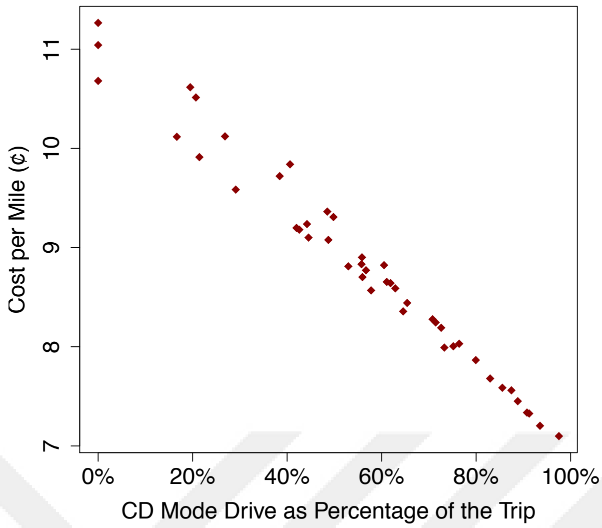

Figure 2.6: Cost per mile values for 45 run results in California dataset

Computational performances for the proposed solution techniques were essentially similar to the ones in the previous part. It is noteworthy that, from both the solution quality and the time perspectives, DHE1 and SP techniques perform reasonably well in these large problem instances. Not only the computational performances but also practical insights we derive in the mesh network cases remain intact. Figure 2.6 shows that the cost per mile values decrease with increasing CD mode travel percentage. This indicates that the results and insights discussed in this study are quite robust against the changes in the underlying network topology.

Figure 2.6 depicts an interesting plot which shows that for every additional 25% CD mode trip, approximately 1 cent per mile is saved. Even though this might not be a significant decrease for individual drivers, it is of great value from the fleet managers' and governments' perspective taking into account the 575 billion miles long-distance travels in a year [15].

2.4 Summary

In this chapter, we introduce the minimum cost path problem for plug-in hybrid electric vehicles. Urban (i.e. short distance) uses of PHEVs have been extensively investigated with all its expected benefits and shortcomings. However, such a comprehensive scientific treatment does not exist for the long-distance trips. As such, utilization of PHEVs in the long-distance transportation appears as an emerging trend in the logistics. The dual-energy source flexibility, however, begets theoretical challenges to solve the minimum cost path problem for PHEVs. In fact, we show that this problem is NP-complete even though there are polynomial time algorithms to solve its single energy source (electricity or gasoline) special cases. Fluctuations in fuel/electricity costs, battery degradation issues and scarcity of charging stations add further challenges to our problem. In our study, we propose exact and heuristic solution techniques to solve this challenging problem. From a practical point of view, our unifying approach reveals important results about the long-distance use of PHEVs both as personal vehicles and business assets.

We conduct extensive computational experiments to test the computational performance of the proposed solution methodologies. Computational studies show that the proposed MIQCP formulation can solve problems with realistic sizes. A dynamic programming based heuristic and a shortest path heuristic methodologies further extend the sizes of the solvable problems drastically and produce near optimal solutions.

Our results underline a significant advantage of PHEVs that they are quite flexible in their use of gasoline and electricity energy. When the cost of electricity is low compared to the gasoline prices, availability of charging infrastructure and driver tolerance for frequent refueling/charging stops is high, PHEVs increase the share of CD-mode drive which entails lower costs and higher environmental benefits. On the other hand, when these conditions are not met, PHEVs mainly operate in CS mode which enables them to still drive the long-distance trips but limits the realization of the potential cost and emission benefits. The contribution of our study is to present a way to quantify the touted benefits of PHEVs for different scenarios. Therefore, the MCPP-PHEV and the solution methods proposed in this study can be a very useful decision support tool for the personal vehicle owners who want to better understand PHEV economics, for the investors who want to asses the possible benefits of incorporating this new technology in their fleets and for the governments who want to better direct incentives to facilitate the transition from the fossil fuels to more economic, secure and environment friendly energy sources.

The methodologies that we present in this chapter are not only applicable for PHEVs, but also for all types of hybrid vehicles that run on two types of energy resources. Note that our solution methodologies naturally encompass single energy source alternative fuel vehicles such as electric and hydrogen. Our study reveals one strategic insight about all those alternative energy vehicles: In the literature, most of the studies related to alternative energy vehicles - EV and PHEV in particular - discuss the problem of availability of refueling and charging stations as a barrier to proliferation of those vehicles. However, the limited range of a non-fossil-fuel-energy drive not only brings the problem of finding charging stations on the route, but also results in frequent charging stops which may not be preferable for most of the drivers. Our study shows that this neglected problem can also be a significant barrier. These are significant results for both infrastructure investors and governments. Decision makers need to consider the drivers' tolerance for stopping and more research must be directed towards determining the utility functions of the drivers' willingness for making frequent stops.

In the following chapter, we further elaborate the impacts of battery characteristics, driver preferences and road network features on travel costs of a PHEV for long-distance trips and compare the results with a similar CV and HEV.

Chapter 3

Impacts of Battery, Driver and Road Characteristics on Long Distance Travel Costs of PHEVs [2]

3.1 Problem Definition

With its electric motor and charging capability, a PHEV offers unique opportunities to decrease the travel costs and GHG emissions. However, various parameters, such as battery characteristics, availability of charging stations and driver preferences affect the magnitude of these improvements. Analyzing the effects of these parameters for long-distance trips is the focal point of this chapter. In this regard, we do not consider the cost of setting up new fast charging stations, but concentrate on the long-distance travel costs of PHEVs that require refueling and/or charging. Note that inclusion of infrastructure costs might affect the results for the charging station case as shown by Neubauer and Pesaran [191].

[2] An extended version of this chapter is authored by Okan Arslan, Barış Yıldız and Oya Ekin Karaşan and is published in Energy Policy, 74:168 178, 2014 [190].

Because of the basic differences between PHEVs, HEVs and CVs, trip characteristics of these vehicles can be quite different. For a simple example, consider a PHEV and a CV traveling between the same departure and destination points. Assume that the shortest path between these points has several refueling stations but no fast charging station and there is an alternative path, only a few miles longer than the shortest path with several fast charging stations. Obviously, the CV prefers to travel on the shortest path to minimize travel costs. On the other hand, assuming price advantage of electricity over the gasoline as a source of energy, the PHEV travels on the longer path for much less travel cost than that of CV. Even if PHEV and CV follow the same path, it is possible that PHEV adheres to a different refueling/charging policy to minimize travel costs. As a result, depending solely on the CV travel data might not be sufficient to derive policy conclusions. In this chapter, we address this issue by simulating long-distance trips in a transportation network with refueling and fast charging stations for drivers with different stopping and distance tolerances.

Widespread deployment of fast charging stations are being offered as a possible remedy for driver's range anxiety. Some research, including Romm [35] and Wang and Lin [87], argue that a limited number of refueling/fast charging stations is a barrier to the proliferation of alternative fuel vehicles. However, a prevalence of fast charging stations might not solely overcome this concern. Because a PHEV may only travel a limited mileage in CD mode, it requires frequent stops when traveling long distances to remain in CD mode. The driver, however, might be reluctant to stop so often. Therefore, the tolerance of the driver for stopping, which we refer to as *stopping tolerance*, is also a key parameter in PHEV travel costs. Similarly, driver's tolerance for longer distances, which we refer to as *distance tolerance*, is another factor that affects PHEV travel costs. If the driver is intolerant for longer trips, then he/she might not accept to deviate from the shortest path to visit a fast charging station and take advantage of the price difference. As a result, PHEV travel costs would be adversely affected by the distance intolerance. Therefore, analyzing PHEV travel costs should be viewed wholistically, taking into account battery characteristics as well as driver preferences, and the location and availability of refueling/fast charging stations. Different than the existing literature, we consider the driver and network aspects of the problem when conducting economics analyses and analyze the path that a PHEV may prefer to take, which may be different than that of a CV. We also consider battery degradation in the analyses, which proves to be a significant component of the overall cost of a PHEV trip due to rather limited lifespan of a typical battery. In this context, we analyze long-distance travel costs of PHEVs in terms of real-world dynamics on three groups of independent factors: battery characteristics, driver preferences and road network features. We investigate the interactions of these factors, and rank the contribution of each level of these factors to the total cost. This analysis provides critical managerial insights which are extremely relevant in shaping future investment decisions about PHEVs and their infrastructure. Ultimately, the findings of this paper hold imperative information for policy makers, governments and investors who would like to fully exploit the opportunities offered by the game changing PHEV technology.

3.2 Material and methods

We consider a long-range trip between a departure and a destination point in a road network with refueling and fast charging stations. We use the road network of California as the network instance and model long-distance trips between urban population clusters on this real world example. We utilize the dynamic programming heuristic solution methodology for solving the Minimum Cost Path Problem for PHEV (MCPP-PHEV) as presented in Chapter 2 to simulate trips for various types of drivers with different stopping and distance tolerances. In the following, we present the basic information related to this methodology and discuss the data and parameter settings pertinent to the analysis.

3.2.1 Data

We compare six different vehicle types: a CV, an HEV and four different PHEVs with all-electric range (AER) of 7, 20, 40 and 60 miles. The data pertaining to the vehicles is depicted in Table 3.1. The battery capacities, electricity and gasoline usage data are as obtained by [118] using the U.S. Department of Energy PSAT Vehicle Physics Simulator. The data accounts for the decreasing efficiency for additional weight due to battery and its structural support. The AER ranges of 7 to 60 miles span the current PHEV types that are available in the market at the time of this research, such as Toyota Prius and Chevrolet Volt.

Table 3.1: Vehicle types and specifications

Vehicle Type	Tank Capacity (gallons)	Battery Capacity (kWh)	Gasoline Usage (gal/mile)	Electricity Usage (kWh/mile)
CV	11.9	N/A	0.0353	N/A
HEV	11.9	N/A	0.0193	N/A
PHEV7	10.6	3.0	0.0194	0.179
PHEV20	10.6	8.2	0.02	0.183
PHEV40	10.6	16.8	0.0204	0.188
PHEV60	10.6	26.4	0.0209	0.197

3.2.2 Road Network Features

For the network instance, we use the California road network shown in Figure 3.1 [192] representing the transportation network of California with 1046 nodes and 3312 arcs.

A refueling station is located at every node in the network, and the gasoline price at any station is assumed to be a random value between a minimum and maximum level. As an experimental factor, we investigate two scenarios:

- In the base case, the minimum and maximum prices for the gasoline are

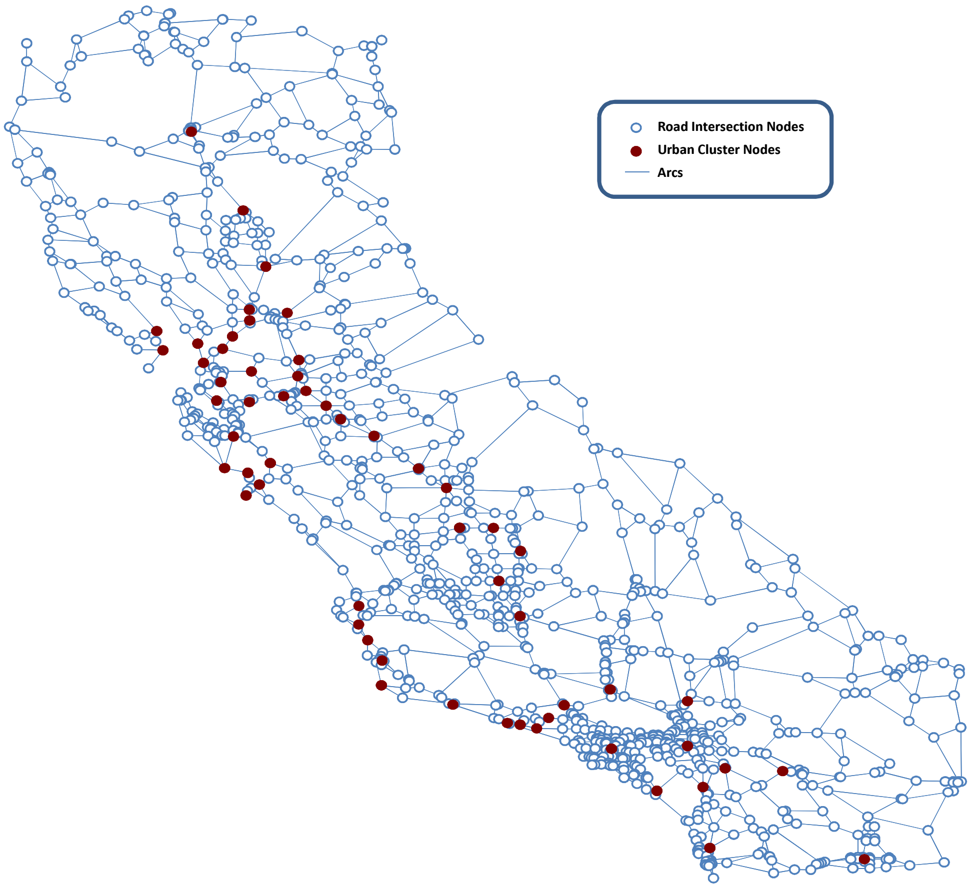

Figure 3.1: California road data with 1046 nodes and 3312 arcs

$3.21 and $4.07, respectively. This is the national average gasoline pricing range for a given day in 2014 [193].

- For the low gasoline pricing range, the minimum and maximum prices are $1.61 and $2.04, respectively. These are the figures for November 2008 [193].

Fast charging stations are located randomly at 0%, 25%, 50%, 75% and 100% of the network nodes. We refer to these percentages as ‘deployment levels’. Similar to the gasoline prices, we model electricity pricing with two scenarios:

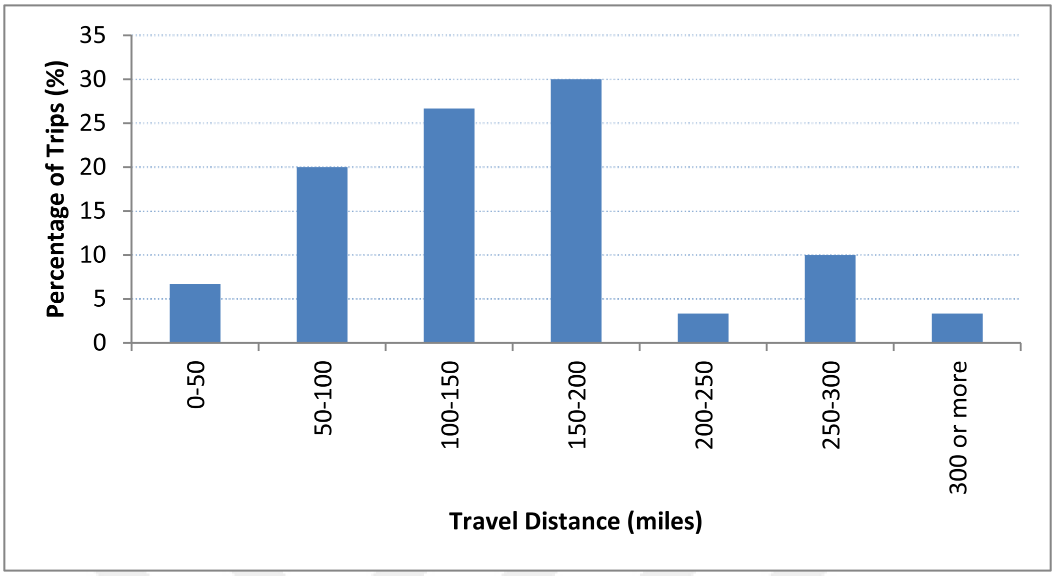

Figure 3.2: Travel distance distribution

- In the base case, the minimum and maximum prices for the electricity are 11.47¢ and 12.61¢, respectively [194].
- For the high electricity pricing range, the base case prices are doubled with minimum and maximum prices of 22.94¢ and 25.22¢, respectively.

There are 57 urban clusters in California with 50,000 or more population count [189] as shown in Figure 3.1. 1345 of the 1596 possible origin-destination pairs between these 57 urban clusters are 60 or more miles apart from each other. For our analyses, we randomly choose 30 trips and simulate each trip with all 6 vehicle types considered in this study. The total travel distance distribution is depicted in Figure 3.2.

3.2.3 Driver Preferences

A PHEV driver is characterized with two parameters: stopping tolerance and distance tolerance. Stopping tolerance represents the monetary value for the inconvenience of refueling/charging stops. Thus, a lower stopping tolerance value implies a higher tolerance for stopping and vice versa. In our simulations, we study stopping tolerance values between 0¢ and 500¢. The rationale behind these levels is as follows: Consider a PHEV60 that requires the least number of stops among PHEVs considered in this study. PHEV60 can travel 507 miles on CS mode with only one refueling stop. On the other hand, the same vehicle needs to stop 9 times in order to travel the same mileage on CD mode. The travel cost of CS mode trip is at most 4314¢ when the gasoline price is assumed to be $4.07 (highest possible value) in all refueling stations. Similarly, the travel cost of CD mode trip is at least 1146¢. Thus, when the stopping cost is above 396¢, it is never profitable to drive on CD mode because the sum of the 9 stopping tolerance values and the cost of electricity exceeds the sum of the gasoline cost and one stopping tolerance value. This limiting value for stopping tolerance changes between 40¢ and 396¢ for the PHEVs considered in this study. Note that stopping tolerance is a measure of the inconvenience to the driver. Thus it can even be zero for some drivers. But when it is above 396¢, gasoline is always preferable, and CS mode drive is always cheaper than CD mode drive. In order to take into account drivers' varying tolerances towards stopping, we consider a wide range of 0¢ (high tolerance) to 500¢ (low tolerance) values with increments of 100¢ in our experimental design. Note that the tolerance levels in parentheses and the tolerance values have an inverse relation. Assuming a refueling or charging time of 10-40 minutes [195], 0-500¢ stopping cost value translates to an inconvenience cost of $0-$30 per hour.

The second parameter is the distance tolerance which is the monetary value of the inconvenience due to each mile traveled. Lower distance tolerance value implies a higher tolerance for longer trips. We consider a wide range from 0¢ to 50¢ distance tolerance values in our experimental design. For an average speed of

60 miles per hour, this translates to an inconvenience cost of \$0 to \$30 for an hour of driving. Note that when the distance tolerance is above a certain level, the cost of deviating from the shortest path gets so high that vehicles never detour from the shortest path.

3.2.4 Battery Characteristics

Battery capacity is an implicit experimental factor in our study. For the PHEV types considered in this study, battery capacities are 3.0, 8.2, 16.8 and 26.4 kWh as shown in Table 3.1. The battery cost is also an experimental factor. The battery costs in 2012 are around \$500 per kWh and the Department of Energy set battery cost targets of \$300 per kWh in 2015 and \$125 per kWh by 2022 for its sponsored research program [196]. For this reason, we consider \$125/kWh, \$300/kWh and \$500/kWh in the experiments.

A PHEV battery has a limited lifespan, and its life shortens at each cycle. It deteriorates through usage and incurs a *battery degradation cost* for each battery charge/discharge cycle. Even though it is an implicit cost, the vehicle owner still needs to bear this cost when replacing his/her battery or when buying/selling the vehicle. We assume that the costs are calculated by smart navigation devices that are widely available for drivers. Hence, the algorithms embedded in the devices take into account these implicit costs and save the battery life. This, in turn, minimizes the cost that a driver has to bear. In our study, we assume that a PHEV owner incurs a battery degradation cost depending on the DoD level upon arrival at a fast charging station. According to theoretical studies, the number of cycles is a nonlinear function of depth of discharge (DoD) [177, 184, 185]. We can determine this cost by evaluating a quadratic function of DoD which depends on the battery cost. A sample cost function for a PHEV40 vehicle with \$300/kWh battery pricing is depicted in Figure 3.3. The DoD is relative to the usable capacity. Thus, a DoD value of 1 implies that the battery is completely depleted, and a value of 0 implies that the battery is at the highest level of its usable capacity. The quadratic cost function is $c^{bat}(\delta) = 151.23 \times \delta^2 + 71.995 \times \delta$ where δ is DoD and $c^{bat}(\delta)$ is the battery degradation cost. On the other hand, [197] report that the real world data shows a linear change of battery life for different DoDs as depicted in the same figure. Linear cost function is $c^{bat}(\delta) = 219.13 \times \delta$. In this study, we investigated the results for both linear and quadratic modeling techniques.

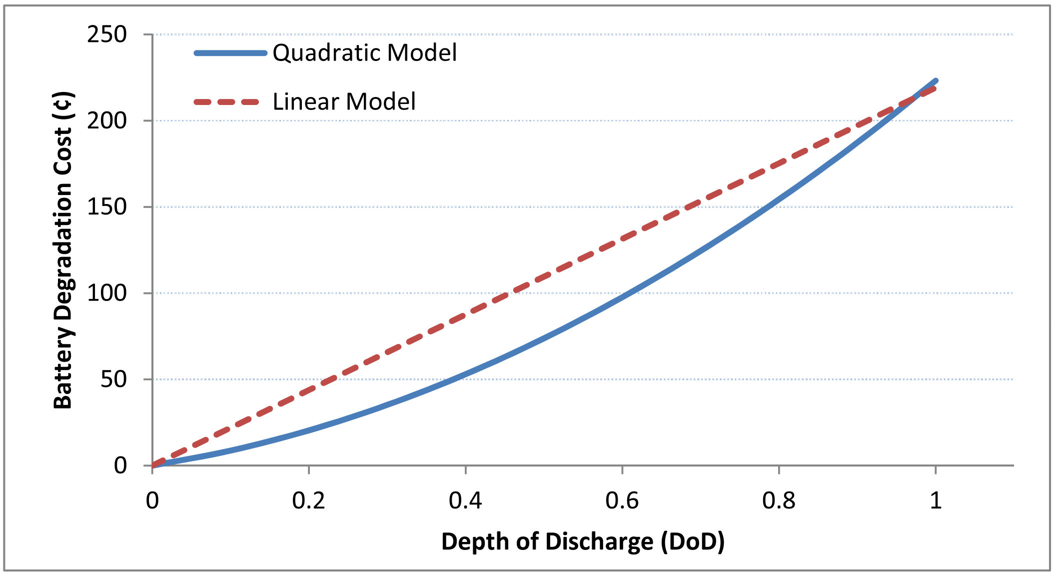

Figure 3.3: Quadratic and linear battery degradation cost functions for different DoD values

3.2.5 Experimental Design

We define a travel simulation as a trip between an origin-destination pair for a specific vehicle type, battery cost, battery modeling technique, stopping and distance tolerance levels, gasoline and electricity pricing levels and fast charging station deployment level in the road network. 30 origin-destination pairs, 6 vehicle types, 5 deployment levels, 3 battery costs, 2 battery modeling techniques, 6 stopping tolerance levels, 5 distance tolerance levels, 2 gasoline pricing levels and 2 electricity pricing levels are considered in this study. In total, there are eight factors with different levels in the experiments (as depicted in Table 3.2), and the total number of trips that are simulated in our experiments is 648,000.

Table 3.2: Experimental factors and their levels to measure the impacts on PHEV travel costs

Experimental Factor	Factor Levels
Vehicle Types	{CV, HEV, PHEV7, PHEV20, PHEV40, PHEV60}
Battery Cost ($/kWh)	{125, 300, 500}
Stopping Tolerance (¢)	{0, 100, 200, 300, 400, 500}
Distance Tolerance (¢)	{0, 5, 10, 20, 50}
Deployment Level (%)	{0, 25, 50, 75, 100}
Gasoline Prices ($)	{(1.61-2.04) (low), (3.21-4.07) (high)}
Electricity Prices (¢)	{(11.47-12.61) (low), (22.94-25.22) (high)}
Battery Degradation Model	{linear, quadratic}

Base case for battery cost is assumed to be $300/kWh. For the tolerance values, we assume that the base case values are zero in order to observe the effects more clearly. With a similar reasoning, the base case for the deployment level is assumed to be 100%. We conducted all the simulation runs on a 4x16C AMD opteron with 96 GB RAM. IBM ILOG CPLEX Optimization Studio 12.4 was used to solve the models. We present the data and the results in the following section.

3.2.6 Cost Metrics

The objective function of the MCPP-PHEV model includes electricity cost, gasoline cost, battery degradation cost, distance tolerance cost and stopping tolerance cost. Observe that the tolerances are parameters to model driver preferences and they do not correspond to an actual cost. For this reason, when comparing a PHEV with an HEV or a CV, we need to compare the actual cost of travel, which excludes the tolerance costs. Hence, we use the cost of electricity, gasoline and battery degradation as cost components for comparison. Furthermore, we use distance-normalized cost values to compare trips with different lengths. Consequently, we refer to the sum of electricity, gasoline and battery degradation cost components per mile as the 'levelized cost per mile' (LCPM) [198]. We define LCPM as:

$$LCPM = c^e \times e^+ + c^g \times g^+ + c^{bat}$$

where c^e is the electricity pricing (¢/kWh), e^+ is the electricity purchase (kWh), c^g is the gasoline pricing (¢/gallon), g^+ is the gasoline purchase (gallons) and c^{bat} is the degradation cost of the PHEV battery corresponding to the electricity load of e^+.

3.3 Results and Discussion

In this section, we present the results with respect to two metrics: distance and LCPM. Initially, we study the driver's path preferences, that is, the driving patterns, and analyze differences with respect to the shortest path. Secondly, we investigate the impacts of factors affecting the LCPM individually and carry out an in-depth analysis on the factors that are identified as significant. Lastly, we put forward the relative impacts of each level of the experimental factors and provide strategic managerial insights.

3.3.1 Driving Pattern Analysis

If refueling and/or charging is not considered in a trip, then the shortest path between two points is the minimum-cost path for a vehicle. However, the driver has the opportunity to reduce travel costs by refueling and/or charging at stations off the shortest path. Out of the 648,000 travel simulations carried out in our experiments, 2.49% of drivers prefer traveling on paths that were not the shortest. The average deviation from the shortest paths is 2.4%. The extra distance traveled depends on driver preferences and network features.

Table 3.3: Average deviation from the shortest paths versus deployment level for different stopping tolerances

	0%	**25%**	**50%**	**75%**	**100%**
CV	2.02	2.02	2.02	2.02	2.02
HEV	2.02	2.02	2.02	2.02	2.02
PHEV7	2.02	3.32	2.37	1.98	1.45
PHEV20	2.02	2.48	1.49	1.23	1.12
PHEV40	2.02	2.81	2.15	1.63	1.15
PHEV60	2.02	2.48	4.04	0.51	0.32

As shown in Table 3.3, the deviation from the shortest path for a CV and an HEV is not affected by the deployment level of the fast charging stations. Similarly, the deviation is fixed for all vehicle types when the deployment level is zero, as expected. For PHEVs, however, the deviation is highest when the deployment level reaches 25-50% since fast charging stations are sparse in the network. Therefore, PHEVs detour from the shortest paths more often to reach those stations in order to travel on cost effective CD mode. Observe that the average deviation from the shortest path decreases by increasing deployment level beyond 50% because fast charging stations are encountered on the shortest paths more often.

In the experimental results, all the vehicle types follow the shortest path regardless of the deployment level when the stopping tolerance is above 200¢. A recent study by Perk et al. [199] reports that the value of travel time might get well above the range of the tolerance values considered in this study. But, increasing the stopping tolerance above 200¢ only implies that the vehicles will follow the shortest path and the LCPM values will stay the same.

Even though the deviation changes with respect to different deployment levels, the average deviation from the shortest paths is not significant. This is due to the fact that longer trips require more fuel and/or electricity consumption. Since the travel cost is minimized, the detour from the shortest paths is not a high percentage of the total travel distance.

3.3.2 Levelized Cost Per Mile (LCPM) Component Breakdown

Figure 3.4 plots LCPM for different fast charging station deployment levels. The LCPM of CV is 11.93¢ (not shown in the graph), and it does not change by deployment level since a CV travels solely on gasoline. When there are no fast charging stations in the network (i.e. zero deployment level), the LCPM values of PHEVs are higher than those of an HEV. The reason is the decreased fuel efficiency of PHEVs due to heavier weights. After the initial deployment of fast charging stations, PHEVs start to benefit from CD mode travel and there is a gradual decrease of LCPM with increasing deployment level. The most significant decrease is for PHEV40 among the PHEVs considered in this study. This interesting result shows that after a certain minimum AER is reached, PHEVs with lower battery capacities start to perform better in terms of total travel costs.

Figure 3.5 depicts the breakdown of LCPM components for all vehicle types. The LCPM of a CV is 11.93¢. The LCPM of a HEV almost halves the cost with 6.52¢. For the PHEVs, the LCPM gradually decreases with increasing AER, but observe that the decrease in cost is not significant among PHEV types. Again, PHEV40 gives the least cost. Note also that the percentage of the degradation cost is notable among the other cost components.

Figure 3.6 plots CD mode travel percentage for PHEVs. Observe that the higher the capacity of the PHEV is, the more the CD mode drive is. This is the result of increased battery capacity.

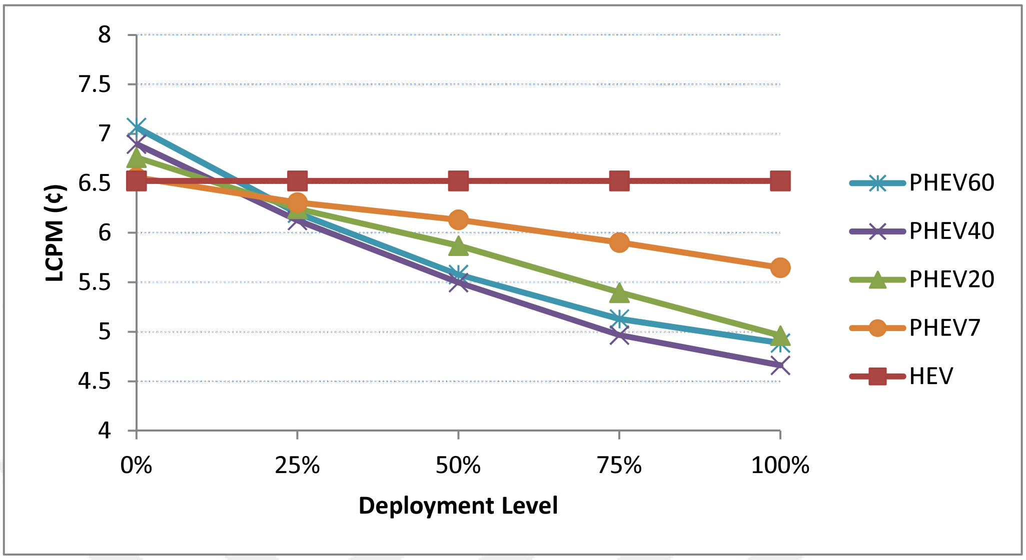

Figure 3.4: Levelized cost per mile change with increasing deployment levels

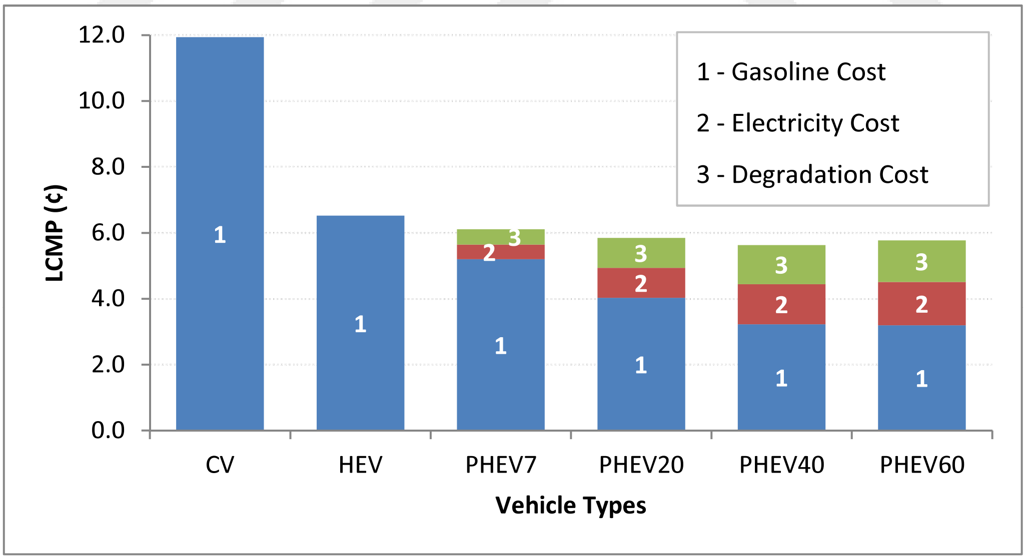

Figure 3.5: Breakdown of LCPM components for different vehicle types

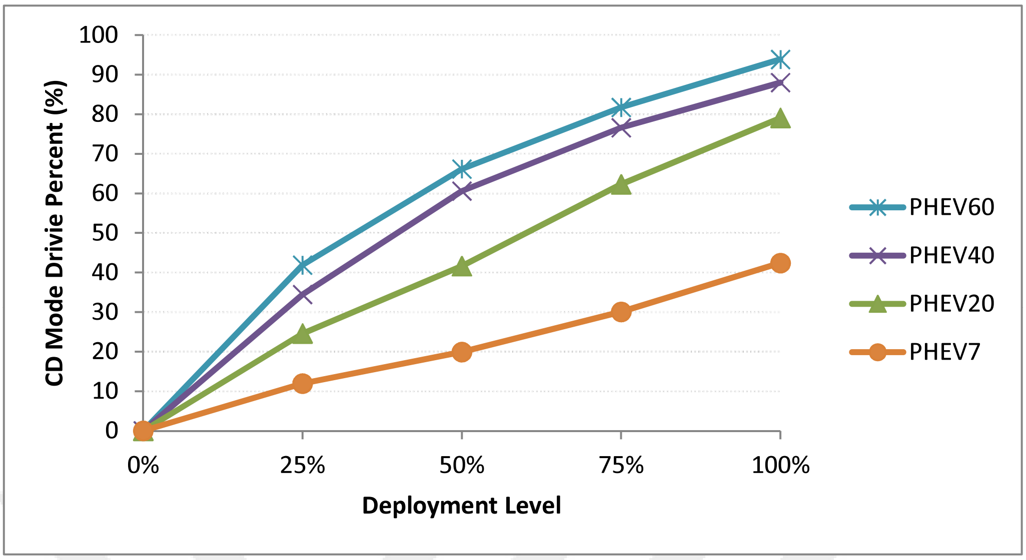

Figure 3.6: CD and CS mode drive percentages versus deployment level

3.3.3 Effects of Experimental Factors on LCPM

The correlation between each experimental factor and the LCPM is used as a way to understand the significance of the impacts on the LCPM. Spearman's Rank Correlation Coefficients [200] between the experimental factors and the LCPM are presented in Figure 3.7.

A negative value indicates an inverse relationship. Observe that LCPM decreases by increasing stopping tolerance or deployment level, and by decreasing gasoline prices, battery costs and electricity prices. The distance tolerance has insignificant effect on LCPM which is due to the fact that the extra mileage requires more gasoline or electricity to be consumed, ultimately increasing the total cost. Increasing the distance tolerance only results in forcing the drivers to follow the shortest paths. As we have observed previously, the total trip distances of a PHEV and CV are very close to each other, and distance tolerance turns out to have an insignificant effect on LCPM.

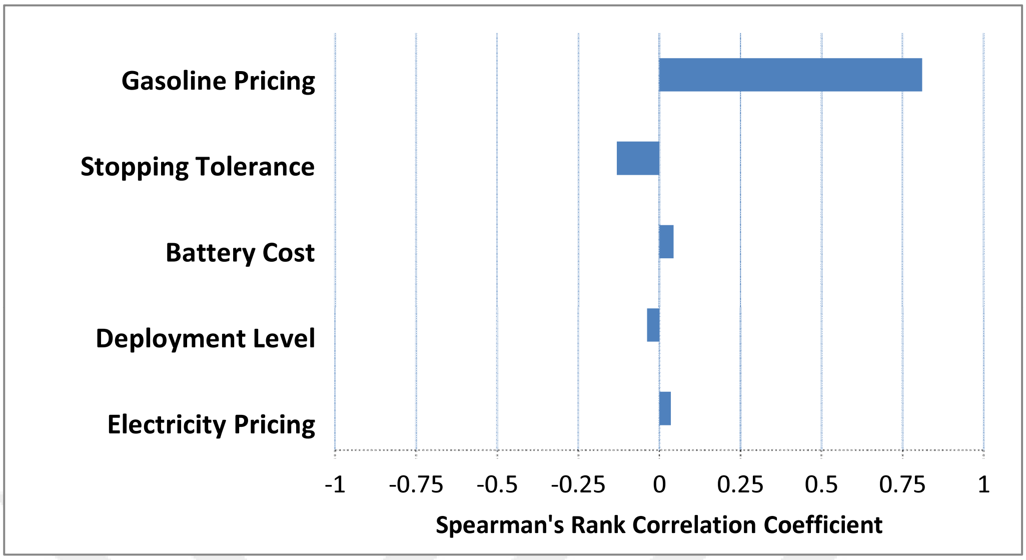

Figure 3.7: Spearman's rank correlation coefficients between each experimental factor and LCPM

Another result is that the battery modeling method, whether linear or quadratic, does not affect the results. In other words, the results for each battery model are not statistically different. This is mainly due to limited AER. The PHEV usually depletes the battery fully before charging again. Thus, the function, whether linear or quadratic, gives a close cost value when evaluated at $\delta = 1$ (i.e. when the battery is completely depleted).

In the following, we further investigate the factors that have significant correlation with LCPM.

3.3.4 Stopping Tolerance and Deployment Level Sensitivity

The impacts of stopping tolerance for the two extreme cases, 0% and 100% deployment levels, are depicted in Figure 3.8. Each curve in the subfigures corresponds to a different vehicle type. On the horizontal axis, higher stopping tolerance values imply less tolerance for stopping.

Consider 0% deployment level. Increasing the stopping tolerance value results in increased LCPM, because the drivers make less number of stops to refuel. Note that the vehicles do not benefit from CD mode trip at 0% deployment level. The LCPM for PHEV60 is the highest when the deployment level is 0%. The decreased efficiency due to additional battery weight is the reason for higher costs. When the deployment level increases to 100%, the LCPM for PHEV60 is the lowest for all stopping tolerance values except zero value. Observe that the LCPM is not changing above a certain tolerance value for all vehicle types for 100% deployment level. This is due to the preference change of the drivers with increasing stopping tolerance value. Thus, there is a critical stopping tolerance at which the driver starts preferring to drive on gasoline rather than electricity; identifying this tolerance correctly is crucial for infrastructure investors. Observe that increasing the deployment level has a positive effect on LCPM, but high stopping tolerance values may hamper this positive impact.

Recall that previously, we had identified PHEV40 as the alternative with the least travel cost for the base case (i.e. when the stopping tolerance value is zero). However, we observe now that PHEV40 is the best alternative for long-distance travels for highly tolerant vehicle drivers. If the driver's intolerance is above zero level, then PHEV60 turns out to be the best alternative from the cost minimization perspective. This is an important result showing that stopping tolerance is a key factor in long-distance travel costs.

Also note that the critical stopping tolerance value is higher for high capacity

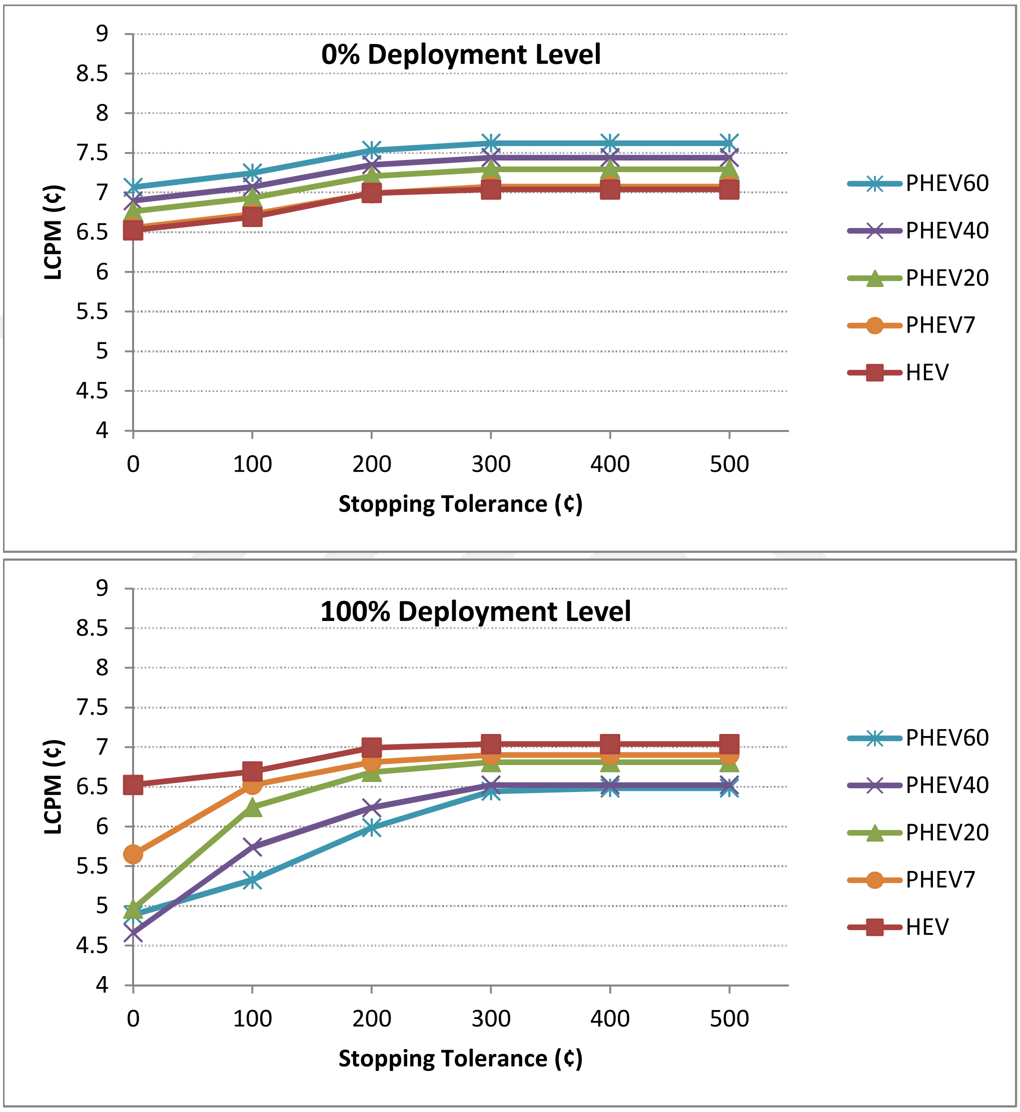

Figure 3.8: Stopping tolerance versus LCPM for 0% and 100% deployment levels

PHEVs. PHEV7 has a fixed LCPM above 200¢ stopping tolerance values, however the critical value is 300¢ for PHEV60. This implies that the higher the mileage that a PHEV can travel nonstop with its fully charged battery, the less the adverse affect of driver stopping intolerance.

3.3.5 Electricity and Gasoline Price Sensitivity

LCPM values for different electricity and gasoline price settings are given in Table 3.4. The low and high price settings for electricity are (11.47¢-12.61¢) and (22.94¢-25.22¢). Similarly, the high and low settings for gasoline are ($3.21-$4.07) and ($1.61-$2.04), respectively.

Table 3.4: Levelized cost per mile for different price settings

	(Electricity & Gasoline) Prices			
	(low & low)	(high & low)	(low & high)	(high & high)
CV	5.98	5.98	11.93	11.93
HEV	3.27	3.27	6.52	6.52
PHEV7	3.29	3.29	5.65	6.45
PHEV20	3.39	3.39	4.96	6.49
PHEV40	3.46	3.46	4.66	6.57
PHEV60	3.54	3.54	4.89	6.85

Observe that for the low gasoline price setting, i.e. the (low & low) and (high & low) columns in Table 3.4, the LCPMs are the same for both low and high electricity price settings. This clearly indicates that when the gasoline prices are low enough, it is always preferable for the drivers to travel using gasoline rather than electricity in order to minimize the costs. Similar results are also obtained in the literature [118]. When the gasoline price setting is high, PHEV7 performs the best when the electricity price is also high. When electricity price is low, larger capacity PHEVs incur less cost and PHEV40 performs the best.

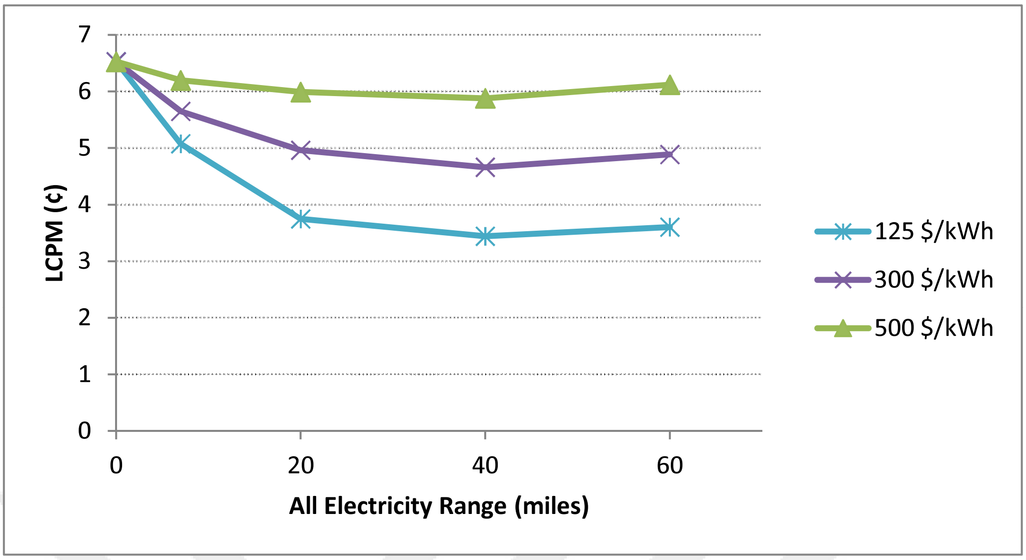

Figure 3.9: Battery Cost Impacts on LCPM

3.3.6 Battery cost impacts on LCPM

Each curve in Figure 3.9 represents a different battery cost. Note that zero AER vehicle is HEV, and the other data points in the figure represent PHEVs with the respective AER.

Observe that all curves follow a similar trend. When the AER increases from 0 to 20 miles, the LCPM reduces more steeply than when AER increases from 20 to 60 miles. Increasing the AER from 20 to 60 miles has little effect on levelized cost regardless of battery cost. Again, PHEV40 performs the best for different battery costs.

3.3.7 Environmental Impacts

One of the major benefits of PHEVs is their lower GHG emissions compared to CVs. In this section, we analyze the impacts of deployment level of fast charging stations on GHG emissions. In this study, we assume 11.34 kg of carbon dioxide equivalent (CO_2e) emission per gallon of gasoline and 0.730 kg of CO_2e emission per kWh of electricity charge [118]. For the gasoline emission data, combustion and supply chain emissions are taken into account. For the electricity emission data, generation at the power plant, transmission and distribution losses are considered. The included GHG emissions are for vehicle operation. We do not consider the emissions due to producing the batteries in this study. Figure 3.10 plots the total CO_2e emission of vehicle types per mile in grams for different deployment levels. A CV produces 40 grams of CO_2e per mile of travel. On the other hand, the other vehicle types produce at most 23.7 grams of CO_2e per mile, mainly due to increased efficiency. Deployment level also causes a decrease in emission per mile due to CD mode travel increase.

Note that in Table 3.4, the electricity pricing does not have a significant impact on the LCPM values. Similarly, the emissions are not affected significantly by the electricity prices. However, gasoline pricing has a significant effect on the emissions. Figure 3.11 plots the CO_2e emissions for low and high gasoline price settings. When the gasoline prices are high, the drivers prefer to drive more on CD mode and the emission decreases in the range of 17% to 36% for the PHEVs.

3.3.8 Discussion

The results of our extensive simulations provide critical insights into travel costs of PHEVs in long-distance trips. First of all, results show that driving patterns are affected by the driver preferences and the network features. The path difference between a CV, an HEV and a PHEV is the largest when the deployment level is

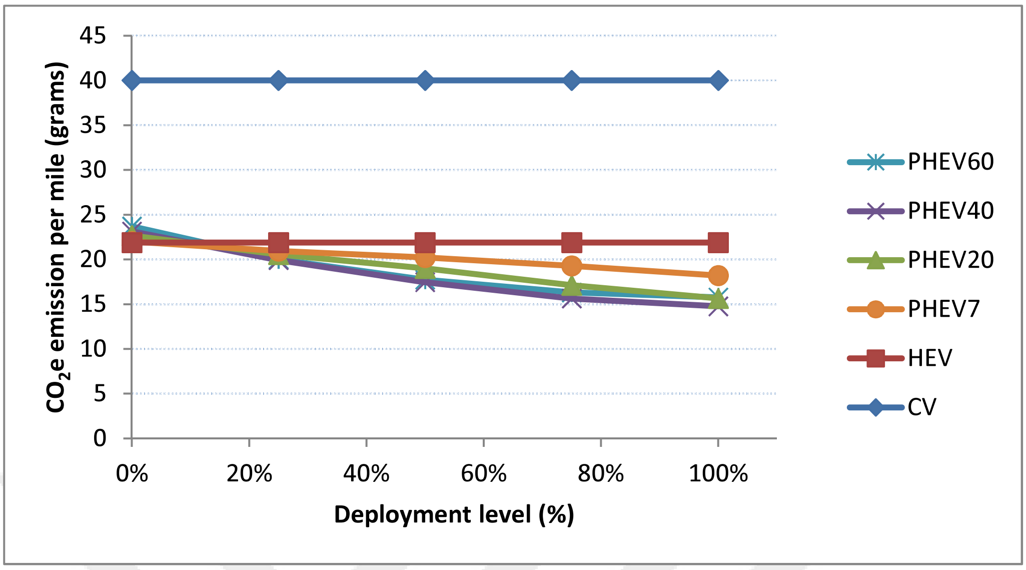

Figure 3.10: CO_2e Emissions per mile for vehicle types and different deployment levels

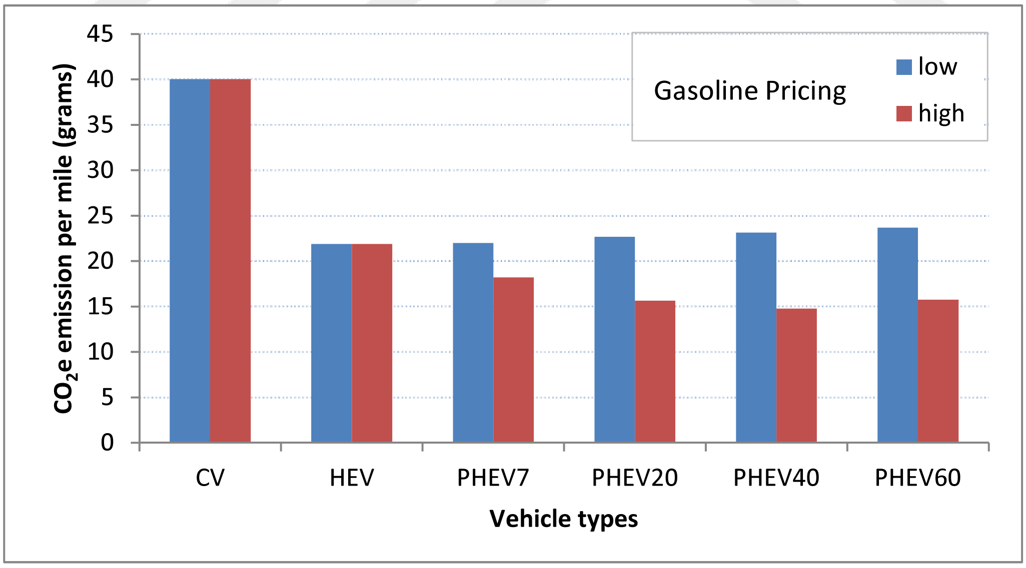

Figure 3.11: CO_2e emissions per mile for vehicle types and gasoline price settings

between 25-50%.

Results also show a gradual decrease of LCPM with increasing deployment level. This is an intuitive result since cost benefit of a PHEV is mainly due to the CD mode travel and high figures for the deployment level enable more CD mode travel for all PHEVs with different AERs. We also observe that the deployment level of fast charging stations needed for a PHEV to be a better alternative than an HEV in terms of long-distance travel costs is between 0% and 25%.

The battery degradation cost proves to be a significant contributer of the LCPM, especially for the PHEVs with longer AER. Numerical experiments also show that there is not a significant difference between the quadratic and linear battery models investigated in this study.

One of the major findings of this study is the strong connection between the stopping tolerance of the driver and the LCPM of a PHEV trip. Stopping intolerance hampers the benefits of PHEVs even for high deployment levels of fast charging stations. However, higher AER is effective to alleviate the adverse effects of low stopping tolerance. Results also show that there is a critical stopping tolerance at which drivers start driving on gasoline rather than electricity, and identifying this tolerance is crucial to make better infrastructure investment decisions. On the other hand, distance tolerance does not play such an important role in long-distance travel costs. Finally, note that the impact of both stopping tolerance and distance tolerance might be related to each other by value of time.

In this research, the results are obtained under some mild assumptions about the road networks. We assume that fast charging stations are randomly dispersed in the road network. This is a future research direction and location models can be combined together with models used in this study to arrive at more accurate results.

3.4 Policy Implications

The benefits of PHEVs for short trips are often touted, but their potential benefits for long distance trips have not attracted much attention. U.S. Department of Transportation [15] reports that in 2009, more than 575 billion vehicle miles were traveled in trips of 50 miles and over, by personally owned vehicles. If only 10% of these vehicles were PHEVs and only an average cost reduction of 2.5¢ per mile were achieved, 1.44 billion dollars could be saved annually.

This chapter highlights the importance of charging infrastructure on the travel costs of a PHEV for long-distance trips and reveals several important factors, especially driver stopping tolerance and AER. In this regard, the deployment level of charging stations should further be pinpointed for better input to policy decisions. Furthermore, the importance of consumers' stopping tolerance is another policy takeaway; identifying the drivers' actual willingness to stop is an important factor to determine the real world impacts of PHEVs for long distance driving.

In this context, we analyze the impacts of battery characteristics, driver preferences and road network features on PHEV long-distance-travel costs. The existing literature usually assumes exogenous driving profiles and builds models on this strong assumption. However, a PHEV is different from a CV and it might follow different paths between the same departure and destination points in order to reduce its travel costs. The travel cost of a PHEV is affected by factors such as location and availability of refueling/fast charging stations, capacity and cost of PHEV batteries and driver tolerance for extra mileage and additional stopping. If infrastructure is not set up to offer a widespread network of battery charging opportunities, or managerial decisions are made without taking into consideration driver preferences, then drivers' cost reduction expectations might not be satisfied. In this research, we analyze the relative importance of the above factors on PHEV travel costs for long-distance trips by investigating the actual path and refueling/fast charging locations that a PHEV may prefer, which may be different from those of a CV or an HEV. Furthermore, we study the environmental impacts of these factors.

Analyses show that the price of gasoline is the most important factor affecting the long-distance costs of PHEVs. The availability of fast charging stations is another important factor. Average transportation cost per mile gradually decreases with increasing fast charging station deployment level in the road network. However, drivers' stopping intolerance might hamper this positive impact. There is a critical stopping tolerance beyond which the drivers prefer not to make frequent stops to reduce transportation costs, but instead prefer to travel using gasoline. Having a larger battery capacity decreases the adverse effects of the stopping intolerance.

The results indicate that after an essential initial setup of fast charging stations in the road network is reached, research must be directed towards battery capacity expansion. This key result is important for managers and infrastructure investors alike.

At this point, setting up the initial level of fast charging stations is identified as a new problem. In the following section, we deal with the charging station location problem from a different perspective and take the PHEVs into account when locating the stations.

Chapter 4

Hybrid Charging Station Location Problem[3]

4.1 Problem Definition

In this section, we discuss the assumptions regarding the common sense in charging logic, formally introduce the Hybrid Charging Station Location Problem (HSCLP) and present its complexity status.

4.1.1 Common Sense in Charging Logic

Charging logic and Range of EVs: The AFVs have a limited range and they need to refuel on their way to the destination before running out of fuel. Taking the limited range into account, Kuby and Lim [34] extensively discuss the refueling

[3]An extended version of this chapter is authored by Okan Arslan and Oya Ekin Karaşan. It is under review for publication.

logic of AFVs. In their study, the AFVs are assumed to have their tank half-full at the origin node and they are required to have at least half-full tank when arriving at the destination node unless a refueling station is located at this node. This ensures that they can make their trip back to the same refueling station again in the following trip. The charging logic of EVs is similar to the refueling logic of AFVs with only one minor difference: they can be charged at their origin and destination nodes since these nodes represent cities and dense residential areas where there exist charging opportunities possibly at the drivers' home, at shopping malls, parking lots or at charging stations. Hence, we assume that the driver has fully charged battery at the origin node, and it is allowed to arrive at the destination node with a depleted battery. When traveling intercity, the EVs require charging stations on the road to facilitate the trip. In this study, we consider the location of such intercity charging facilities. Note that this is not a restrictive assumption from the methodological perspective and our solution methodology presented in the following section can easily be adapted to model different charging logics in different applications.

Charging logic and Range of PHEVs: Using its internal combustion engine, a PHEV can travel on gasoline similar to a conventional vehicle. It can also charge its battery at a charging station and travel using electricity until a minimum state of charge is reached, similar to an EV. Existing studies suggest that PHEVs actively search for electricity usage opportunities to avoid the use of gasoline [8, 139]. A recent survey carried out by Axsen and Kurani [201] reveals that early PHEV consumers are generally enthusiastic about any available opportunity to charge their batteries [139]. Considering the price effect of the gasoline on the consumer behavior [202, 203], He et al. [8] also points out that PHEVs benefit from the available charging opportunities due to the cost difference between gasoline and electricity. With the sparsely located charging stations especially in the initial stages of infrastructure establishment, we also assume PHEVs will stop at available charging stations to decrease transportation costs. Observe that this critical assumption, similar to the assumption made in He et al. [8], can easily be relaxed in future studies as data become available on the stopping behavior of the drivers, and a possible upper bound can be considered on the mileage per charging stop.

One-way trip: When considering the connectivity of an origin-destination pair, similar to FRLP, we consider the shortest path between the OD pairs. Without loss of generality, only the one-way trip is considered. Note that for EVs, enabling this trip ensures that the round-trip between the same OD pair is also feasible. On the PHEV side, consider two consecutive nodes that a PHEV stops for charging. Regardless of the direction that the PHEV is traveling between these two nodes, the distance that it can travel on electricity is the same on this connection. Thus, enabling a one-way trip also ensures the round trip feasibility for PHEVs.

4.1.2 Hybrid Charging Station Location Problem

Definition 8. *Let $G = (N, E)$ represent our transportation network where N is the set of nodes and E is the set of edges. Let A be the set of arcs induced by edges in E, that is, $A = \{(i, j) \cup (j, i) : \{i, j\} \in E\}$. An EV demand q is a four-tuple $\{s(q), t(q), f_{ev}^q, L_{ev}\}$, where $s(q)$, $t(q) \in N$ are the origin and the destination nodes of the demand, respectively; f_{ev}^q is the EV flow traveling on the shortest path between $s(q)$ and $t(q)$; and L_{ev} is the electric range of the particular EV. A PHEV demand $q = \{s(q), t(q), f_{phev}^q, L_{phev}\}$, is similarly defined.*

The sets of EV and PHEV demands are referred to as Q^{ev} and Q^{phev}, respectively. The demand set Q is the union of two sets, i.e., $Q = Q^{ev} \cup Q^{phev}$.

Definition 9. *An HCSLP instance is a four tuple $\{G, Q, K, p\}$ where G is the transportation network, Q is the set of demands, $K \subseteq N$ is the set of candidate nodes, and $p \leq |K|$ is a positive integer. Given such an instance, the HCSLP problem is defined as finding the set of nodes with cardinality p such that the distance to be covered on electricity is maximized.*

4.1.3 Complexity

Proposition 2. *The hybrid charging station location problem is NP-Complete.*

Proof. Given an HCSLP instance, it is easy to check the feasibility of the problem. Thus, HCSLP is in NP. In order to show that HCSLP is NP-Complete, we now provide a transformation from the FRLP. Consider an FRLP instance $\{G, F, K, p\}$, with network G, demand set F, candidate facility nodes $K \subseteq N$, and the number of stations to be located p. For the HCSLP instance, let $Q^{phev} = \emptyset$, and $Q^{ev} = F$ with $f^q_{ev} = f^q_{afv}/d^q$ where d^q is the shortest distance between $s(q)$ and $t(q)$. For the corresponding network G', we add two dummy nodes $s'(q)$ and $t'(q)$ for each $q \in F$, and two dummy arcs $(s'(q), s(q))$ and $(t(q), t'(q))$ with lengths of $L_{ev}/2$. Observe that solving this HCSLP instance is equivalent to solving the corresponding FRLP instance. Thus, HCSLP is NP-Complete. $\square$

4.2 Mathematical Model

In this section, the required notation and the hybrid charging station location model (HCSLM) are presented. Given an HSCLP instance, let $N^q \subseteq N$ and $A^q \subseteq A$ be the sets of nodes and arcs, respectively, on the shortest path between $s(q)$ and $t(q)$, $\forall q \in Q$. Let d_a, $\forall a \in A^q$ be the arc distance and d^q be the distance of the shortest path. In other words, $d^q = \sum_{a \in A^q} d_a$. Now, for a given $q \in Q^{ev}$, consider an arc $a \in A^q$, and a node $i \in N^q$ appearing on the shortest path prior to traversing arc a. Observe that if the distance between node i and head node of arc a on the shortest path between $s(q)$ and $t(q)$ is less than or equal to L_{ev}, then an EV can charge at node i and traverse arc a completely. In this context, let K^q_a be the set of nodes $i \in K$ that enable complete traversal of the directional arc $a \in A^q$ by an EV. For a given $q \in Q^{phev}$, partial traversal of an arc is also plausible. Let d^{qi}_a be the distance on arc $a \in A^q$ that can be traveled be a PHEV using electricity if there exists a charging station at node $i \in N^q$, and let R_a^q be the set of candidate sites that enable at least partial traversal of the directional arc $a \in A^q$ by a PHEV using electricity. We need the following decision variables:

$$x_k = \begin{cases} 1, & \text{if a refueling station is located at node } k \in K \\ 0, & \text{otherwise} \end{cases}$$

$$z_q = \begin{cases} 1, & \text{if EV demand } q \text{ is covered} \\ 0, & \text{otherwise} \end{cases}$$

$$y_a^{qi} = \begin{cases} 1, & \text{if PHEV demand on arc } a \text{ travels at least partially on electricity} \\ & \text{by charging at node } i \\ 0, & \text{otherwise} \end{cases}$$

$\overline{\text{HCSLM}}$ formulation is as follows:

$$\text{maximize} \quad \sum_{q \in Q^{ev}} f_{ev}^q d^q z^q + \sum_{\substack{q \in Q^{phev} \\ a \in A^q \\ i \in R_a^q}} f_{phev}^q d_a^{qi} y_a^{qi} \tag{4.1}$$

subject to

$$y_a^{qi} \leq x_i \qquad \forall q \in Q^{phev}, a \in A^q, i \in R_a^q \setminus s(q) \tag{4.2}$$

$$\sum_{i \in R_a^q} y_a^{qi} \leq 1 \qquad \forall q \in Q^{phev}, a \in A^q \tag{4.3}$$

$$z^q \leq \sum_{i \in K_a^q} x_i \qquad \forall q \in Q^{ev}, a \in A^q \tag{4.4}$$

$$\sum_{k \in K} x_k = p \tag{4.5}$$

$$x_k \in \{0, 1\} \qquad \forall k \in K \tag{4.6}$$

$$y_a^{qi} \in \{0, 1\} \qquad \forall q \in Q^{phev}, a \in A^q, i \in R_a^q \tag{4.7}$$

$$z^q \in \{0, 1\} \qquad \forall q \in Q^{ev} \tag{4.8}$$

The objective function maximizes the distance traveled using electricity by both EVs and PHEVs. Constraints (4.2) ensure that if the PHEV associated with demand q travels using electricity on an arc a by refueling at node i, then node i must have a charging station except when $i = s(q)$ due to the charging logic. Constraints (4.3) make sure that an arc a is not counted more than once in the objective function. Constraints (4.4) are for setting z^q equal to 1 only if all of the path between $s(q)$ and $t(q)$ is traversable using electricity by the EV associated with demand q. These constraints are inherited from the study by Capar et al. [131]. Constraints (4.5) set the number of open facilities to p. Constraints (4.6)-(4.8) are domain restrictions.

4.2.1 Variable Relaxation

Proposition 3. *The variables y_a^{qi} and z^q necessarily assume binary values in an extreme point of the polyhedron that is formed by relaxing their integrality requirement in the $\overline{HCSLM}$ formulation.*

Proof. Let $\overline{\text{HCSLM-R}}$ be the polyhedron that is formed by relaxing the y_a^{qi} and z^q variables in the $\overline{\text{HCSLM}}$ formulation. Observe that $0 \leq y_a^{qi} \leq 1$ due to the relaxation of Constraints (4.7). Now, assume that there exists an extreme point of $\overline{\text{HCSLM-R}}$, say $\xi = (y; z)$, with some fractional entries in y. For a given $\hat{q} \in Q^{phev}$ and $\hat{a} \in A^q$, let $T_{\hat{a}}^{\hat{q}} = \{i \in R_{\hat{a}}^{\hat{q}} : 0 < y_{\hat{a}}^{\hat{q}i} < 1\}$. Consider the unit vector e^i (of length $|R_a^q \setminus s(q)|$ with i^{th} entry equal to 1 and the remaining entries equal to 0), and the zero vector $\mathbf{0}$ (of length $|R_a^q \setminus s(q)|$ with all entries equal to zero). Note that ($\mathbf{0}$; z), $(e^i; z) \in \overline{\text{HCSLM-R}}$, $\forall i \in T_{\hat{a}}^{\hat{q}}$ due to Constraints (4.2) and (4.3). Observe that the point ξ can be represented as a strict convex combination of $(e^i; z)$ and the zero vector ($\mathbf{0}$; z). Thus ξ cannot be an extreme point and y variables necessarily assume binary values. With a similar reasoning, it is easy to see that the z variables also assume binary values in a solution of $\overline{\text{HCSLM-R}}$. □

4.2.2 Variable Elimination

For a given $q \in Q$, the set A^q contains all the arcs on the shortest path between $s(q)$ and $t(q)$ and the number of variables and constraints depends on the size of this set. However, due to the charging logic of EVs and PHEVs, the size of the set A^q can be significantly reduced. Let B^q_{ev} and B^q_{phev} be the sets of arcs on the shortest path between $s(q)$ and $t(q)$ that can be completely covered by an EV or PHEV, respectively, by charging at the origin node (i.e. the distance between the origin node and the head node of an arc in sets B^q_{ev} and B^q_{phev} is less than the range of EV and PHEV, respectively). Since we assume that the EVs and PHEVs begin their trip fully charged at the origin node, the arcs in sets B^q_{ev} and B^q_{phev} can always be completely traversed using electricity.

Let A^q_{ev} and A^q_{phev} be the sets of arcs on the shortest path between $s(q)$ and $t(q)$ excluding B^q_{ev} and B^q_{phev}, respectively. More formally, $A^q_{ev} = \{a \in A^q : a \notin B^q_{ev}\}$ and $A^q_{phev} = \{a \in A^q : a \notin B^q_{phev}\}$. By considering these sets rather than the set A^q, variables y^{qi}_a, $\forall q \in Q^{phev}, a \in B^q_{phev}, i \in R^q_a$ are eliminated from the formulation, and the number of Constraints (4.2)-(4.4) are reduced. Then, the final formulation, which we shall refer to as HCSLM becomes:

$$\text{maximize} \quad \sum_{q \in Q^{ev}} f^q_{ev} d^q z^q + \sum_{\substack{q \in Q^{phev} \\ a \in A^q_{phev} \\ i \in R^q_a}} f^q_{phev} d^{qi}_a y^{qi}_a + \sum_{\substack{q \in Q^{phev} \\ a \in B^q_{phev}}} f^q_{phev} d_a \tag{4.9}$$

subject to

$$y^{qi}_a \le x_i \qquad \forall q \in Q^{phev}, a \in A^q_{phev}, i \in R^q_a \setminus s(q) \tag{4.10}$$

$$\sum_{i \in R^q_a} y^{qi}_a \le 1 \qquad \forall q \in Q^{phev}, a \in A^q_{phev} \tag{4.11}$$

$$z^q \le \sum_{i \in K^q_a} x_i \qquad \forall q \in Q^{ev}, a \in A^q_{ev} \tag{4.12}$$

$$\sum_{k \in K} x_k = p \tag{4.13}$$

$$z^q \leq 1 \qquad \forall q \in Q^{ev} \tag{4.14}$$

$$y_a^{qi} \geq 0 \qquad \forall q \in Q^{phev}, a \in A^q_{phev}, i \in R^q_a \tag{4.15}$$

$$z^q \geq 0 \qquad \forall q \in Q^{ev} \tag{4.16}$$

$$x_k \in \{0,1\} \qquad \forall k \in K \tag{4.17}$$

Let $\mathcal{F}= \sum_{\substack{q \in Q^{phev} \\ a \in B^q_{phev}}} f^q_{phev} d_a$, as it appears in the objective function. Since $\mathcal{F}$ is fixed for a given HCSLM instance, we exclude it from the formulations in the following parts of the paper for conciseness. Note that, a covered arc contributes to the objective function for the PHEVs, but not for the EVs. Therefore, there does not exist a fixed term in the objective function related to EVs and the set B^q_{ev}. If all of the arcs on a given path of EV demand $\hat{q} \in Q^{ev}$ can be covered by charging at the origin, then Constraints (4.12) are eliminated for $\hat{q}$ in the formulation and $z_{\hat{q}}$ variable naturally assumes a value of 1.

4.3 Benders Decomposition

Considering PHEVs beside EVs further compound the challenge in the charging station location problem. Therefore, we propose a Benders decomposition [204] algorithm as an exact solution technique. A location problem is a well-fit for Benders Decomposition, since generally there is a set of binary variables associated with location decisions and fixing these variables might render the problem into a relatively easier model from a solution perspective. Thus, there are several successful implementations in the recent literature [205–217]. In this section, we propose a Benders Decomposition algorithm as the solution technique and apply enhancements to improve the solution-time of the algorithm by efficiently solving the subproblem and constructing Pareto-optimal cuts in closed form expressions.

Observe that in our particular case, fixing the location variables x turns the formulation into a linear programming model due to Proposition 3. In our presentation, we use a similar notation to the study by Üster and Kewcharoenwong [218].

4.3.1 Benders Subproblem

For a given $\hat{x} \in \{0,1\}^{|K|}$, the subproblem of the HCSLM, referred to as $SP(y, z|\hat{x})$ is presented below:

$$\text{maximize} \quad \sum_{q \in Q^{ev}} f^q_{ev} d^q z^q + \sum_{\substack{q \in Q^{phev} \\ a \in A^q_{phev} \\ i \in R^q_a}} f^q_{phev} d^{qi}_a y^{qi}_a \tag{4.18}$$

subject to

$$y^{qi}_a \leq \hat{x}_i \qquad \forall q \in Q^{phev}, a \in A^q_{phev}, i \in R^q_a \setminus s(q) \tag{4.19}$$

$$\sum_{i \in R^q_a} y^{qi}_a \leq 1 \qquad \forall q \in Q^{phev}, a \in A^q_{phev} \tag{4.20}$$

$$z^q \leq \sum_{i \in K^q_a} \hat{x}_i \qquad \forall q \in Q^{ev}, a \in A^q_{ev} \tag{4.21}$$

$$z^q \leq 1 \qquad \forall q \in Q^{ev} \tag{4.22}$$

$$y^{qi}_a \geq 0 \qquad \forall q \in Q^{phev}, a \in A^q_{phev}, i \in R^q_a \tag{4.23}$$

$$z^q \geq 0 \qquad \forall q \in Q^{ev} \tag{4.24}$$

Note that setting all the variables equal to zero is a feasible solution to the subproblem. Therefore, the subproblem is always feasible. Due to Constraints (4.19)-(4.22), it is also bounded.

Let $\mu, \rho,$ ϕ and σ be the dual variables associated with constraints (4.19), (4.20), (4.21) and (4.22), respectively. Then, the dual subproblem, referred to as $SPD(\mu, \rho, \phi, \sigma|\hat{x})$, is expressed as follows:

$$\text{minimize} \quad \sum_{\substack{q \in Q^{phev} \\ a \in A^q_{phev} \\ i \in R^q_a \setminus s(q)}} \hat{x}_i \mu^{qi}_a + \sum_{\substack{q \in Q^{phev} \\ a \in A^q_{phev}}} \rho^q_a + \sum_{\substack{q \in Q^{ev} \\ a \in A^q_{ev} \\ i \in K^q_a}} \hat{x}_i \phi^q_a + \sum_{q \in Q^{ev}} \sigma_q \tag{4.25}$$

subject to

$$\sum_{a \in A^q_{ev}} \phi^q_a + \sigma_q \geq f^q_{ev} d^q \qquad \forall q \in Q^{ev} \tag{4.26}$$

$$\mu^{qi}_a + \rho^q_a \geq f^q_{phev} d^{qi}_a \qquad \forall q \in Q^{phev}, a \in A^q_{phev}, i \in R^q_a \setminus s(q) \tag{4.27}$$

$$\rho^q_a \geq f^q_{phev} d^{qs(q)}_a \qquad \forall q \in Q^{phev}, a \in A^q_{phev}, s(q) \in R^q_a \tag{4.28}$$

$$\mu^{qi}_a, \rho^q_a \geq 0 \qquad \forall q \in Q^{phev}, a \in A^q_{phev}, i \in R^q_a \setminus s(q) \tag{4.29}$$

$$\phi^q_a, \sigma_q \geq 0 \qquad \forall q \in Q^{ev}, a \in A^q_{ev} \tag{4.30}$$

4.3.2 Benders Master Problem

Let $\mathcal{D}(SPD)$ denote the set of extreme points of $SPD(\mu, \rho, \phi, \sigma|\hat{x})$. Then, we can construct the master problem, referred to as MP, as follows:

$$\text{maximize } \varsigma \tag{4.31}$$

subject to

$$\varsigma \leq \sum_{\substack{q \in Q^{phev} \\ a \in A^q_{phev} \\ i \in R^q_a \setminus s(q)}} x_i \mu^{qi}_a + \sum_{\substack{q \in Q^{phev} \\ a \in A^q_{phev}}} \rho^q_a + \sum_{\substack{q \in Q^{ev} \\ a \in A^q_{ev} \\ i \in K^q_a}} x_i \phi^q_a + \sum_{q \in Q^{ev}} \sigma_q \quad \forall (\mu, \rho, \phi, \sigma) \in \mathcal{D}(SPD) \tag{4.32}$$

$$\sum_{k \in K} x_k = p \tag{4.33}$$

$$x_k \in \{0, 1\} \qquad \forall k \in K \tag{4.34}$$

We have now transformed the HCSLM model into an equivalent mixed integer programming model with $|K|$ binary and one continuous variables. In order to handle the exponential number of constraints of the MP model due to the set $\mathcal{D}(SPD)$, we apply a branch and cut approach. Using the dual variable values obtained from the subproblem, a *cut* is added to the master problem at each iteration in the form of an inequality (4.32). Note that since the primal subproblem is always feasible and bounded, by strong duality, the dual is also feasible and bounded. Therefore, the cuts added at each iteration are optimality cuts and only remove solutions that are known not to be optimal.

The classical Benders implementation solves the master problem to optimality before solving the subproblem. This entails the possibility of unnecessarily revisiting the same solutions again in the master problem. Therefore, we solve our problem in a single branch and bound tree similar to Codato and Fischetti [219]. At every potential incumbent solution encountered in the search tree, we solve the subproblem and add an optimality cut, if necessary. In our computational studies, we implement this method using the *lazy constraint callback* of the CPLEX Concert Technology.

4.3.3 Subproblem Solution

Observe that the subproblem $SP(y, z|\hat{x})$ can be decomposed based on the vehicle type. The first term in the objective function and Constraints (4.21), (4.22) and (4.24) are related to EVs, while the remaining parts are related to PHEVs. We refer to the former problem as $SP^{ev}(z|\hat{x})$, and the latter as $SP^{phev}(y|\hat{x})$. Observe that $SP^{ev}(z|\hat{x})$ can further be decomposed on the basis of demand. For a given demand $q \in Q^{ev}$, we refer to the partition which is formulated below as $SP^{ev}_q(z|\hat{x})$.

$$\text{maximize } f^q_{ev} d^q z^q \tag{4.35}$$

subject to

$$z^q \leq \sum_{i \in K_a^q} \hat{x}_i \qquad \forall a \in A_{ev}^q \tag{4.36}$$

$$z^q \leq 1 \tag{4.37}$$

$$z^q \geq 0 \tag{4.38}$$

Let $K^\star(\hat{x}) = \{k \in K : \hat{x}_k = 1\}$. Observe that identifying if the path between $s(q)$ and $t(q)$ can be traveled by an EV without running out of electricity can be done by checking the existence of an open station to cover every arc on the path. Hence, the following variable construction is an optimal solution for $SP_q^{ev}(z|\hat{x})$.

$$z^q = \begin{cases} 1, & \text{if } |K_a^q \cap K^\star(\hat{x})| \geq 1, \forall a \in A_{ev}^q \\ 0, & \text{otherwise} \end{cases} \tag{4.39}$$

As for the PHEVs, the $SP^{phev}(y|\hat{x})$ problem can be decomposed on the basis of demand and arc. For a given demand $q \in Q^{phev}$ and $a \in A_{phev}^q$, we refer to the partition which is formulated below as $SP_{qa}^{phev}(y|\hat{x})$:

$$\text{maximize} \sum_{i \in R_a^q} f_{phev}^q d_a^{qi} y_a^{qi} \tag{4.40}$$

subject to

$$y_a^{qi} \leq \hat{x}_i \qquad \forall i \in R_a^q \setminus s(q) \tag{4.41}$$

$$\sum_{i \in R_a^q} y_a^{qi} \leq 1 \tag{4.42}$$

$$y_a^{qi} \geq 0 \qquad \forall i \in R_a^q \tag{4.43}$$

Similar to the case with EVs, the solution can easily be constructed. Observe that, for the demand q, the distance that can be traveled on the arc a using electricity is equal to $\max\limits_{j \in R_a^q \cap (K^\star(\hat{x}) \cup s(q))} \{d_a^{qj}\}$ in which case the associated variable

y_a^{qj} assumes a value of 1. That is,

$$y_a^{qi} = \begin{cases} 1, & \text{if } i = \text{argmax}_{j \in R_a^q \cap (K^\star(\hat{x}) \cup s(q))}\{d_a^{qj}\} \\ 0, & \text{otherwise} \end{cases} \tag{4.44}$$

4.3.4 Benders Cut Characterization

In the dual subproblem $SPD(\mu, \rho, \phi, \sigma|\hat{x})$, variables ϕ and σ and Constraints (4.26) and (4.30) are related to the EVs, while variables μ and ρ and Constraints (4.27), (4.28) and (4.29) are related to PHEVs. Therefore $SPD(\mu, \rho, \phi, \sigma|\hat{x})$ problem can also be decomposed into two: $SPD^{ev}(\phi, \sigma|\hat{x})$ and $SPD^{phev}(\mu, \rho|\hat{x})$. Note that the former problem can also be decomposed on the basis of demand. Let q^{th} partition of the $SPD^{ev}(\phi, \sigma|\hat{x})$ problem be defined as $SPD_q^{ev}(\phi, \sigma|\hat{x})$, which is stated as follows:

$$\text{minimize} \sum_{\substack{a \in A_{ev}^q \\ i \in K_a^q}} \hat{x}_i \phi_a^q + \sigma_q \tag{4.45}$$

subject to

$$\sum_{a \in A_{ev}^q} \phi_a^q + \sigma_q \geq f_{ev}^q d^q \tag{4.46}$$

$$\phi_a^q, \sigma_q \geq 0 \qquad \forall a \in A_{ev}^q \tag{4.47}$$

Observe that this is a continuous knapsack problem. Therefore we can construct the solution of this problem in closed form. Before we proceed, we need some further definitions. Let $\mathcal{A}_0^q(\hat{x})$ and $\mathcal{A}_1^q(\hat{x})$ be the sets of arcs in A_{ev}^q, induced by $\hat{x}$, that cannot be covered by any of the open stations and that can only be covered by a single station, respectively. Formally, $\mathcal{A}_0^q(\hat{x}) = \{a \in A_{ev}^q : |K_a^q \cap K^\star(\hat{x})| = 0\}$ and $\mathcal{A}_1^q(\hat{x}) = \{a \in A_{ev}^q : |K_a^q \cap K^\star(\hat{x})| = 1\}$. Note that $\mathcal{A}_1^q(\hat{x})$ might be empty even if $z_q = 1$, e.g. if all arcs on the path between $s(q)$ and $t(q)$ can be covered by at least two open stations. But we have a non-empty $\mathcal{A}_0^q(\hat{x})$ set for any q with $z_q = 0$.

Proposition 4. *For a given $\hat{x}$, and path $\hat{q} \in Q^{ev}$, the following is the characterization of optimal solutions to $SPD^{ev}_{\hat{q}}$.*

Case (1) *If path $\hat{q}$ is not chargeable (i.e., $z_{\hat{q}} = 0$), then:*

(a) For all $\alpha \in \mathcal{A}^{\hat{q}}_0(\hat{x})$, the following solution is optimal:

- $\sigma_{\hat{q}} = 0$
- $\phi^{\hat{q}}_{\alpha} = f^{\hat{q}}_{ev} d^{\hat{q}}$
- $\phi^{\hat{q}}_{a} = 0$, $\forall a \in (A^{\hat{q}}_{ev} \setminus \alpha)$.

Case (2) *If path $\hat{q}$ is chargeable (i.e., $z_{\hat{q}} = 1$), then:*

(a) For all $\alpha \in \mathcal{A}^{\hat{q}}_1(\hat{x})$, the following solution is optimal:

- $\sigma_{\hat{q}} = 0$
- $\phi^{\hat{q}}_{\alpha} = f^{\hat{q}}_{ev} d^{\hat{q}}$
- $\phi^{\hat{q}}_{a} = 0, \forall a \in (A^{\hat{q}}_{ev} \setminus \alpha)$

(b) The following is also an optimal solution:

- $\sigma_{\hat{q}} = f^{\hat{q}}_{ev} d^{\hat{q}}$
- $\phi^{\hat{q}}_{a} = 0, \forall a \in A^{\hat{q}}_{ev}$

Proof. All results follow trivially from the fact that $SPD^{ev}_q(\phi, \sigma|\hat{x})$ is a continuous knapsack problem. □

Note that any convex combination of alternative optimal solutions is also optimal for $SPD^{ev}_q(\phi, \sigma|\hat{x})$.

The subproblem for PHEVs which we refer to as $SPD^{phev}(\mu, \rho|\hat{x})$ can be decomposed on the basis of demand and arc. We refer to the partition of a^{th} arc of the q^{th} demand as $SPD^{phev}_{qa}(\mu, \rho|\hat{x})$, which is stated as follows:

$$\text{minimize} \sum_{i \in R^q_a \setminus s(q)} \hat{x}_i \mu^{qi}_a + \rho^q_a \tag{4.48}$$

subject to

$$\mu_a^{qi} + \rho_a^q \geq f_{phev}^q d_a^{qi} \qquad \forall i \in R_a^q \setminus s(q) \tag{4.49}$$

$$\rho_a^q \geq f_{phev}^q d_a^{qs(q)} \qquad s(q) \in R_a^q \tag{4.50}$$

$$\mu_a^{qi}, \rho_a^q \geq 0 \qquad \forall i \in R_a^q \setminus s(q) \tag{4.51}$$

The following result can be attained through complementary slackness conditions:

Proposition 5. *For a given path $\hat{q}$ and arc $\hat{a} \in A_{phev}^{\hat{q}}$, the following is the characterization of optimal solutions to $SPD_{\hat{q}\hat{a}}^{phev}(\mu, \rho|\hat{x})$.*

Case (1) *If $\sum_{i \in R_{\hat{a}}^{\hat{q}}} y_{\hat{a}}^{\hat{q}i} = 0$, then the following solution is optimal:*

- $\rho_{\hat{a}}^{\hat{q}} = 0$
- $\mu_{\hat{a}}^{\hat{q}i} = f_{phev}^{\hat{q}} d_{\hat{a}}^{\hat{q}i}$, $\forall i \in R_{\hat{a}}^{\hat{q}} \setminus s(\hat{q})$

Case (2) *If $y_{\hat{a}}^{\hat{q}s(\hat{q})} = 1$, then the following solution is optimal:*

- $\rho_{\hat{a}}^{\hat{q}} = f_{phev}^{\hat{q}} d_{\hat{a}}^{\hat{q}s(\hat{q})}$
- $\mu_{\hat{a}}^{\hat{q}i} = max\{0, f_{phev}^{\hat{q}} d_{\hat{a}}^{\hat{q}i} - \rho_{\hat{a}}^{\hat{q}}\}$, $\forall i \in R_{\hat{a}}^{\hat{q}} \setminus s(\hat{q})$

Case (3) *If $y_{\hat{a}}^{\hat{q}j} = 1$ for $j \neq s(\hat{q})$, then the following are the conditions for optimality:*

- $\mu_{\hat{a}}^{\hat{q}j} + \rho_{\hat{a}}^{\hat{q}} = f_{phev}^{\hat{q}} d_{\hat{a}}^{\hat{q}j}$,
- $\mu_{\hat{a}}^{\hat{q}i} = 0$, *and* $\rho_{\hat{a}}^{\hat{q}} \geq f_{phev}^{\hat{q}} d_{\hat{a}}^{\hat{q}i}$, $\forall i \in R_{\hat{a}}^{\hat{q}} : i \in K^\star(\hat{x}), i \neq s(\hat{q}), i \neq j$,
- $\mu_{\hat{a}}^{\hat{q}i} + \rho_{\hat{a}}^{\hat{q}} \geq f_{phev}^{\hat{q}} d_{\hat{a}}^{\hat{q}i}$, $\forall i \in R_{\hat{a}}^{\hat{q}} : i \notin K^\star(\hat{x}), i \neq s(\hat{q}), i \neq j$,
- $\rho_{\hat{a}}^{\hat{q}} \geq f_{phev}^{\hat{q}} d_{\hat{a}}^{\hat{q}s(\hat{q})}$, if $s(\hat{q}) \in R_{\hat{a}}^{\hat{q}}$,
- $\mu_{\hat{a}}^{\hat{q}i}, \rho_{\hat{a}}^{\hat{q}} \geq 0$, $\forall i \in R_{\hat{a}}^{\hat{q}}, i \notin K^\star(\hat{x}), i \neq s(\hat{q})$.

Proof. Since $\sum_{i \in R_{\hat{a}}^{\hat{q}}} y_{\hat{a}}^{\hat{q}i} = 0$, we have $y_{\hat{a}}^{\hat{q}i} = 0$, $\forall i \in R_{\hat{a}}^{\hat{q}}$. We then have $|R_{\hat{a}}^{\hat{q}} \cap K^\star(\hat{x})| = 0$, that is $\hat{x}_i = 0, \forall i \in R_a^q \setminus s(q)$. Therefore, Case (1) follows. When

$\sum_{i \in R_{\hat{a}}^{\hat{q}}} y_{\hat{a}}^{\hat{q}i} = 1$, either $y_{\hat{a}}^{\hat{q}s(\hat{q})} = 1$ or $y_{\hat{a}}^{\hat{q}j} = 1$ for $j \neq s(\hat{q})$. In the former case, we have $d_{\hat{a}}^{\hat{q}s(\hat{q})} \geq d_{\hat{a}}^{\hat{q}i}$, $\forall i \in R_{\hat{a}}^{\hat{q}}, i \in K^{\star}(\hat{x}), i \neq s(\hat{q})$ since $y_{\hat{a}}^{\hat{q}s(\hat{q})} = 1$. Thus, we have $\mu_{\hat{a}}^{\hat{q}j} + \rho_{\hat{a}}^{\hat{q}} = f_{phev}^{\hat{q}} d_{\hat{a}}^{\hat{q}j}$. This implies that $\mu_{\hat{a}}^{\hat{q}i} = 0$, $\forall i \in R_{\hat{a}}^{\hat{q}}, i \in K^{\star}(\hat{x}), i \neq s(\hat{q})$. For $i \in R_{\hat{a}}^{\hat{q}}, i \notin K^{\star}(\hat{x}), i \neq s(\hat{q})$, we have $\mu_{\hat{a}}^{\hat{q}i} = max\{0, f_{phev}^{\hat{q}} d_{\hat{a}}^{\hat{q}i} - \rho_{\hat{a}}^{\hat{q}}\}$ due to Constraints (4.49). In the latter case, we have $y_{\hat{a}}^{\hat{q}j} = 1$ for $j \neq s(\hat{q})$. This implies that $d_{\hat{a}}^{\hat{q}j} \geq d_{\hat{a}}^{\hat{q}i}$, $\forall i \in R_{\hat{a}}^{\hat{q}}, \forall i \in K^{\star}(\hat{x}), i \neq s(\hat{q}), i \neq j$. Since we have $\hat{x}_i = 1$ for $i \in R_{\hat{a}}^{\hat{q}}, \forall i \in K^{\star}(\hat{x}), i \neq s(\hat{q}), i \neq j$, we have the first two conditions as given in Case (3). Since we can have $d_{\hat{a}}^{\hat{q}j} < d_{\hat{a}}^{\hat{q}i}$ for $i \in R_{\hat{a}}^{\hat{q}}, i \notin K^{\star}(\hat{x}), i \neq s(\hat{q}), i \neq j$, we keep Constraints (4.49) in the third bullet of Case (3). The remaining two bullets are also inherited from the constraint set of $SPD_{qa}^{phev}(\mu, \rho | \hat{x})$. This completes the proof. $\square$

Remark 1. *Both Propositions 4 and 5 assume primal feasibility as given, and present the properties of optimal solutions for their respective problems.*

Remark 2. *A Benders cut can be constructed by first solving the subproblem using (4.39) and (4.44), and then by generating the dual variables μ, ρ, ϕ and σ that satisfy the conditions given in Propositions 4 and 5. The generated cut can be added to the master problem as an inequality of the form (4.32).*

In the following, we propose three different cut selection schemes. The first one produces a single cut for each subproblem solved. This cut is used as a benchmark in the computational study section to compare the efficiencies of the remaining two cut selection schemes. The next scheme is multicut generation scheme in which several cuts are added at each iteration. In the last scheme, we generate a Pareto-optimal cut.

4.3.5 Cut Selection Scheme 1: Single Cut

For a given $\hat{x}$, we can construct the primal subproblem solutions $z^q, \forall q \in Q^{ev}$ and $y_a^{qi}, \forall q \in Q^{phev}, a \in A_{phev}^q, i \in R_a^q$. Consider the corresponding dual solution presented in Algorithm 1. Parts of the algorithm that are analogous to cases in Propositions 4 and 5 are explicitly shown. The dual variables obtained can be used to construct a single cut to be added to the master problem at each iteration as an inequality of type (4.32).

4.3.6 Cut Selection Scheme 2: Multicut

Birge and Louveaux [220] considered addition of several cuts in a single iteration in the context of two-stage stochastic linear programs. Multicut version of Benders Decomposition has successfully been implemented in different applications [209, 221–223]. To implement the multicut version, we need to modify our master problem. For this purpose, let β_q^{ev} and δ_{qa}^{phev} be new surrogate variables associated with $SPD_q^{ev}(\phi,\sigma|\hat{x})$ and $SPD_{qa}^{phev}(\mu,\rho|\hat{x})$, respectively; $\mathcal{D}(SPD_q^{ev})$ and $\mathcal{D}(SPD_{qa}^{phev})$ be the set of extreme points for the respective problems. Then the modified master problem can be expressed as:

$$\text{maximize} \sum_{q\in Q^{ev}} \beta_q^{ev} + \sum_{\substack{q\in Q^{phev}\\ a\in A_{phev}^q}} \delta_{qa}^{phev} \tag{4.52}$$

subject to

$$\beta_q^{ev} \leq \sum_{\substack{a\in A_{ev}^q\\ i\in K_a^q}} x_i\phi_a^q + \sigma_q \qquad \forall q\in Q^{ev}, (\phi,\sigma)\in\mathcal{D}(SPD_q^{ev}) \tag{4.53}$$

$$\delta_{qa}^{phev} \leq \sum_{i\in R_a^q\setminus s(q)} x_i\mu_a^{qi} + \rho_a^q \qquad \forall q\in Q^{phev}, a\in A_{phev}^q, (\mu,\rho)\in\mathcal{D}(SPD_{qa}^{phev}) \tag{4.54}$$

$$\sum_{k\in K} x_k = p \tag{4.55}$$

$$x_k\in\{0,1\} \qquad \forall k\in K \tag{4.56}$$

Algorithm 1: Single Cut Construction

Input: $\hat{x}$
Output: A valid cut

foreach $\hat{q} \in Q^{ev}$ **do**
  Calculate $z_{\hat{q}}$ using $\hat{x}$ and (4.39)
  if $z_{\hat{q}} = 0$ **then** `// Prop.3 - Case(1)`
    $\sigma_{\hat{q}} \leftarrow 0$
    $\phi^{\hat{q}}_{\alpha} \leftarrow f^{\hat{q}}_{ev} d^{\hat{q}}$ where $\alpha \in \mathcal{A}^{\hat{q}}_{0}(\hat{x})$ is the first uncovered arc on the path
    $\phi^{\hat{q}}_{a} \leftarrow 0$, $\forall a \in (A^{\hat{q}}_{ev} \setminus \alpha)$
  else `// Prop.3 - Case(2)`
    $\sigma_{\hat{q}} \leftarrow f^{\hat{q}}_{ev} d^{\hat{q}}$
    $\phi^{\hat{q}}_{a} \leftarrow 0, \forall a \in A^{\hat{q}}_{ev}$

foreach $\hat{q} \in Q^{phev}$ *and* $\hat{a} \in A^{\hat{q}}_{phev}$ **do**
  foreach $i \in R^{\hat{q}}_{\hat{a}}$ **do**
    Calculate $y^{\hat{q}i}_{\hat{a}}$ using $\hat{x}$ and (4.44)
  if $\sum_{i \in R^{\hat{q}}_{\hat{a}}} y^{\hat{q}i}_{\hat{a}} = 0$ **then** `// Prop.4 - Case(1)`
    $\rho^{\hat{q}}_{\hat{a}} \leftarrow 0$
    $\mu^{\hat{q}i}_{\hat{a}} \leftarrow f^{\hat{q}}_{phev} d^{\hat{q}i}_{\hat{a}}$, $\forall i \in R^{\hat{q}}_{\hat{a}} \setminus s(\hat{q})$
  else if $\sum_{i \in R^{\hat{q}}_{\hat{a}}} y^{\hat{q}i}_{\hat{a}} = 1$ *and* $y^{\hat{q}s(\hat{q})}_{\hat{a}} = 1$ **then** `// Prop.4 - Case(2)`
    $\rho^{\hat{q}}_{\hat{a}} \leftarrow f^{\hat{q}}_{phev} d^{\hat{q}s(\hat{q})}_{\hat{a}}$
    $\mu^{\hat{q}i}_{\hat{a}} \leftarrow max\{0, f^{\hat{q}}_{phev} d^{\hat{q}i}_{\hat{a}} - \rho^{\hat{q}}_{\hat{a}}\}$, $\forall i \in R^{\hat{q}}_{\hat{a}} \setminus s(\hat{q})$
  else `// Prop.4 - Case(3)`
    $\rho^{\hat{q}}_{\hat{a}} \leftarrow f^{\hat{q}}_{phev} d^{\hat{q}j}_{\hat{a}}$
    $\mu^{\hat{q}j}_{\hat{a}} \leftarrow 0$
    $\mu^{\hat{q}i}_{\hat{a}} \leftarrow 0$, $\forall i \in R^{\hat{q}}_{\hat{a}} : i \in K^{\star}(\hat{x}), i \neq s(\hat{q}), i \neq j$
    $\mu^{\hat{q}i}_{\hat{a}} \leftarrow max\{0, f^{\hat{q}}_{phev} d^{\hat{q}i}_{\hat{a}} - \rho^{\hat{q}}_{\hat{a}}\}$, $\forall i \in R^{\hat{q}}_{\hat{a}} : i \notin K^{\star}(\hat{x}), i \neq s(\hat{q}), i \neq j$

---

return $\varsigma \leq \sum_{\substack{q \in Q^{phev} \\ a \in A^{q}_{phev} \\ i \in R^{q}_{a} \setminus s(q)}} x_i \mu^{qi}_{a} + \sum_{\substack{q \in Q^{phev} \\ a \in A^{q}_{phev}}} \rho^{q}_{a} + \sum_{\substack{q \in Q^{ev} \\ a \in A^{q}_{ev} \\ i \in K^{q}_{a}}} x_i \phi^{q}_{a} + \sum_{q \in Q^{ev}} \sigma_q$

For a given $\hat{x}$, multiple extreme points for each subproblem as presented in Propositions 4 and 5 exist. By modifying the master problem, we can now use the information that is available for each subproblem and add a cut corresponding to each extreme point, as presented in Algorithm 2. In this fashion, a cut pool is collected at each iteration.

4.3.7 Cut Selection Scheme 3: Pareto-optimal Cut

Reducing the number of Benders iterations is of great value to accelerate the implementation. However, as we have identified above, conditions in Propositions 4 and 5 imply that several cuts can be generated for a given vector $\hat{x}$. Out of these cuts, the simple cut generation scheme selects one cut to be added at each iteration, and the multicut implementation adds several cuts at once. One other option is to select a cut that might help us reduce the number of iterations. In this section, we present the Pareto-optimal cut generation scheme in the sense of the study by Magnanti and Wong [224]. Let $\mathcal{X}$ be the feasible set of the master problem in the first iteration (i.e. $\mathcal{X}= \{x \in \{0,1\}^{|K|} : \sum_{k\in K} x_k = p\}$), $\mathbf{opt}(\mathcal{P})$ be the optimal objective function value of the problem $\mathcal{P}$, and the function $\mathcal{C}(x,\mu,\rho,\phi,\sigma)$ be defined as the following:

$$\mathcal{C}(x,\mu,\rho,\phi,\sigma) = \sum_{\substack{q\in Q^{phev}\\ a\in A^q_{phev}\\ i\in R^q_a\setminus s(q)}} x_i\mu^{qi}_a + \sum_{\substack{q\in Q^{phev}\\ a\in A^q_{phev}}} \rho^q_a + \sum_{\substack{q\in Q^{ev}\\ a\in A^q_{ev}\\ i\in K^q_a}} x_i\phi^q_a + \sum_{q\in Q^{ev}} \sigma_q \tag{4.57}$$

In their seminal paper, Magnanti and Wong [224] presented the notion of cut domination in the Benders Decomposition framework. The cut generated by the dual solution $(\hat{\mu},\hat{\rho},\hat{\phi},\hat{\sigma})$ is said to dominate the cut generated by the dual solution $(\tilde{\mu},\tilde{\rho},\tilde{\phi},\tilde{\sigma})$, if and only if $\mathcal{C}(x,\hat{\mu},\hat{\rho},\hat{\phi},\hat{\sigma}) \leq \mathcal{C}(x,\tilde{\mu},\tilde{\rho},\tilde{\phi},\tilde{\sigma})$ for all $x\in\mathcal{X}$ with a strict

Algorithm 2: Multicut Construction

Input: $\hat{x}$
Output: Cut pool $\mathcal{G}$

foreach $\hat{q} \in Q^{ev}$ **do**
  Calculate $z_{\hat{q}}$ using $\hat{x}$ and (4.39)
  if $z_{\hat{q}} = 0$ **then** `// Prop.3 - Case(1)`
    foreach $\alpha \in \mathcal{A}_0^{\hat{q}}(\hat{x})$ **do**
      $\sigma_{\hat{q}} \leftarrow 0$
      $\phi_{\alpha}^{\hat{q}} \leftarrow f_{ev}^{\hat{q}} d^{\hat{q}}$
      $\phi_{a}^{\hat{q}} \leftarrow 0, \forall a \in (A_{ev}^{\hat{q}} \setminus \alpha)$
      $\mathcal{G} \leftarrow \mathcal{G} \cup \{\ \beta_{\hat{q}}^{ev} \le \sum_{i \in K_{\alpha}^{\hat{q}}} x_i \phi_{\alpha}^{\hat{q}}\ \}$
  else `// Prop.3 - Case(2)`
    foreach $\alpha \in \mathcal{A}_1^{\hat{q}}(\hat{x})$ **do**
      $\sigma_{\hat{q}} \leftarrow 0$
      $\phi_{\alpha}^{\hat{q}} \leftarrow f_{ev}^{\hat{q}} d^{\hat{q}}$
      $\phi_{a}^{\hat{q}} \leftarrow 0, \forall a \in (A_{ev}^{\hat{q}} \setminus \alpha)$
      $\mathcal{G} \leftarrow \mathcal{G} \cup \{\ \beta_{\hat{q}}^{ev} \le \sum_{i \in K_{\alpha}^{\hat{q}}} x_i \phi_{\alpha}^{\hat{q}}\ \}$
    $\sigma_{\hat{q}} \leftarrow f_{ev}^{\hat{q}} d^{\hat{q}}$
    $\phi_{a}^{\hat{q}} \leftarrow 0, \forall a \in A_{ev}^{\hat{q}}$
    $\mathcal{G} \leftarrow \mathcal{G} \cup \{\ \beta_{\hat{q}}^{ev} \le \sigma_{\hat{q}}\ \}$

foreach $\hat{q} \in Q^{phev}$ *and* $\hat{a} \in A_{phev}^{\hat{q}}$ **do**
  foreach $i \in R_{\hat{a}}^{\hat{q}}$ **do**
    Calculate $y_{\hat{a}}^{\hat{q}i}$ using $\hat{x}$ and (4.44)
  if $\sum_{i \in R_{\hat{a}}^{\hat{q}}} y_{\hat{a}}^{\hat{q}i} = 0$ **then** `// Prop.4 - Case(1)`
    $\rho_{\hat{a}}^{\hat{q}} \leftarrow 0$
    $\mu_{\hat{a}}^{\hat{q}i} \leftarrow f_{phev}^{\hat{q}} d_{\hat{a}}^{\hat{q}i}, \forall i \in R_{\hat{a}}^{\hat{q}} \setminus s(\hat{q})$
    $\mathcal{G} \leftarrow \mathcal{G} \cup \{\ \delta_{\hat{q}\hat{a}}^{phev} \le \sum_{i \in R_{\hat{a}}^{\hat{q}} \setminus s(\hat{q})} x_i \mu_{\hat{a}}^{\hat{q}i}\ \}$
  else if $y_{\hat{a}}^{\hat{q}s(\hat{q})} = 1$ **then** `// Prop.4 - Case(2)`
    $\rho_{\hat{a}}^{\hat{q}} \leftarrow f_{phev}^{\hat{q}} d_{\hat{a}}^{\hat{q}s(\hat{q})}$
    $\mu_{\hat{a}}^{\hat{q}i} \leftarrow max\{0, f_{phev}^{\hat{q}} d_{\hat{a}}^{\hat{q}i} - \rho_{\hat{a}}^{\hat{q}}\}, \forall i \in R_{\hat{a}}^{\hat{q}} \setminus s(\hat{q})$
    $\mathcal{G} \leftarrow \mathcal{G} \cup \{\ \delta_{\hat{q}\hat{a}}^{phev} \le \sum_{i \in R_{\hat{a}}^{\hat{q}} \setminus s(\hat{q})} x_i \mu_{\hat{a}}^{\hat{q}i} + \rho_{\hat{a}}^{\hat{q}}\ \}$
  else `// Prop.4 - Case(3)`
    $\rho_{\hat{a}}^{\hat{q}} \leftarrow f_{phev}^{\hat{q}} d_{\hat{a}}^{\hat{q}j}$
    $\mu_{\hat{a}}^{\hat{q}j} \leftarrow 0$
    $\mu_{\hat{a}}^{\hat{q}i} \leftarrow 0, \forall i \in R_{\hat{a}}^{\hat{q}} : i \in K^{\star}(\hat{x}), i \neq s(\hat{q}), i \neq j$
    $\mu_{\hat{a}}^{\hat{q}i} \leftarrow max\{0, f_{phev}^{\hat{q}} d_{\hat{a}}^{\hat{q}i} - \rho_{\hat{a}}^{\hat{q}}\}, \forall i \in R_{\hat{a}}^{\hat{q}} : i \notin K^{\star}(\hat{x}), i \neq s(\hat{q}), i \neq j$
    $\mathcal{G} \leftarrow \mathcal{G} \cup \{\ \delta_{\hat{q}\hat{a}}^{phev} \le \sum_{i \in R_{\hat{a}}^{\hat{q}} \setminus s(\hat{q})} x_i \mu_{\hat{a}}^{\hat{q}i} + \rho_{\hat{a}}^{\hat{q}}\ \}$
    $\rho_{\hat{a}}^{\hat{q}} \leftarrow \max\{f_{phev}^{q} d_{a}^{qs(q)}, \max_{i \in R_a^q \cap K^{\star}(\hat{x}), i \neq j, i \neq s(q)} \{f_{phev}^{q} d_{a}^{qi}\}\}$
    $\mu_{\hat{a}}^{\hat{q}j} \leftarrow 0$
    $\mu_{\hat{a}}^{\hat{q}i} \leftarrow 0, \forall i \in R_{\hat{a}}^{\hat{q}} : i \in K^{\star}(\hat{x}), i \neq s(\hat{q}), i \neq j$
    $\mu_{\hat{a}}^{\hat{q}i} \leftarrow max\{0, f_{phev}^{\hat{q}} d_{\hat{a}}^{\hat{q}i} - \rho_{\hat{a}}^{\hat{q}}\}, \forall i \in R_{\hat{a}}^{\hat{q}} : i \notin K^{\star}(\hat{x}), i \neq s(\hat{q}), i \neq j$
    $\mathcal{G} \leftarrow \mathcal{G} \cup \{\ \delta_{\hat{q}\hat{a}}^{phev} \le \sum_{i \in R_{\hat{a}}^{\hat{q}} \setminus s(\hat{q})} x_i \mu_{\hat{a}}^{\hat{q}i} + \rho_{\hat{a}}^{\hat{q}}\ \}$

return $\mathcal{G}$

inequality for at least one point. A cut is called *Pareto-optimal*, if no other cuts dominate it. To obtain a Pareto-optimal cut induced by $\hat{x}$, we need to solve the following linear programming problem:

$$\text{minimize} \;\; \mathcal{C}(\bar{x}, \mu, \rho, \phi, \sigma) \tag{4.58}$$

subject to

(4.26) – (4.30)

$$\mathcal{C}(\hat{x}, \mu, \rho, \phi, \sigma) = \mathbf{opt}(SPD(\mu, \rho, \phi, \sigma | \hat{x})) \tag{4.59}$$

where $\bar{x} \in ri(\mathcal{X}^c)$, a point in the relative interior of the convex hull of the set $\mathcal{X}$, is called a *core point*. We refer to this LP as $MW(\mu, \rho, \phi, \sigma | \hat{x}, \bar{x})$. Our initial core point is a vector of length $|K|$ with all entries equal to $\frac{p}{|K|}$. In the following Benders iterations, we use the average of the current core point and the active solution of the MP, similar to [225].

At this point, note that Constraint (4.59) and fractional coefficients $\bar{x}_i$ may prevent obtaining an efficient optimal-dual solution, as is the case for the study by Contreras et al. [210]. However, as we present in the following parts, we can cleverly exploit the knapsack nature of the subproblems to find the optimal solutions for the MW problem using Remark (1).

4.3.8 Magnanti-Wong Problem Solution

Similar to the subproblem and the dual of the subproblem, the $MW(\mu, \rho, \phi, \sigma | \hat{x}, \bar{x})$ problem can also be decomposed. The EV problem partition for a given demand $q \in Q^{ev}$, which we refer to as $MW_q^{ev}(\phi, \sigma | \hat{x}, \bar{x})$ is formulated as:

$$\text{minimize} \sum_{\substack{a \in A_{ev}^q \\ i \in K_a^q}} \bar{x}_i \phi_a^q + \sigma_q \tag{4.60}$$

subject to

$$\sum_{\substack{a\in A_{ev}^q \\ i\in K_a^q}} \hat{x}_i\phi_a^q + \sigma_q = \mathbf{opt}(SPD_q^{ev}(\phi,\sigma|\hat{x})) \tag{4.61}$$

$$\sum_{a\in A_{ev}^q} \phi_a^q + \sigma_q \geq f_{ev}^q d^q \tag{4.62}$$

$$\phi_a^q, \sigma_q \geq 0 \qquad \forall a \in A_{ev}^q \tag{4.63}$$

Observe that the constraint set enforces the solution to be optimal for the $SPD_q^{ev}(\phi,\sigma|\hat{x})$ problem for which we have the optimal solutions presented in Proposition 3. Therefore we can construct the optimal variable values of the $MW_q^{ev}(\phi,\sigma|\hat{x},\bar{x})$ in the following proposition:

Proposition 6. *The following solution is optimal for* $MW_q^{ev}(\phi,\sigma|\hat{x},\bar{x})$.

$$\phi_a^q = \begin{cases} f_{ev}^q d^q, & \textit{if } z(q)=1, |\mathcal{A}_1^q(\hat{x})| \neq 0, a = \text{argmin}_{b\in\mathcal{A}_1^q(\hat{x})}\{\sum_{i\in K_b^q}\bar{x}_i\} \text{ and } \sum_{i\in K_a^q}\bar{x}_i \leq 1 \\ f_{ev}^q d^q, & \textit{if } z(q)=0 \text{ and } a = \text{argmin}_{b\in\mathcal{A}_0^q(\hat{x})}\{\sum_{i\in K_b^q}\bar{x}_i\} \\ \mathit{0}, & \text{otherwise} \end{cases} \tag{4.64}$$

$$\sigma_q = \begin{cases} f_{ev}^q d^q, & \textit{if } z(q)=1 \text{ and } \sum_{i\in K_a^q}\bar{x}_i > 1, \forall a \in \mathcal{A}_1^q(\hat{x}) \\ f_{ev}^q d^q, & \textit{if } z(q)=1 \text{ and } |\mathcal{A}_1^q(\hat{x})| = 0 \\ \mathit{0}, & \text{otherwise} \end{cases} \tag{4.65}$$

Proof. Let $\mathcal{P}(\phi,\sigma|\hat{x})$ be the set of optimal dual variables for $SPD_q^{ev}(\phi,\sigma|\hat{x})$ problem as identified in Proposition 4. Then we can remodel the problem without the complicating Constraints (4.61) as follows:

$$\text{minimize} \sum_{\substack{a\in A_{ev}^q \\ i\in K_a^q}} \bar{x}_i\phi_a^q + \sigma_q \tag{4.66}$$

subject to

$$(\sigma_q, \phi_a^q) \in \mathcal{P}(\phi,\sigma|\hat{x}) \tag{4.67}$$

Note that we have two conditions in Proposition 4 depending on the optimal value of $z(q)$.

Case (1) If the path $q \in Q$ is not chargeable (i.e., $z_q = 0$), then the optimal solution of $MW_q^{ev}(\phi, \sigma|\hat{x}, \bar{x})$ problem is $\phi_a^q = f_{ev}^q d^q$ for $a = \text{argmin}_{b \in \mathcal{A}_0^q(\hat{x})}\{\sum_{i \in K_b^q} \bar{x}_i\}$ and all of the remaining variables are equal to zero.

Case (2) If a given path $q \in Q^{ev}$ is chargeable (i.e., $z_q = 1$), then we can find the optimal solution of the $MW_q^{ev}(\phi, \sigma|\hat{x}, \bar{x})$ problem by investigating the tradeoff between the objective function coefficients of σ and ϕ. First of all, observe that if $|\mathcal{A}_1^q(\hat{x})| = 0$, then the only optimal solution can be attained by letting $\sigma_q = f_{ev}^q d^q$ and all of the remaining variables equal to zero. Otherwise, if $|\mathcal{A}_1^q(\hat{x})| \geq 1$, then we check if $\sum_{i \in K_a^q} \bar{x}_i > 1$, $\forall a \in \mathcal{A}_1^q(\hat{x})$ in which case, assigning $\sigma = f_{ev}^q d^q$ and all of the remaining variables equal to zero produces the optimal solution for $MW_q^{ev}(\phi, \sigma|\hat{x}, \bar{x})$. Lastly, if $|\mathcal{A}_1^q(\hat{x})| \neq 0$ and $\sum_{i \in K_a^q} \bar{x}_i \leq 1$, then we select the arc with $a = \text{argmin}_{b \in \mathcal{A}_1^q(\hat{x})}\{\sum_{i \in K_b^q} \bar{x}_i\}$ and assign $\phi_a^q = f_{ev}^q d^q$ and all of the remaining variables equal to zero. We now have the desired result as presented in Proposition 6. $\square$

In a similar fashion, we can construct the optimal variable values of the $MW_{qa}^{phev}(\mu, \rho|\hat{x}, \bar{x})$ problem, which is defined as:

$$\text{minimize} \quad \sum_{i \in R_a^q \setminus s(q)} \bar{x}_i \mu_a^{qi} + \rho_a^q \tag{4.68}$$

subject to

$$\sum_{i \in R_a^q \setminus s(q)} \hat{x}_i \mu_a^{qi} + \rho_a^q = \mathbf{opt}(SPD_{qa}^{phev}(\mu, \rho|\hat{x})) \tag{4.69}$$

$$\mu_a^{qi} + \rho_a^q \geq f_{phev}^q d_a^{qi} \qquad \forall i \in R_a^q \setminus s(q) \tag{4.70}$$

$$\rho_a^q \geq f_{phev}^q d_a^{qs(q)} \qquad s(q) \in R_a^q \tag{4.71}$$

$$\mu_a^{qi}, \rho_a^q \geq 0 \qquad \forall i \in R_a^q \setminus s(q) \tag{4.72}$$

Proposition 7. *The following solution is optimal for* $MW_{qa}^{phev}(\mu, \rho|\hat{x}, \bar{x})$.

1) **If** $y_{\hat{a}}^{\hat{q}j} = 1$ *for* $j \neq s(\hat{q})$*, then:*

$$\rho_a^q = \text{argmin}_{\lambda \in S_a^q}\Big(\sum_{\substack{i \in R_a^q \setminus s(q) \\ i \notin K^\star(\hat{x})}} \big(\bar{x}_i \max\{0, f_{phev}^q d_a^{qi} - \lambda\}\big) + (1 - \bar{x}_j)\lambda \Big)$$

where $\rho_{max} = f_{phev}^q d_a^{qj}$ *and* $\rho_{min} = \max\{f_{phev}^q d_a^{qs(q)}, \max_{i \in R_a^q \cap K^\star(\hat{x}), i \neq j, i \neq s(q)} f_{phev}^q d_a^{qi}\}$ *(Note that* ρ_{max} *and* ρ_{min} *are constants)* and $S_a^q = \{\rho_{min}, \rho_{max}\} \cup \{f_{phev}^q d_a^{qi} : \rho_{min} \leq f_{phev}^q d_a^{qi} \leq \rho_{max}$ *and* $i \in R_a^q, \forall i \notin K^\star(\hat{x}), i \neq s(q), i \neq j\}$

else if $y_{\hat{a}}^{\hat{q}s(\hat{q})} = 1$ *then,* $\rho_a^q = f_{phev}^q d_a^{qs(q)}$

else $\rho_a^q = 0$.

2) $\mu_a^{qi} = \max\{0, f_{phev}^q d_a^{qi} - \rho_a^q\}, \ i \in R_a^q \setminus s(q)$

Proof. Similar to the $MW_q^{ev}(\phi, \sigma|\hat{x}, \bar{x})$ problem, $MW_{qa}^{phev}(\mu, \rho|\hat{x}, \bar{x})$ can also be modeled using the conditions in Proposition 5. Note that we have three conditions in Proposition 5 depending on the optimal value of y_a^{qi}. There is a unique optimal solution for both *Case (1)* and *Case (2)*. They are also optimal for the $MW_{qa}^{phev}(\mu, \rho|\hat{x}, \bar{x})$ problem. When we have $y_a^{qj} = 1$ for $j \neq s(q)$, that is *Case (3)*, $MW_{qa}^{phev}(\mu, \rho|\hat{x}, \bar{x})$ can be written as:

$$\text{minimize} \quad \sum_{i \in R_a^q \setminus s(q)} \bar{x}_i \mu_a^{qi} + \rho_a^q \tag{4.73}$$

subject to

$$\mu_a^{qj} + \rho_a^q = f_{phev}^q d_a^{qj} \tag{4.74}$$

$$\mu_a^{qi} = 0 \qquad \forall i \in R_a^q, \forall i \in K^\star(\hat{x}), i \neq s(q), i \neq j \tag{4.75}$$

$$\rho_a^q \geq f_{phev}^q d_a^{qi} \qquad \forall i \in R_a^q, \forall i \in K^\star(\hat{x}), i \neq s(q), i \neq j \tag{4.76}$$

$$\mu_a^{qi} + \rho_a^q \geq f_{phev}^q d_a^{qi} \qquad \forall i \in R_a^q, \forall i \notin K^\star(\hat{x}), i \neq s(q), i \neq j \tag{4.77}$$

$$\rho_a^q \geq f_{phev}^q d_a^{qs(q)} \qquad \text{if } s(q) \in R_a^q \tag{4.78}$$

$$\mu_a^{qi}, \rho_a^q \geq 0 \qquad \forall i \in R_a^q, i \notin K^\star(\hat{x}), i \neq s(q) \tag{4.79}$$

Note that the optimality conditions given in Proposition 5 are simply appended as constraints to the above model. This ensures that our optimal solution for $MW_{qa}^{phev}(\mu,\rho|\hat{x},\bar{x})$ is also optimal for $SPD^{phev}(\mu,\rho|\hat{x})$. In this model, we have $\mu_a^{qj} = f_{phev}^q d_a^{qj} - \rho_a^q$ due to Constraints (4.74). Rewriting μ_a^{qj}, and letting $\mu_a^{qi} = 0$, $\forall i \in R_a^q, \forall i \in K^\star(\hat{x}), i \neq s(q), i \neq j$, we have an equivalent model:

$$\bar{x}_j f_{phev}^q d_a^{qj} + \text{ minimize } \sum_{\substack{i \in R_a^q \setminus s(q) \\ i \notin K^\star(\hat{x})}} \bar{x}_i \mu_a^{qi} + (1-\bar{x}_j)\rho_a^q \tag{4.80}$$

subject to

$$\rho_a^q \geq f_{phev}^q d_a^{qi} \qquad \forall i \in R_a^q, i \in K^\star(\hat{x}), i \neq s(q), i \neq j \tag{4.81}$$

$$\mu_a^{qi} + \rho_a^q \geq f_{phev}^q d_a^{qi} \qquad \forall i \in R_a^q, \forall i \notin K^\star(\hat{x}), i \neq s(q), i \neq j \tag{4.82}$$

$$\rho_a^q \geq f_{phev}^q d_a^{qs(q)} \qquad \text{if } s(q) \in R_a^q \tag{4.83}$$

$$f_{phev}^q d_a^{qj} - \rho_a^q \geq 0 \tag{4.84}$$

$$\mu_a^{qi}, \rho_a^q \geq 0 \qquad \forall i \in R_a^q, i \notin K^\star(\hat{x}), i \neq s(q) \tag{4.85}$$

Observe that Constraints (4.81), (4.83) and (4.84) can be combined as $\rho_{max} \geq \rho_a^q \geq \rho_{min}$, where $\rho_{max} = f_{phev}^q d_a^{qj}$ and $\rho_{min} = \max\{f_{phev}^q d_a^{qs(q)}, \max_{i \in R_a^q \cap K^\star(\hat{x}), i \neq j, i \neq s(q)} f_{phev}^q d_a^{qi}\}$. The model is then:

$$\bar{x}_j f_{phev}^q d_a^{qj} + \text{ minimize } \sum_{\substack{i \in R_a^q \setminus s(q) \\ i \notin K^\star(\hat{x})}} \bar{x}_i \mu_a^{qi} + (1-\bar{x}_j)\rho_a^q \tag{4.86}$$

subject to

$$\mu_a^{qi} + \rho_a^q \geq f_{phev}^q d_a^{qi} \qquad \forall i \in R_a^q, \forall i \notin K^\star(\hat{x}), i \neq s(q), i \neq j \tag{4.87}$$

$$\rho_{max} \geq \rho_a^q \geq \rho_{min} \tag{4.88}$$

$$\mu_a^{qi} \geq 0 \qquad \forall i \in R_a^q, i \notin K^\star(\hat{x}), i \neq s(q) \tag{4.89}$$

In this model, we can determine the optimal μ values once we know the optimal value of ρ. At this point, note that the set of values that ρ can assume are from the set $S_a^q = \{\rho_{min}, \rho_{max}\} \cup \{f_{phev}^q d_a^{qi} : \rho_{min} \leq f_{phev}^q d_a^{qi} \leq \rho_{max}$ and $i \in R_a^q, \forall i \notin K^\star(\hat{x}), i \neq s(q), i \neq j\}$. Any other possible value for the ρ variable would either be suboptimal or infeasible. Thus, the following solution is optimal for $MW_{qa}^{phev}(\mu, \rho | \hat{x}, \bar{x})$.

$$\rho_a^q = \text{argmin}_{\lambda \in S_a^q}\Big(\sum_{\substack{i \in R_a^q \setminus s(q) \\ i \notin K^\star(\hat{x})}} \big(\bar{x}_i \max\{0, f_{phev}^q d_a^{qi} - \lambda\}\big) + (1 - \bar{x}_j)\lambda\Big) \tag{4.90}$$

$$\mu_a^{qi} = \max\{0, f_{phev}^q d_a^{qi} - \rho_a^q\} \tag{4.91}$$

Observe that the solution given in Proposition 7, are the solutions of the models given in the above cases. This completes the proof. □

Remark 3. *In a regular MW framework, two different LP problems are needed to be solved for every subproblem, one to obtain the optimal value of the the subproblem, and one for the MW problem. However, in our particular case, we are able to construct the primal subproblem solution, the dual subproblem solution and a Pareto-optimal cut directly, without any need to build an LP.*

4.4 Computational Study

In this section, we present performance analyses of the HCSLM model and the BD algorithm with three different cut selection schemes. Note that in all three decomposition implementations, we only construct one search tree, and solve the master problem using branch and cut method. In order to compare the computational performances of the solution techniques, computational studies are carried out on two datasets. The first one, shown in Figure 4.1, is a 25-node dataset commonly used in the literature [34, 130, 226]. A second dataset is a real-world representation of the California (CA) road network as presented in Figure 4.2 [48, 125]. The data related to network specifications are presented in Table 4.1.

Table 4.1: Road network features

				node degree		
network	#nodes	# OD pair nodes	#edges	min	max	mean
25-node	25	300	86	1	6	3.36
California (CA)	339	1167	1234	1	7	3.64

All of the instances are run on a desktop computer with 3.16GHz 2xDuo CPU, 2.00GB RAM. The algorithms are implemented using Java and CPLEX 12.5 [227] with Concert Technology.

4.4.1 25-node Road Network

In the 25-node road network, all nodes are assumed to be origin and destination nodes similar to previous studies. Following the convention in the literature, we assume that the demand between OD pairs is directly proportional with the populations of the origin and the destination nodes, and inversely proportional with the distance between the OD pair, and the calculation of the vehicle flow is due to gravity model by Hodgson [226]. The ranges considered in the 25-node network in previous studies are 4, 8, and 12. Since we can handle multiple vehicle types in the same problem, we consider EVs and PHEVs with ranges 4, 8 and 12 for every OD pair with equal flows as attained from the gravity model. With these settings, we solved the problem using the BD algorithm with singlecut, multicut and Pareto-optimal cut generation schemes. The p value range is from 1 to 25. The results are presented in Table 4.2. In the table, the second column represents the optimal solution value. We express this value as the percentage of covered distance with respect to the *total coverable distance*. Total coverable distance is defined as the difference in the objective function value of the HCSLM model when a charging station is located at all of the nodes in the network and when no charging station is located in the network. Corresponding to each of the three solution methods, there are seven columns. *# Subproblems* shows the number of subproblems solved,

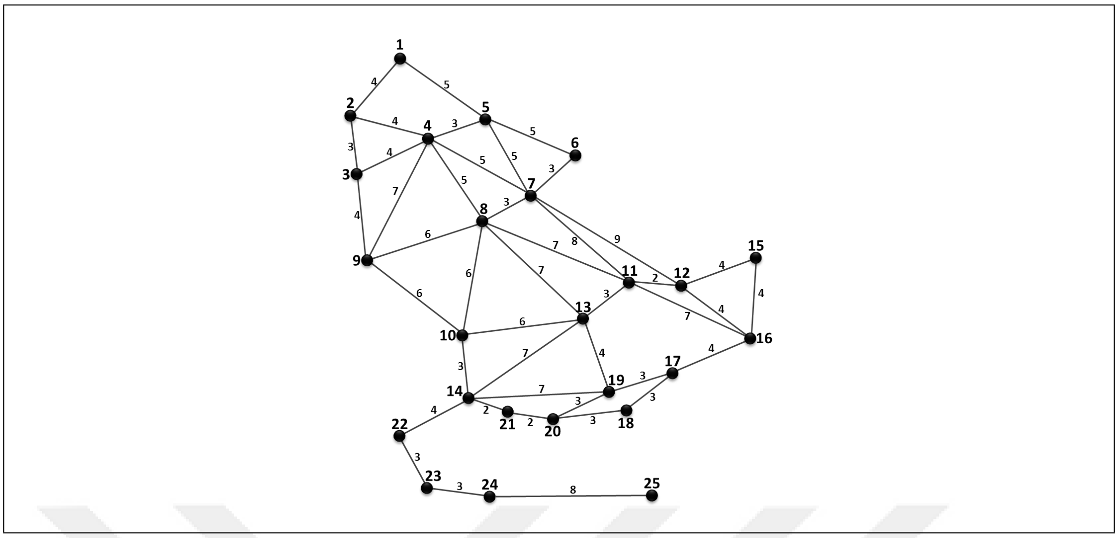

Figure 4.1: 25-node road network

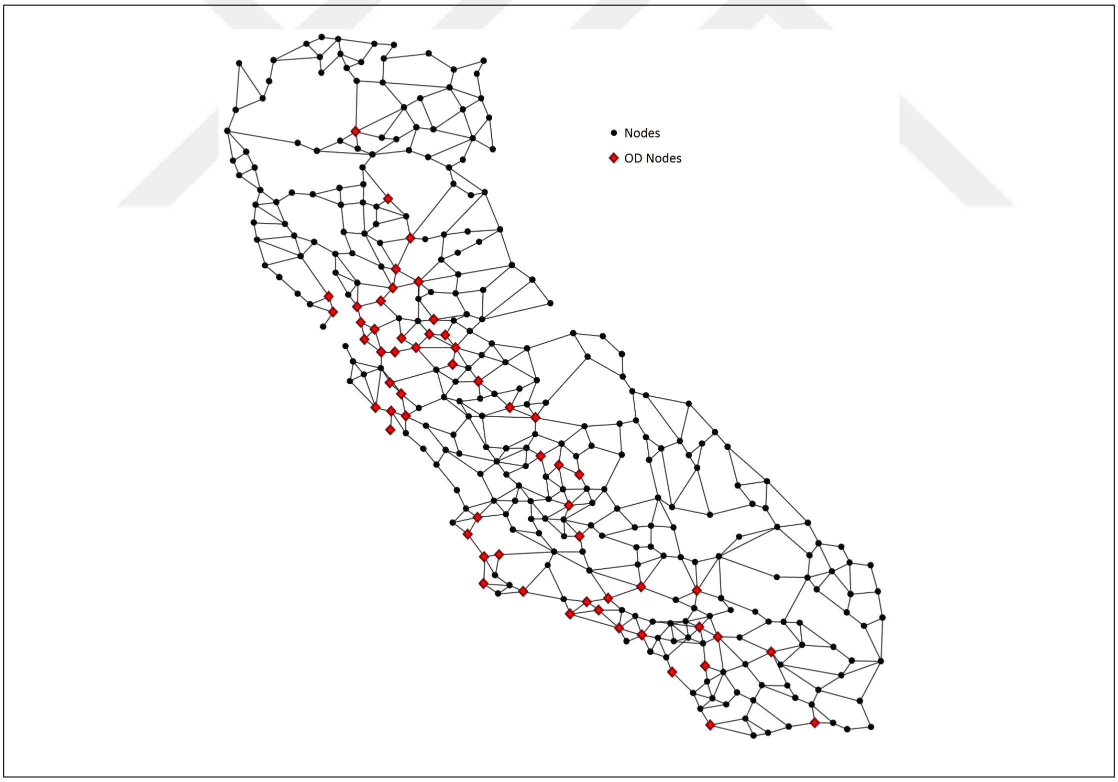

Figure 4.2: California state road network

Cuts is the total number of cuts added, *Preprocessing Time, Master Sol.Time* and *Subp.Sol.Time* show the preprocessing time, master problem solution time and the subproblem solution time, respectively. *Avg.Subp.Sol.Time* is the average solution time of a single subproblem, found by dividing the *Subp.Sol.Time* by the *# Subproblems*. *Total Sol.Time* column is the total running time, which equals to the summation of preprocessing, subproblem and master problem solution times.

There are some critical insights regarding the nature of the solution techniques. BD algorithm with singlecut implementation generally solves the most number of subproblems while the multicut implementation requires to solve the least number of subproblems to arrive at the optimal solution. However, the number of cuts added to the master problem is far more in multicut implementation than the other two cut implementations. The Pareto-optimal cut implementation solves more subproblems than the multicut, but the cuts added are far less in number. On the average, the Pareto-optimal cut generation scheme solves the problems faster than the other two cut generation techniques. As it will be apparent in the following parts, similar line of results can be observed in larger sized networks.

Table 4.2: 25-node road network results

Problem		HCSLM	Singlecut Implementation							Multicut Implementation							Pareto-optimal Cut Implementation						
p	Opt.Sol. (%)	Total Sol. Time (s)	# Subproblems	# Cuts	Prep. Sol.Time (s)	Master Sol.Time (s)	Subp. Sol.Time (s)	Avg. Subp. Sol. Time (s)	Total Sol. Time (s)	# Subproblems	# Cuts	Prep. Sol.Time (s)	Master Sol.Time (s)	Subp. Sol.Time (s)	Avg. Subp. Sol. Time (s)	Total Sol. Time (s)	# Subproblems	# Cuts	Prep. Sol.Time (s)	Master Sol.Time (s)	Subp. Sol.Time (s)	Avg. Subp. Sol. Time (s)	Total Sol. Time (s)
1	23.07	1.35	3	2	0.03	0.07	0.09	0.03	0.18	2	4212	0.03	0.08	0.27	0.13	0.37	3	2	0.05	0.12	0.11	0.04	0.28
2	32.60	0.60	10	9	0.04	0.01	0.13	0.01	0.19	4	4638	0.08	0.14	0.44	0.11	0.65	9	7	0.05	0.19	0.29	0.03	0.52
3	40.76	0.89	34	30	0.02	0.02	0.44	0.01	0.48	6	4948	0.04	0.19	0.60	0.10	0.83	15	11	0.05	0.18	0.37	0.02	0.60
4	50.55	0.53	42	37	0.02	0.04	0.53	0.01	0.58	4	4862	0.03	0.17	0.43	0.11	0.63	16	13	0.05	0.18	0.41	0.03	0.64
5	59.17	0.64	51	47	0.02	0.05	0.65	0.01	0.72	4	4947	0.04	0.15	0.45	0.11	0.65	15	11	0.05	0.18	0.40	0.03	0.62
6	66.38	0.50	56	52	0.02	0.07	0.71	0.01	0.79	4	5071	0.03	0.19	0.48	0.12	0.71	11	9	0.05	1.45	0.30	0.03	1.81
7	71.29	0.47	85	80	0.02	0.12	1.07	0.01	1.20	5	5188	0.03	0.15	0.70	0.14	0.88	17	14	0.05	0.18	0.46	0.03	0.69
8	75.88	0.41	125	118	0.02	0.18	1.56	0.01	1.76	7	5192	0.03	0.15	0.82	0.12	1.01	15	13	0.05	0.17	0.42	0.03	0.65
9	80.17	0.38	138	132	0.02	0.20	1.72	0.01	1.94	6	5246	0.03	0.15	0.77	0.13	0.96	13	9	0.05	0.17	0.37	0.03	0.59
10	84.75	0.32	105	99	0.02	0.15	1.42	0.01	1.58	5	5249	0.03	0.11	0.70	0.14	0.84	9	6	0.05	0.15	0.27	0.03	0.47
11	87.55	0.31	103	95	0.02	0.16	1.28	0.01	1.46	9	5420	0.03	0.13	1.14	0.13	1.30	18	12	0.05	0.20	0.51	0.03	0.76
12	90.16	0.31	112	102	0.02	0.15	1.39	0.01	1.56	7	5555	0.03	0.13	0.91	0.13	1.08	13	11	0.05	0.17	0.40	0.03	0.62
13	92.78	0.35	95	89	0.02	0.11	1.17	0.01	1.30	7	5578	0.03	0.14	0.86	0.12	1.03	16	12	0.05	0.18	0.43	0.03	0.66
14	95.11	0.29	63	58	0.02	0.06	0.79	0.01	0.87	6	5584	0.03	0.11	0.78	0.13	0.92	12	9	0.05	0.17	0.38	0.03	0.60
15	97.12	0.27	45	35	0.02	0.03	0.56	0.01	0.61	6	5632	0.03	0.11	0.79	0.13	0.93	9	8	0.05	0.15	0.28	0.03	0.48
16	98.69	0.26	27	21	0.02	0.02	0.34	0.01	0.38	6	5627	0.03	0.12	0.78	0.13	0.94	7	6	0.05	0.15	0.25	0.04	0.45
17	99.58	0.22	26	21	0.02	0.02	0.32	0.01	0.36	4	5657	0.03	0.07	0.52	0.13	0.62	8	6	0.05	0.17	0.30	0.04	0.52
18	99.86	0.29	22	17	0.02	0.02	0.28	0.01	0.31	4	5683	0.07	0.06	0.53	0.13	0.66	4	3	0.05	0.15	0.18	0.04	0.37
19	100.00	0.22	6	4	0.02	0.01	0.08	0.01	0.11	4	5730	0.03	0.05	0.50	0.12	0.59	4	3	0.05	0.15	0.18	0.04	0.37
20	100.00	0.22	3	2	0.02	0.01	0.04	0.01	0.07	3	5709	0.03	0.05	0.42	0.14	0.50	3	2	0.05	0.14	0.13	0.04	0.32
21	100.00	0.22	3	2	0.02	0.01	0.04	0.01	0.07	3	5709	0.03	0.04	0.51	0.17	0.59	3	2	0.05	0.14	0.13	0.04	0.32
22	100.00	0.23	3	2	0.02	0.01	0.04	0.01	0.06	3	5709	0.03	0.05	0.44	0.15	0.52	3	2	0.05	0.14	0.13	0.04	0.32
23	100.00	0.22	3	2	0.02	0.01	0.04	0.01	0.06	3	5709	0.03	0.05	0.39	0.13	0.47	3	2	0.05	0.14	0.13	0.04	0.32
24	100.00	0.30	3	2	0.02	0.01	0.05	0.02	0.07	3	5709	0.04	0.06	0.41	0.14	0.51	3	2	0.05	0.14	0.13	0.04	0.32
25	100.00	0.12	2	1	0.02	0.01	0.03	0.01	0.05	2	2719	0.03	0.02	0.27	0.13	0.32	2	1	0.05	0.14	0.11	0.05	0.30

4.4.2 California Road Network

CA dataset is a real world representation of the California road network with 339 nodes and 1234 arcs. 57 centers with a population of 50,000 or above are selected as the origin and destination nodes. Similar to Yıldız et al. [125], we consider all pairings of these nodes with a 30 miles or more distance in between. There are 1167 such pairings as presented in Table 4.1. As done in the 25-node network case, the vehicle flows between pairings are calculated using the gravity model [226].

Related to EV and PHEV sales numbers, Center for Sustainable Energy [140] reports new-vehicle rebates on behalf of the California Air Resource Boards Clean Vehicle Rebate Project (CVRP). We can extract EV and PHEV sales versus brands, and obtain Tables 4.3 and 4.4. The tables show the EV and PHEV sales in California state for vehicles with different ranges, respectively. 25.43% of the total EV sales have an extended range of 426 kilometers (265 miles), and 45.13% of the PHEVs have a range of 61 kilometers (38 miles). Therefore, we have 6 copies for each of the 1167 OD pairs, three of them representing the EVs with different ranges, and the remaining three representing the PHEVs with different ranges.

Table 4.3: EV sales

Designator	Range (km)	Percentage in total EV sales (%)
EV-1	426	25.43
EV-2	142	19.58
EV-3	132	54.99

Table 4.4: PHEV sales

Designator	Range (km)	Percentage in total PHEV sales (%)
PHEV-1	61	45.13
PHEV-2	32	20.46
PHEV-3	19	34.41

Table 4.5: California road network results

Problem		HCSLM	Singlecut Implementation						Multicut Implementation					Pareto-optimal Cut Implementation				
p	Opt.Sol. (%)	Total Sol. Time (s)	# Subproblems	# Cuts	Master Sol.Time (s)	Subp. Sol.Time (s)	Total Sol. Time (s)	Gap (%)	# Subproblems	# Cut	Master Sol.Time (s)	Subp. Sol.Time (s)	Total Sol. Time (s)	# Subproblems	# Cuts	Master Sol.Time (s)	Subp. Sol.Time (s)	Total Sol. Time (s)
1	40.84	1438.72	6	5	0.26	4.07	7.86	-	2	58665	10.33	31.70	48.24	3	2	0.14	2.49	6.10
2	59.04	1258.87	20	14	0.03	13.45	16.42	-	2	58665	4.19	31.28	40.87	8	5	0.14	6.85	10.46
3	66.38	1335.37	53	46	0.25	36.91	40.10	-	4	66563	11.37	98.20	114.96	12	8	0.13	11.02	14.61
4	70.27	1547.52	215	209	1.20	150.74	154.89	-	8	73896	29.77	172.13	207.32	18	11	0.15	17.49	21.11
5	73.64	1626.40	572	559	9.36	413.04	425.44	-	7	75363	33.96	155.03	194.42	24	17	0.16	24.90	28.53
6	76.92	1352.06	792	782	25.70	561.75	590.39	-	5	78716	29.85	113.36	148.65	20	15	0.15	20.46	24.09
7	79.47	1850.89	1397	1384	128.41	996.71	1128.11	-	7	85985	32.07	179.31	216.60	28	19	0.16	30.10	33.75
8	82.02	1576.26	1247	1238	198.84	882.96	1084.82	-	6	88099	27.50	166.40	199.18	35	23	0.20	39.17	42.85
9	84.27	1128.04	1023	1009	162.98	734.19	900.09	-	8	85900	30.61	220.09	256.28	22	16	0.18	27.54	31.20
10	86.02	1136.14	991	975	208.00	726.91	937.92	-	5	88709	36.31	133.95	175.97	28	21	0.23	31.35	35.05
11	87.58	1318.24	850	836	222.13	622.46	847.60	-	5	88912	41.66	132.07	179.93	24	17	0.23	26.51	30.22
12	89.10	880.49	463	447	157.83	330.18	490.99	-	5	88577	20.76	131.76	158.70	30	20	0.26	34.73	38.47
13	90.30	879.33	373	354	79.50	272.73	355.14	-	6	90106	27.84	179.12	213.63	30	20	0.22	33.64	37.32
14	91.28	656.85	318	303	136.29	226.66	365.88	-	5	89886	31.81	155.67	194.13	29	19	0.23	32.76	36.45
15	91.94	631.22	662	650	915.42	485.42	1403.86	-	4	89693	52.89	133.40	193.04	33	24	0.23	37.99	41.69
16	92.53	674.54	1384	1373	2615.08	984.84	3602.89	0.19	6	90455	41.31	184.44	232.62	36	26	0.29	41.61	45.37
17	93.07	648.92	2267	2246	1985.06	1614.86	3602.88	0.29	6	90523	38.41	208.56	254.84	46	34	0.26	54.42	58.14
18	93.58	640.30	2008	1989	2135.91	1464.04	3602.98	0.38	9	93020	36.89	306.72	351.38	48	34	0.44	56.84	60.75
19	94.05	569.41	2912	2897	1487.57	2112.40	3602.92	0.44	8	93526	34.42	314.92	357.77	54	39	0.42	64.21	68.10
20	94.49	643.31	2692	2671	1684.34	1915.58	3602.86	0.41	7	93856	46.54	297.96	353.66	52	42	0.55	62.95	66.99
30	97.19	643.48	3289	3260	1239.46	2360.48	3602.97	0.51	15	101608	75.82	314.60	396.63	94	73	1.07	117.83	122.38
40	98.57	508.04	3278	3247	1266.05	2334.53	3603.56	0.32	15	105093	200.75	315.07	521.23	90	74	3.66	115.79	122.91
50	99.31	378.55	3177	3147	1357.27	2242.65	3602.89	0.19	12	106324	178.92	284.71	469.03	102	80	2.32	131.88	137.67
60	99.74	409.56	1419	1383	2608.32	991.69	3602.96	0.06	20	106796	242.35	458.60	706.33	110	88	5.79	142.47	151.72
70	99.93	237.89	291	258	3400.67	200.70	3604.88	0.01	10	106910	120.71	229.34	355.45	81	61	0.67	103.26	107.40
80	99.97	179.91	185	158	3.15	126.46	132.59	-	7	107154	74.11	191.22	270.73	77	55	0.60	98.59	102.66
90	99.98	123.81	146	124	0.81	98.14	101.90	-	7	106825	41.91	181.78	229.04	53	38	0.40	67.15	71.02
100	100.00	208.42	130	112	0.71	84.89	89.11	-	4	106568	27.03	119.42	151.66	44	37	0.25	55.92	59.63

Table 4.6: Summary of computational results

Parameter	HCSLM	Singlecut	Multicut	Pareto-optimal
Avg. # Subproblems	-	1148.57	7.32	43.96
Avg. # Cuts	-	1131.29	89871.18	32.79
Avg. Prep. Sol.Time (s)	-	3.03	6.12	3.47
Avg. Master Sol.Time (s)	-	786.81	56.43	0.70
Avg. Subp. Sol.Time (s)	-	821.05	194.31	53.21
Avg. Subp. Sol. Time (s)	-	0.71	26.91	1.14
Avg. Total Sol. Time (s)	874.38	>1610.88	256.87	57.38

Regarding the solution of the California road network instances, the results are presented in Table 4.5. We present the results for the problem instances ranging from $p = 1$, through $p = 20$ with increments of one. After 20 charging stations where the coverage reaches to 94.49%, we increased p by 10, through 100, where the coverage reaches to 100.00%. Optimal solutions could be obtained by the HCSLM model and the BD algorithm with multicut and Pareto-optimal cut implementations. However singlecut implementation terminated with an optimality gap of less than %0.51 for $p = 16$ to $p = 70$ within an hour time-limit. The multicut implementation solution time is much smaller than singlecut implementation, however, it performs worse than the HCSLM model for instances with $p = 50$ to $p = 90$. Also note that the number of cuts added are, on the average, 89871.18 (Table 4.6). The results indicate that the number of subproblems and the solution time of the Pareto-optimal cut implementation do not get overwhelmed for increasing values of p. As seen in Table 4.6, the average number of subproblems is 43.96 with an average solution time of less than one minute, which is on the average 15 times faster than the HCSLM model. Our BD algorithm with Pareto-optimal cut construction performs much faster than the HCSLM model and the other two cut construction techniques especially for smaller p values. The average speedup is nearly 30 times for $p \leq 20$. For greater p values, the runtime of the HCSLM model also decreases and gets closer to the runtimes of the Pareto-optimal cut implementation of the BD algorithm. It is worth noting that even though Benders Decomposition algorithm is mostly used with the objective of solving problems of larger sizes rather than efficiency concerns, our implementation not only guarantees larger problem sizes (due to decomposition) but also presents promising results for the solution time reduction as well. To confirm this assertion, we also doubled the EV and PHEV demands for the CA network. That is, we consider 12 copies of demand for each OD pair rather than 6. In that case, the results of Pareto-optimal cut implementation are presented in Table 4.7. The HCSLM model cannot even write the problem into the memory and results in out-of-memory error for every instance. However, Benders Decomposition algorithm does not explicitly create all the variables in the solution and continues to solve these large-scale instances within reasonable runtimes. Duplicating the demand does not change the number of binary variables in the HCSLM problem, however the increase in the number of variables (namely the y and z variables) is drastic. Thus, the HCSLM model fails to solve the problem. For the BD algorithm, the subproblem solutions and the cuts are constructed in closed form, and this reduces the requirement for extensive memory.

Table 4.8 lists the optimal charging station locations for $p = 1$ through 20. The first column shows the p value. For a given row, an '$\times$' sign shows that the corresponding node, as depicted in Figure 4.3, is selected. For example, for $p = 4$, nodes 2, 3, 5 and 6 are the optimal locations of the charging stations. Observe that the optimal locations of the charging stations are robust in the sense that a node appearing in one solution shows up again in several different forthcoming solutions with increasing p values.

If a node does not show up again, it is generally substituted by other nodes. For instance, node 1 shows up in most of the optimal solutions for $p = 1$ through 9. Then, nodes 12 and 13 start showing up in the optimal solutions for $p = 10$ and onwards. Looking at Figure 4.3, we observe that these nodes are geographically right next to each other. The same is also true for different node combinations as well. In particular,

- Node 1 leaves and nodes 12 and 13 enter the optimal solution set.

Table 4.7: California road network results with demand doubled

Problem		Pareto-optimal cut implementation					
p	Opt.Sol. (%)	# Subproblems	Prep. Sol.Time (s)	Master Sol.Time (s)	Subp. Sol.Time (s)	Avg. Subp. Sol. Time (s)	Total Sol.Time (s)
1	40.84	3	9.85	0.14	75.95	25.32	85.94
2	59.04	8	9.88	0.12	224.42	28.05	234.43
3	66.38	12	9.89	0.13	360.94	30.08	370.96
4	70.27	18	9.88	0.15	578.17	32.12	588.19
5	73.64	24	9.89	0.16	861.42	35.89	871.47
6	76.92	20	9.87	0.15	713.06	35.65	723.09
7	79.47	28	9.90	0.16	1064.44	38.02	1074.50
8	82.02	35	9.89	0.20	1421.13	40.60	1431.22
9	84.27	22	9.90	0.17	876.52	39.84	886.60
10	86.02	28	9.88	0.21	1138.07	40.65	1148.15
11	87.58	24	9.90	0.18	974.51	40.60	984.58
12	89.10	30	9.90	0.22	1275.83	42.53	1285.95
13	90.30	30	9.88	0.17	1244.35	41.48	1254.40
14	91.28	29	9.90	0.18	1209.51	41.71	1219.60
15	91.94	33	9.91	0.19	1422.25	43.10	1432.35
16	92.53	35	9.90	0.37	1523.78	43.54	1534.05
17	93.07	49	9.88	0.24	2210.21	45.11	2220.32
18	93.58	48	9.89	0.41	2197.71	45.79	2208.01
19	94.05	53	9.88	0.34	2429.80	45.85	2440.02
20	94.49	60	9.88	0.32	2866.34	47.77	2876.54
30	97.19	79	9.88	1.28	4000.15	50.63	4011.31
40	98.57	86	9.90	3.83	4545.76	52.86	4559.48
50	99.31	101	9.89	6.66	5388.40	53.35	5404.95
60	99.74	99	9.90	7.06	5317.02	53.71	5333.98
70	99.93	83	9.89	0.60	4411.93	53.16	4422.42
80	99.97	65	9.88	0.42	3427.71	52.73	3438.01
90	99.98	46	9.88	0.31	2413.95	52.48	2424.14
100	100.00	43	9.88	0.20	2248.53	52.29	2258.61

- Node 7 leaves and nodes 2 and 4 enter the optimal solution set.
- Node 8 leaves and nodes 16 and 17 enter the optimal solution set.
- Node 11 leaves and node 14 enters the optimal solution set.
- Node 14 leaves and node 11 reenters the optimal solution set.

For $p = 20$, all nodes shown in Figure 4.3 except 1, 7, 8 and 14 are selected as charging station locations. These 4 nodes, as shown above, are substituted by other nodes in the network.

Table 4.8: Optimal charging station locations for California road network

p	1	2	3	4	5	6	7	8	9	10	11	12	13	14	15	16	17	18	19	20	21	22	23	24
1	×																							
2		×	×																					
3	×			×	×																			
4		×	×		×	×																		
5	×		×		×	×	×																	
6	×		×		×	×	×	×																
7	×		×		×	×	×	×	×															
8	×		×		×	×	×	×	×	×														
9	×	×	×	×	×			×	×	×	×													
10		×	×	×	×			×	×	×	×	×	×											
11		×	×	×	×	×		×	×	×		×	×	×										
12		×	×	×	×	×		×	×	×		×	×	×	×									
13		×	×	×	×	×			×	×		×	×	×	×	×	×							
14		×	×	×	×	×			×	×		×	×	×	×	×	×	×						
15		×	×	×	×	×			×	×	×	×	×		×	×	×	×	×					
16		×	×	×	×	×			×	×	×	×	×		×	×	×	×	×	×				
17		×	×	×	×	×			×	×	×	×	×		×	×	×	×	×	×	×			
18		×	×	×	×	×			×	×	×	×	×		×	×	×	×	×	×	×	×		
19		×	×	×	×	×			×	×	×	×	×		×	×	×	×	×	×	×	×	×	
20		×	×	×	×	×			×	×	×	×	×		×	×	×	×	×	×	×	×	×	×

The initial charging stations start showing up in the middle regions of the state on the highway nodes. Then, the selected nodes start spreading over to north and to the south of the initially selected node. The first 7 charging stations gradually cover the highway nodes to connect the northern cities to the southern cities. The 8^{th} charging station node connects Los Angeles to San Diego. Similarly, the 9^{th} selected node connects San Fransisco to Sacramento. According to the results, initially connecting the northern region to the southern region is critical.

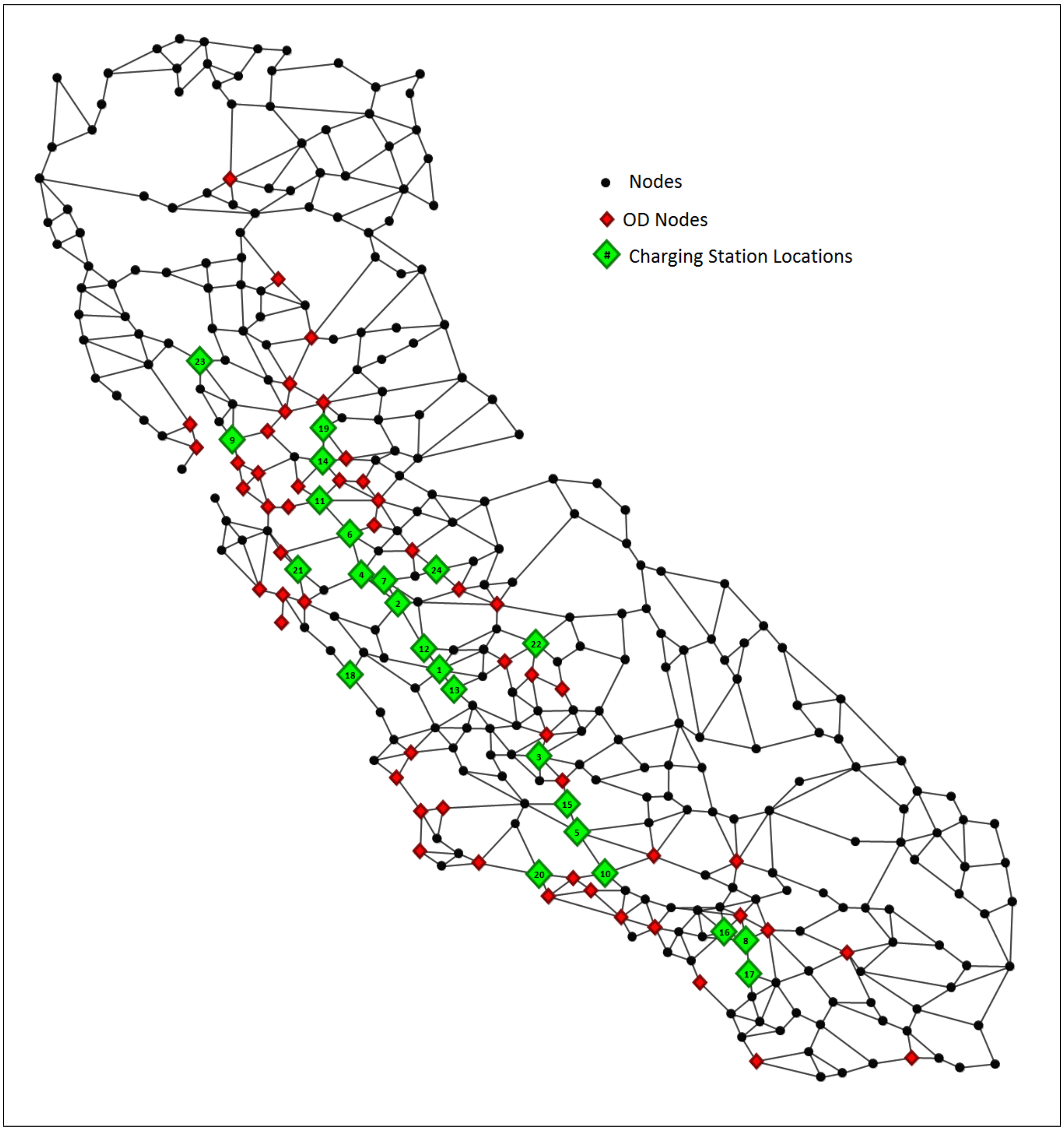

Figure 4.3: Optimal charging station locations for California road network

4.5 Summary

Potential environmental benefits of alternative fuel vehicles (AFVs) such as electric vehicles (EVs) and plug-in hybrid electric vehicles (PHEVs) are widely discussed in the existing literature. Maximizing the vehicle flow might be tricky when it comes to maximizing the environmental benefits, because hybrid vehicles can drive on both regular gasoline and alternative forms of fuels. Even though they are not considered in location decisions, they also widely contribute to the environmental benefits and maximal utilization of alternative-fuels need to be considered as well. Maximizing the electricity usage in transportation is also equivalent to minimizing the total cost under the current cost structure between the electricity and the gasoline.

To this end, we present the hybrid charging station location problem (HCSLP) as an extension of the flow refueling location problem (FRLP). Different than previous studies, we consider hybrid vehicles in addition to single-type fueled vehicles when locating the charging stations. Rather than considering solely the vehicle flows, our objective is to maximize the exploitation of the alternative fuels. With this green viewpoint, we maximize the environmental benefits.

Additionally considering the PHEVs beside EVs complicate the already-difficult FRLP problem. In particular, we deal with this challenge by proposing an effective Benders Decomposition technique. Using the special structure of the formulation, we are able to construct subproblem solutions and associated cuts without the need to build and solve LPs. Furthermore, we can cleverly 'pick' the Pareto-optimal cuts among several alternative cuts. We tested alternative cut construction techniques and results indicate that Pareto-optimal cut generation effectively decreases the solution times in orders of magnitude. Computational studies show that the Benders Algorithm is capable to solve realistic-sized road network instances.

The scope of our problem and algorithm is not limited with PHEVs. It can easily be adapted for all types of hybrid vehicles with minor modifications. Future research in this area can be directed towards considering capacities of the stations. As the number of EVs and PHEVs increase, the capacities of the stations may arise as a critical factor. Furthermore, considering the deviations of the drivers from the shortest paths might be another research direction.

In a different context, we approach the energy management problem in PHEV-penetrated electricity networks in the following chapter.

Chapter 5

Virtual Power Plant Formation in PHEV-penetrated Networks[4]

5.1 Problem Definition

Not only the drivers but also the infrastructure are affected by the introduction of PHEVs into the transportation system, but also the electricity network needs to adapt itself to this new technology. In this context, our problem is the energy management of a VPP in a PHEV-penetrated network. We assume that a group of people come together to form the VPP in order to minimize the cumulative cost and to benefit from the economies of scale. In the present setting, this group is obtaining electricity from the national grid with respect to different tariffs. With the VPP formation, they will become eligible to attain energy from a different set of EPs for potential cost reduction. In this context, there are a number of EPs, including, but not limited to, photovoltaic units, solar and wind farms, fuel cells, hydrogen fuel cells, biomass units and the national grid. The cost for obtaining

[4]An extended version of this chapter is authored by Okan Arslan and Oya Ekin Karaşan and is published in Energy, 60(0): 116-124, 2013 [69].

energy from EPs varies through time. Each EP has an efficiency percentage and a minimum and a maximum power limit. The VPP is responsible for obtaining the required level of energy from the EPs and delivering the energy to a set of consumers with TE and TIE loads. If required, the VPP can also obtain energy from PHEV batteries by discharging them. Preemption (job splitting) is allowed for PHEV battery charging. The PHEV battery has a charging efficiency, which is the percentage of the provided energy that it can actually store. Similarly, the discharge efficiency is the percentage of the energy that it can provide to the VPP from the energy stored in its batteries. Each PHEV has an initial level of charge; and it charges, discharges and consumes energy throughout the day. PHEVs need a minimum level of energy and the battery charge level cannot go below this level. A PHEV travels in a charge-depleting (CD) mode as long as the state-of-charge of the battery is above the minimum level, and switches to a charge-sustaining (CS) mode, traveling using gasoline, once the battery reaches the minimum charge level.

Charge and discharge scheduling is a shared decision between the PHEV owner and the VPP. The PHEV owner decides when to connect, how long the connection will last and the mileage to be traveled in each trip. The VPP is responsible for charge and discharge scheduling decisions and it provides the energy for the PHEV, taking into account the gasoline and electricity generation costs. The VPP achieves this responsibility by dispatching the EPs as necessary.

5.2 Modeling the Problem

This section is made up of two subsections: the first introduces the VPP energy management model, and the second deals with the battery degradation cost modeling.

5.2.1 VPP Energy Management Model

The objective of the VPP energy management model is to minimize the total cost of energy in order to satisfy the loads and to generate the charging and discharging schedules of the PHEVs. The parameters and the variables to be used are presented below:

- *Parameters*

V, U, T	:	Set of PHEVs, EPs and time periods
$I_{v,t}$	:	1 if PHEV v is available for charging during period t, and 0 otherwise
l_t^{TIE}	:	Energy demand to meet the TIE loads during period t (kWh)
$\overline{G}_{u,t}, \underline{G}_{u,t}$	:	Maximum and minimum energy supply by EP u during period t, respectively (kWh)
$\overline{P}_v, \underline{P}_v$	:	Battery maximum and minimum energy capacity of PHEV v, respectively (kWh)
$P0_v$	:	Initial energy stored in battery of PHEV v (kWh)
ρ_v^+, ρ_v^-	:	Total energy transferable to/from PHEV v during one time period, respectively (kWh)
τ_u^+, τ_u^-	:	Minimum up and down times of EP u
η_u^{EP}	:	Efficiency of EP u due to plant side and transformer losses
η_v^+, η_v^-	:	Battery charge and discharge efficiency of PHEV v, respectively
$c_{u,t}^{EP}$	:	Price of obtaining energy from EP u during period t (paid by VPP to EPs)(¢/kWh)
c_t^{gas}	:	Price of gasoline during period t (¢/gallon)
cs_v	:	Average gasoline usage of PHEV v (gallon/mile)
$d_{v,t}^{total}$	:	Total travel distance during period t by PHEV v (miles)
E_v	:	Energy required to run PHEV v on electricity for one mile (kWh)

- *Variables*

$e_{u,t}^{EP}$	:	Energy supply by EP u during period t (kWh)
$e_{v,t}^{PHEV}$	:	Battery energy level of PHEV v at the end of period t (kWh)
$e_{v,t}^{+}, e_{v,t}^{-}$	:	Energy transferred to/from PHEV v during period t (kWh)
$\varphi_{v,t}$	:	1 if PHEV v is charged during period t, 0 otherwise
$d_{v,t}^{CD}, d_{v,t}^{CS}$	:	Travel distance in charge-depleting (CD) and charge-sustaining (CS) mode during period t by PHEV v, respectively (miles)
$E_{v,t}^{req}$	:	Required energy for PHEV v during period t (kWh)
$\delta_{v,t}$	:	Depth of Discharge (DoD) for PHEV v during period t
$c^{bat}(\delta)$	:	Expected battery replacement cost as a function of DoD
$o_{u,t}, s_{u,t}, z_{u,t}$	:	1 if EP u is online, started up or shut down respectively in period t, 0 otherwise
$r_{v,t}$	:	The cost variable of battery deterioration of PHEV v at period t, (used in battery degradation cost function modeling)

The cost minimization model is as follows:

$$\text{minimize} \sum_{t\in T}\Bigg[\sum_{u\in U} c_{u,t}^{EP}\times e_{u,t}^{EP} + \sum_{u\in U} c_{u}^{SU}\times s_{u,t} + \sum_{v\in V}\Big(c_t^{gas}\times cs_v\times d_{v,t}^{CS} + \big[c^{bat}(\delta_{v,t}) - c^{bat}(\delta_{v,t-1})\big]^{+}\Big)\Bigg] \tag{5.1}$$

subject to

$$\underline{P}_v \le e_{v,t}^{PHEV} \le \overline{P}_v; \forall v\in V, \forall t\in T \tag{5.2}$$

$$e_{v,t}^{PHEV} = e_{v,t-1}^{PHEV} + \eta_v^{+}\times e_{v,t}^{+} - \frac{1}{\eta_v^{-}}\times e_{v,t}^{-} - E_{v,t}^{req};\ \forall v\in V, \forall t\in T \tag{5.3}$$

$$e_{v,0}^{PHEV} = P0_v;\ \forall v\in V \tag{5.4}$$

$$e_{v,t}^{+} \le \rho_v^{+}\times I_{v,t}\times\varphi_{v,t};\ \forall v\in V, \forall t\in T \tag{5.5}$$

$$e_{v,t}^{-} \le \rho_v^{-}\times I_{v,t}\times(1-\varphi_{v,t});\ \forall v\in V, \forall t\in T \tag{5.6}$$

$$d_{v,t}^{CD} \le d_{v,t}^{total}; \forall v\in V, \forall t\in T \tag{5.7}$$

$$d_{v,t}^{CD} \le \frac{(e_{v,t-1}^{PHEV} - \underline{P}_v)}{E_v}; \forall v\in V, \forall t\in T \tag{5.8}$$

$$d_{v,t}^{CS} = d_{v,t}^{total} - d_{v,t}^{CD}; \forall v \in V, \forall t \in T \tag{5.9}$$

$$E_{v,t}^{req} = d_{v,t}^{CD} \times E_v; \forall v \in V, \forall t \in T \tag{5.10}$$

$$\delta_{v,t} = 1 - \frac{e_{v,t}^{PHEV}}{\overline{P}_v}; \forall v \in V, \forall t \in T \tag{5.11}$$

$$\sum_{u \in U} \eta_u^{EP} \times e_{u,t}^{EP} + \sum_{v \in V} e_{v,t}^{-} = \sum_{v \in V} e_{v,t}^{+} + l_t^{TIE}; \forall t \in T \tag{5.12}$$

$$o_{u,t} \times \underline{G}_{u,t} \leq e_{u,t}^{EP} \leq o_{u,t} \times \overline{G}_{u,t};\ \forall u \in U, \forall t \in T \tag{5.13}$$

$$o_{u,t} - o_{u,t-1} = s_{u,t} + z_{u,t}; \forall u \in U, \forall t \in T \tag{5.14}$$

$$\sum_{y=t-\tau_u^{+}} s_{u,y} \leq o_{u,t}; \forall u \in U, \forall t \in T \tag{5.15}$$

$$\sum_{y=t-\tau_u^{-}} z_{u,y} \leq 1 - o_{u,t}; \forall u \in U, \forall t \in T \tag{5.16}$$

$$\varphi_{v,t}, o_{u,t}, s_{u,t}, z_{u,t} \in \{0,1\}; \forall u \in U, \forall v \in V, \forall t \in T \tag{5.17}$$

$$e_{u,t}^{EP}, e_{v,t}^{PHEV}, e_{v,t}^{+}, e_{v,t}^{-}, E_{v,t}^{req}, d_{v,t}^{CD}, d_{v,t}^{CS}, \delta_{v,t} \geq 0;\ \forall t \in T,\ \forall v \in V, \forall u \in U \tag{5.18}$$

The objective function minimizes the cost of satisfying the residential loads and PHEV travel requirements. The cost components are: cost of energy generation, startup costs of EPs, gasoline prices and battery degradation cost which is a function of depth of discharge (DoD). Details of this function are presented in the following subsection. Constraints (5.2)-(5.11) are related to PHEVs. (5.2) enforces the minimum and maximum charge limits for each PHEV. (5.3) is the PHEV battery storage balance equation between periods. If the battery is charged (discharged), the stored energy level in the battery in the following period is increased (decreased) accordingly. (5.4) sets the initial battery level of each PHEV. (5.5) and (5.6) jointly ensure that charging and discharging do not occur simultaneously in each period and that either can only occur when the PHEV is connected to the grid. (5.7) and (5.8) together force the distance traveled in CD mode to be the minimum of the 'actual trip distance' and 'possible travel distance with the available energy left in the PHEV battery'. (5.9) sets the CS mode travel distance. (5.10) calculates the energy required to travel the trip distance and (5.11) calculates the DoD for each period. Constraints (5.12)-(5.16) are related to EPs. (5.12) is the energy balance equation. The sum of the total energy obtained from EPs and the discharged energy from the batteries equals the supplied energy for the PHEVs and the TIE loads. (5.13) ensures that the minimum and maximum capacities of each EP are met, and forces the binary variable $o_{u,t}$ to take value 1 if energy is generated by EP u in period t. (5.14) sets the startup and shutdown binary variables to correct values. Constraints (5.15) and (5.16) enforce the minimum and maximum up and down times of EPs. Finally, (5.17) defines the binary variables and (5.18) forces the non-negativity on the variables.

Proposition 8. *In an optimal solution of the VPP Energy Management Model, simultaneous charging and discharging do not occur for any PHEV in any period when the binary variable $\varphi_{v,t}$ is omitted from the formulation.*

Proof. Assume that charging and discharging simultaneously occur for PHEV w during period p in an optimal solution of the above formulation when the binary variable $\varphi_{v,t}$ is omitted. Let $e^{+}_{w,p} = a > 0$ and $e^{-}_{w,p} = b > 0$. Then the VPP supplies a units of energy for the PHEV w and receives b units of energy from the PHEV w. Therefore, the net energy generation required is $a - b$ units. On the other hand, due to the charging and discharging efficiencies of the PHEV w, it actually stores $\eta^{+}_{w} \times a$ units of energy and loses $\frac{1}{\eta^{-}_{w}} \times b$ units of energy back to the VPP. Then, the net energy stored in the PHEV w battery is $c := \eta^{+}_{w} \times a - \frac{1}{\eta^{-}_{w}} \times b$. But c units of energy could be directly provided by only charging $\frac{1}{\eta^{+}_{w}} \times c$ units of energy, which is equal to $a - \frac{1}{(\eta^{+}_{w} \times \eta^{-}_{w})} \times b$. Since $\eta^{+}_{w} < 1$ and $\eta^{-}_{w} < 1$, we have $\frac{1}{\eta^{+}_{w}} \times c < a - b$. Thus, the same level of storage for the battery of PHEV w during period p could be achieved by generating less energy, which means less cost. This contradicts that the solution with simultaneous charging and discharging is the optimal (i.e., the least-cost) solution. □

In other words, because the batteries are not 100% efficient when charging or discharging, it is less costly to charge the required energy directly rather than first charging more energy and then discharging the batteries. Note the non-restrictive underlying assumption that the more energy obtained from EPs, the more cost the VPP incurs. As a result of this theorem, binary variable $\varphi_{v,t}$ can be omitted from the energy management model.

Solving the above model gives the least cost that can be achieved by the VPP. Observe that if we solve the model for only a given vehicle v by taking into account the grid as the single EP, then we obtain the least cost of this PHEV for traveling the desired trip mileage if it was in the national grid domain.

5.2.2 Modeling the Battery Degradation Cost

In order to model the battery degradation cost, we follow a similar methodology to that of Sioshansi and Denholm [228]. The battery of the PHEV has a limited lifespan and it deteriorates through usage. Therefore discharging or depleting the battery shortens its life; and after enough many times, the battery needs to be replaced. Therefore the VPP incurs a cost each time a battery is used. The lifetime of a PHEV battery is inversely proportional with the DoD [229] as shown in Figure 5.1.

Therefore, the more the energy is discharged, the less the lifespan of the battery is; and this implies more cost for deeper discharging. The nonlinearity in the battery deterioration cost as a function of DoD can be approximated with a piecewise linear function. An example battery degradation function for a battery that costs \$4189 is depicted in Figure 5.2. Approximations by a linear function and a 2-piece piecewise linear function are also depicted in this figure.

To handle the linearization of the battery degradation cost function, we adopted the methodology presented in Nemhauser and Wolsey [230]. Consider a piecewise linear function with K pieces and let a_v^i be the DoD values at the break points, and $c^{bat}(a_v^i)$ be the function values evaluated at each a_v^i for $i \in \{1, \ldots, K\}$. Let $r_{v,t} = [c^{bat}(\delta_{v,t}) - c^{bat}(\delta_{v,t-1})]^+$ be the cost variable of battery deterioration of PHEV

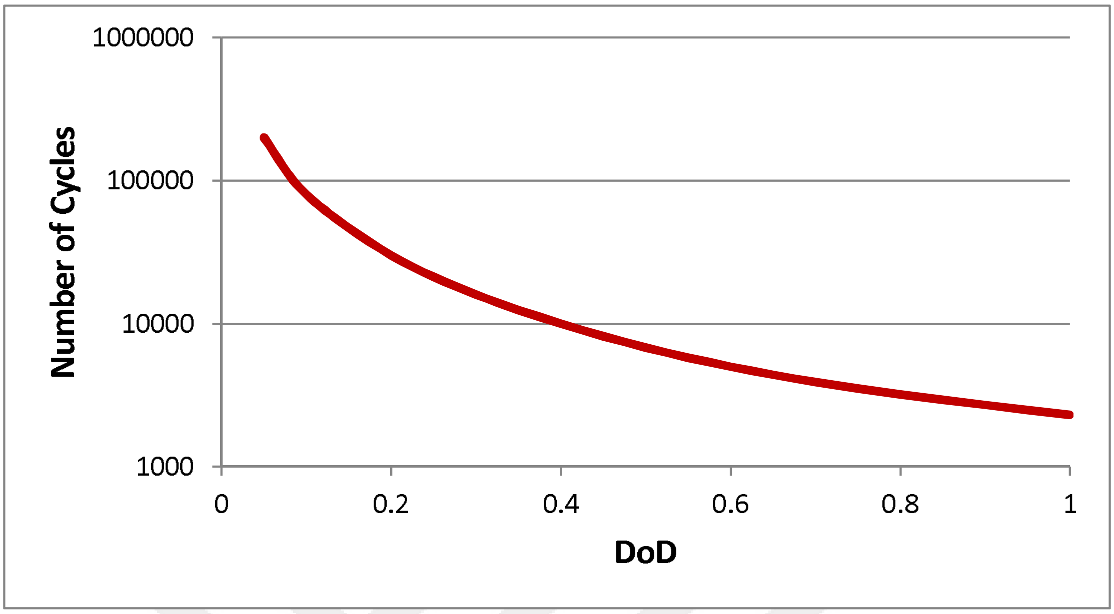

Figure 5.1: Cycle life of PHEV batteries as a function of DoD

v at period t; and $\pi^i_{v,t}$ and $h_{v,t}$ be the auxiliary variables used in linearization. Then, in order to deal with $[c^{bat}(\delta_{v,t}) - c^{bat}(\delta_{v,t-1})]^+$ term, we incorporate the following integer linear program into our model:

$$\text{minimize} \sum_{t \in T} \sum_{v \in V} r_{v,t} \tag{5.19}$$

subject to

$$r_{v,t} \geq \sum_{i=1}^{K} \pi^i_{v,t} \times c^{bat}(a^i_v) - \sum_{i=1}^{K} \pi^i_{v,t-1} \times c^{bat}(a^i_v); \forall v \in V, \forall t \in T \tag{5.20}$$

$$r_{v,t} \geq 0; \forall v \in V, \forall t \in T \tag{5.21}$$

$$\delta_{v,t} = \sum_{i=1}^{K} \pi^i_{v,t} \times a^i_v; \forall v \in V, \forall t \in T \tag{5.22}$$

$$\pi^1_{v,t} \leq h^1_{v,t}; \forall v \in V, \forall t \in T \tag{5.23}$$

$$\pi^i_{v,t} \leq h^i_{v,t} + h^{i-1}_{v,t}; \forall v \in V, \forall t \in T, i = 2, ..., K-1 \tag{5.24}$$

$$\pi^K_{v,t} \leq h^{K-1}_{v,t}; \forall v \in V, \forall t \in T \tag{5.25}$$

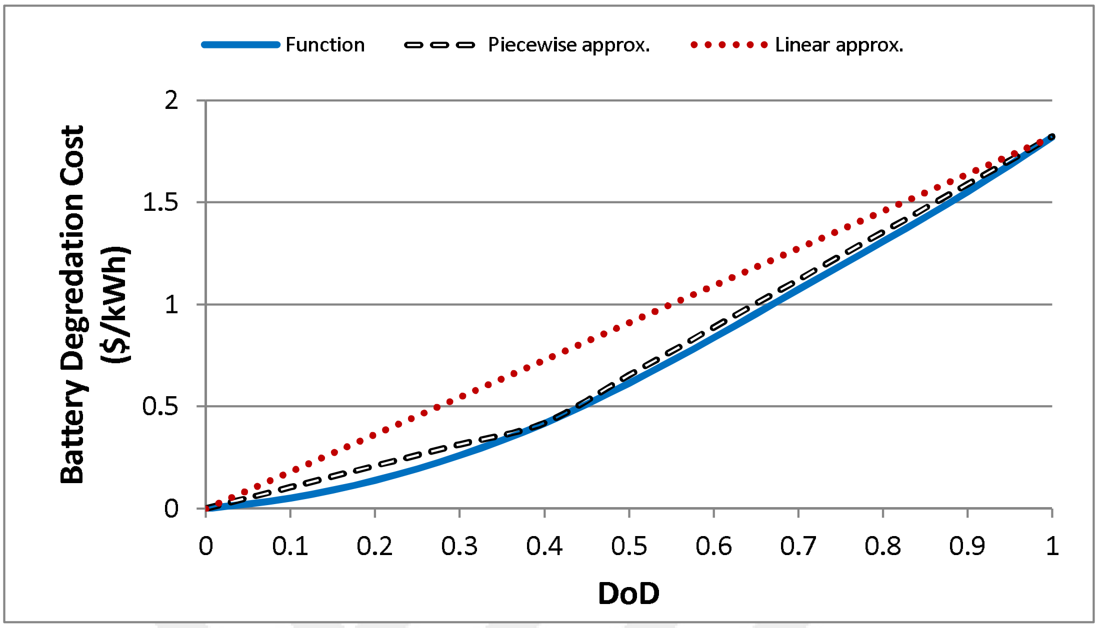

Figure 5.2: Battery degradation cost function and approximating functions

$$\sum_{i=1}^{K} \pi^i_{v,t} = 1; \forall v \in V, \forall t \in T \tag{5.26}$$

$$\sum_{i=1}^{K-1} h^i_{v,t} = 1; \forall v \in V, \forall t \in T \tag{5.27}$$

$$\pi^i_{v,t} \geq 0; \forall v \in V, \forall t \in T \tag{5.28}$$

$$h^i_{v,t} \in \{0,1\}; \forall v \in V, \forall t \in T, i = 1, ..., K-1 \tag{5.29}$$

If $\sum_{t\in T}\sum_{v\in V}[c^{bat}(\delta_{v,t}) - c^{bat}(\delta_{v,t-1})]^+$ term in the objective function of the VPP energy management model is replaced with $\sum_{t\in T}\sum_{v\in V} r_{v,t}$, and constraints (5.20)-(5.29) are appended to (5.2)-(5.18), we obtain an MILP for the energy management problem. The higher the number of the pieces, the better the approximation is of the nonlinear form.

5.3 Case Study

Our research aim is to analyze the cost and emission impacts of VPP formation in PHEV-penetrated networks. In order to achieve this goal, we consider a group of people forming a VPP in the state of California. We compare the cost and emission values to the case when the group members obtain energy from the national grid with respect to the individually optimized tariffs. This way, we are able to measure the value of VPP formation. Furthermore, we consider the VPP formation with and without PHEVs so that we evaluate the value of PHEVs in this formation. We also carry out sensitivity analyses on the gasoline prices, battery prices, energy prices and generation capacities.

5.3.1 Data

We gathered travel patterns, electricity consumption and pricing data for the state of California. The travel data is based on the U.S. Department of Transportation's National Household Travel Survey [231]. We include 26,408 trips, made by 213 compact cars, mid-size cars, large cars and small SUVs in an urban area in the case study. Using this data, we study a hypothetical VPP that serves 574 houses with 213 PHEVs. The data is regarded as a representation of driving patterns for 30 generic days, which accounts to 4.132 different trips daily for each PHEV. The gasoline prices for 30 days are assumed to vary between \$3.037 and \$3.059. Actual trip distances ($d^{total}_{v,t}$) are extracted from the trip data. We assume that all PHEVs and houses are in the VPP's area of responsibility and that the electricity demand of the houses and PHEVs is controlled by the VPP.

Hourly electricity demand per household for TIE loads is obtained from Pacific Gas and Electric Company (PG&E) [232] for 30 days. Hourly TIE load data is multiplied by 574 to obtain the TIE load data (l^{TIE}_t). The hourly TIE load for each of the 30 days changes between the minimum and maximum limits, as shown in Figure 5.3. The peak power is 0.967 MW.

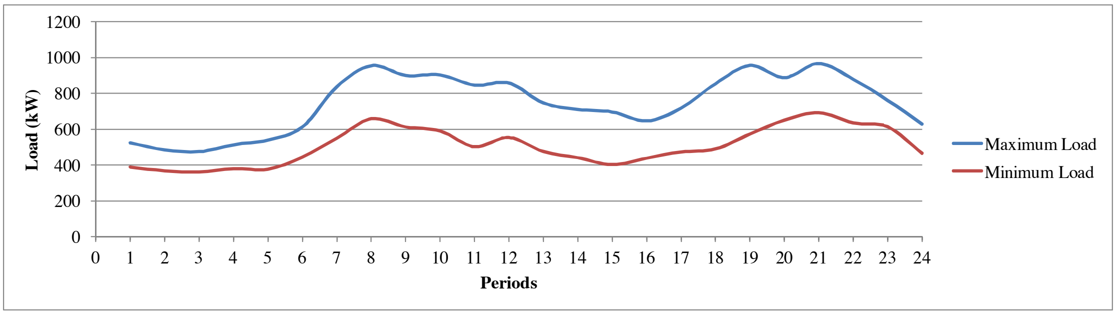

Figure 5.3: Hourly maximum and minimum TIE load data

A day is represented by 24 hourly periods. Similar to previous studies, including [178], PHEVs that are available for a whole hour are regarded as available for charging, and $I_{v,t}$ is set to 1. Average number of PHEVs on road for each time period is shown in Figure 5.4.

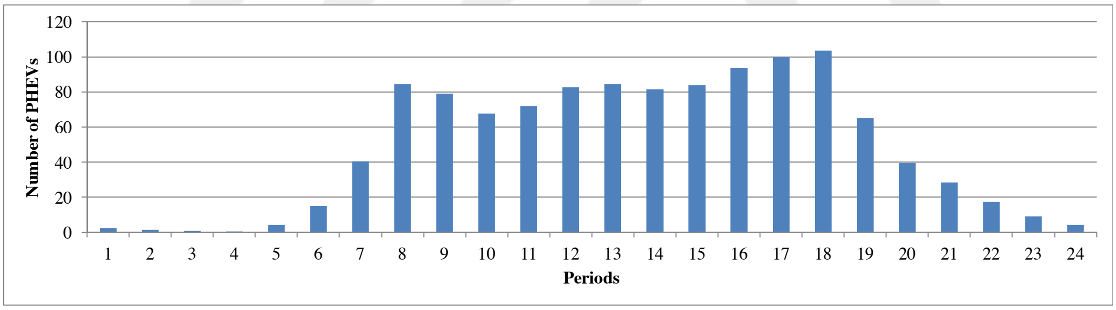

Figure 5.4: Average number of PHEVs on road versus time periods

Table 5.1 lists the energy requirements per mile (E_v), battery capacities ($\overline{P}_v$), battery costs, and the mileage that can be travelled per gallon of gasoline (MPG) in CS mode for each type of vehicle. E_v values are estimated by the Pacific Northwest National Laboratory [233]. We calculate the average gasoline usage of a PHEV (cs_v) as the reciprocal of MPG. The minimum battery storage level ($\underline{P}_v$) and the initial energy stored in batteries ($P0_v$) are assumed to be 10% and 30% of their capacities, respectively. Charging and discharging efficiencies of the batteries (η_v^+ and η_v^-) are 90%. The charge and discharge limits per period (ρ_v^+ and ρ_v^-) are taken as 2.4 kW for all PHEVs.

Table 5.1: Vehicle type specifications

Vehicle Class	Energy Requirement [kWh/mile]	Battery Capacity [kWh]	Battery Cost [$]	MPG in CS-mode
Compact	0.26	8.6	3178	30.2
Mid-Size	0.30	9.9	3377	26.4
Large	0.38	12.5	3776	20.6
Small SUV	0.46	15.2	4189	18

The battery costs shown in Table 5.1 are estimated using the BatPaC 2.1© tool by Argonne National Laboratory [234] and they are used to estimate the expected battery replacement cost function ($c^{bat}(\delta)$) of the batteries. At this point, we note that the expected battery replacement cost functions for each vehicle type for the DoD values between 0 and 1 can be approximated by a single linear function or 2-piece linear function (See Figure 5.2). Solving our model for 30 days with both linear and piecewise linear models, we observe no statistically significant differences in results, but longer solution times for piecewise linear models. Thus, we assume a linear model in the subsequent experimentations in this study.

Thirty-four EPs are included in the case study. The data pertaining to EPs is extracted from the California Energy Comission DER Guide [235] and the Comparative Costs of California Central Station Electricity Generation Report [236] and is shown in Table 5.2 ($\overline{G}_{u,t}$, $c_{u,t}^{EP}$ and η_u^{EP}). For simplicity of the presentation, the minimum and maximum limits of all EPs are assumed to be time invariant. However, our model is capable of handling time-variant data provided that proper data is attainable. The minimum limit ($\underline{G}_{u,t}$) is assumed to be 5 kWh for all EPs, and the minimum up and down times are assumed to be one period for each EP. The VPP can also obtain energy from the national grid if the capacity of the existing EPs is not enough to satisfy the demand load. The startup costs for non-dispatchable units such as wind turbines are simply zero. We assume that the startup cost for dispatchable EPs is the cost of running the unit at full power for an hour.

Table 5.2: EP data

DER Type	Number of Units	Maximum Limit [kWh]	Price [¢/kWh]	EP Efficiency [%]
Microturbine	2	50	24.43	95.8
Photovoltaics	7	25	26.22	76.0
Wind Turbine	8	50	7.24	99.9
Biomass	5	28	10.83	93.0
Fuel Cell	3	50	26.65	85.0
Small Hydro	5	15	8.65	87.0
Geothermal	4	15	8.31	90.0

We consider 4 different residential tariff structures of PG&E [237]: E1, E6, E7 and E9, from which the consumers can select if they individually obtain energy from the national grid. The tariff structures are presented in Figure 5.5. E1 is a fixed pricing throughout the day, E6, E7 and E9 are different time-of-use (ToU) tariffs, in which consumers are charged with respect to the time of the day.

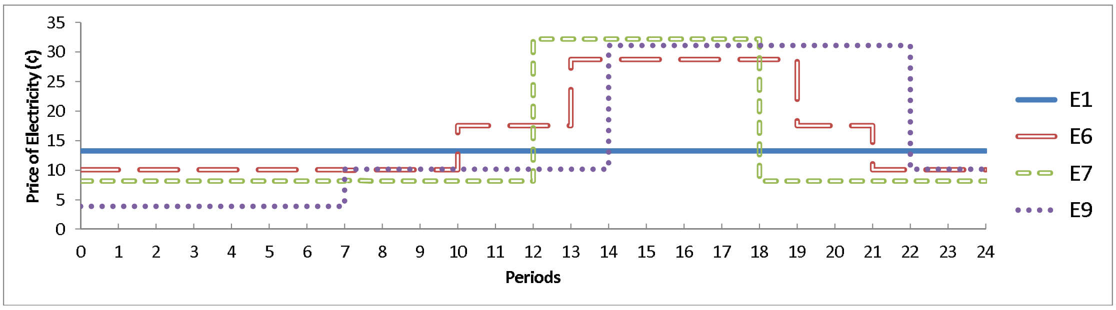

Figure 5.5: E1, E6, E7 and E9 tariffs of PG&E

Conventional (gasoline powered) vehicles and EPs emit nitrogen oxides (NO_x) and carbon dioxide (CO_2), both of which are hazardous to human health and detrimental to nature. The CO_2 and NO_x emission data in Table 5.3 is obtained from U.S. DOE Energy Efficiency and Renewable Energy (EERE) [238, 239] and U.S. Environmental Protection Agency [240]. Photovoltaics, wind turbine, small hydro and geothermal are assumed to have insignificant/zero amounts of emission.

Table 5.3: Emission data

Technology	CO_2	NO_x	Unit
Microturbine	539.8	0.2223	grams/kWh
Biomass	0	0.034	
Fuel Cell	385.6	0.0068	
Grid (average)	544.3	2.267	
Compact car	291.0	0.07	grams/mile (in CS mode)
Mid-size car	335.0	0.07	
Large car	395.0	0.07	
Small SUV	480.0	0.07	

We solve the VPP Energy Scheduling Model with different settings. The model under consideration has 60,125 (2,625 binary) variables and 118,486 constraints. We solve the models using IBM's ILOG CPLEX 12.5 Optimization Studio® on a computer with 2.00 GHz dual-core processor and 2.00 GB RAM.

5.3.2 Value of VPP and PHEVs

We consider 5 scenarios presented in Table 5.4. In the 1st scenario, all of the vehicles are considered to be running on gasoline, and the grid supplies energy for the residential loads. The consumers choose one of the following tariffs individually: E1, E6, E7, or E9. We assume that they behave rationally and select the tariff that gives the least cost. In the 2nd scenario, the vehicles again run on gasoline; but this time, the VPP manages the energy to minimize the total cost. For each of the scenarios, we run the optimization model for 30 times with individualized data pertaining to daily residential loads and driving profiles. The reported cost and emission values are the averages of these 30 runs. The daily average cost in grid domain is \$2720.4, which amounts to an average of \$142.1 monthly bill per house. The average cost in the VPP domain reduces to \$2045.8 and the cost saving of VPP formation is \$674.6 per day; in other words, an average of \$35 saving per house in the monthly bill. Even though both scenarios supply the same level of energy for the residential loads, the emission reduction is also drastic when the VPP is formed, because of the fact that the average emission values of the grid are much higher than those of renewable energy resources.

Table 5.4: Daily average cost and emission comparison of VPP and the grid

Scenario #	Domain	PHEV	V2G	Cost [\$]	CO_2 [kg]	NO_x [kg]
1	Grid	-	-	2720.4	10226.8	33.6
2	VPP	-	-	2045.8	3217.7	4.5
3	Grid	+	-	2628.7	9648.2	38.0
4	VPP	+	-	1854.3	2031.3	6.3
5	VPP	+	+	1850.7	2042.4	6.4

When the PHEVs are introduced in 3rd and 4th scenarios, cost reduction is attained in both domains, but the cost reduction is less in grid domain. Daily average cost savings of VPP formation with respect to grid in PHEV-penetrated network is \$774.4, an average of 29.5% cost reduction. This amounts to \$40.5 reduction in the monthly bill. Emission is again much less in the VPP domain when compared with the grid domain. 79% CO_2 and 83% NO_x emission reductions are attained as shared benefits of consumers in PHEV-penetrated networks.

PHEVs are running on electricity rather than gasoline in 3rd and 4th scenarios. Hence, the electricity generation increases with respect to 1st and 2nd scenarios. Because average electricity generation NO_x emission is higher than the PHEV NO_x emission (see Table 5.3), NO_x emission is increasing in both domains when PHEVs are introduced to the network. Note that CO_2 reduces in both VPP and grid domains when PHEVs are introduced into the network.

Besides VPP and PHEVs, we also include the Vehicle-to-grid (V2G) capability of the PHEV in the 5th scenario (Actually the technology is Vehicle-to-VPP in our case). Observe that the cost reduction is not statistically significant. This is because the electricity cost reduction due to discharging is neutralized by the increase in the battery degradation cost. Refer to Table 5.5 for the breakdown of cost, distance and emission values. The energy generation is slightly more in the 5^{th} scenario with respect to the 4^{th} scenario due to charge and discharge cycles and therefore the emissions increase with V2G accordingly. Though cost and emission gains seem to be insignificant, Sioshansi and Denholm [228] show that the spinning reserve cost reduction can be very rewarding in the grid domain when V2G capability is included.

Table 5.5 lists daily average distance, cost and emission breakdowns for the considered 19 scenarios. The daily average trip distance, 6463.6 miles for each scenario, is traveled either in CS or CD mode. The cost values correspond to the total of battery deterioration cost, electricity cost and gasoline cost. The emissions are categorized by the source: tailpipe emissions (T.P.) and emissions due to electricity generation by EPs (Gen.).

Table 5.5: Daily average generation, distance, cost and emission breakdowns

Scn.	Generation	Distance [miles]		Costs [$]			CO_2 [kg]		NO_x [kg]	
#	[MW]	CD	CS	Bat.	Elec.	Gas.	T.P.	Gen.	T.P.	Gen.
1	14.92	0	6463.5	0	1934.3	786.1	2268.7	7958.2	0.5	33.2
2	15.04	0	6463.5	0	1259.6	786.1	2268.7	949.0	0.5	4.0
3	16.73	4956.5	1507.0	227.5	2213.2	188.0	542.6	9105.6	0.1	37.9
4	16.92	4923.4	1540.2	226.0	1436.4	191.9	554	1477.4	0.1	6.2
5	16.95	4922.9	1540.6	241.8	1416.9	192.0	554.2	1488.2	0.1	6.2
6	15.08	1.1	6462.5	15.4	1238.6	386.6	2268.3	887.5	0.5	3.7
7	15.47	713.1	5750.4	54.1	1272.3	438.3	1934.4	923.1	0.4	3.9
8	16.91	4813.6	1649.9	236.8	1410.3	168.0	591.5	1466.9	0.1	6.2
9	16.95	4922.9	1540.6	241.8	1416.9	192.0	554.2	1488.2	0.1	6.2
10	16.96	4955.3	1508.2	244.9	1418.4	246.8	543	1495.4	0.1	6.3
11	16.95	4922.9	1540.6	241.8	1416.9	192.0	554.2	1488.2	0.1	6.2
12	16.96	4954.0	1509.5	175.0	1418.2	188.3	543.6	1497.5	0.1	6.3
13	16.96	4956.5	1507.0	105.1	1418.3	188.0	542.6	1499.6	0.1	6.3
14	17.08	4956.5	1507.0	0	1398.0	188.0	542.6	1678.4	0.1	7
15	16.95	4922.9	1540.6	241.8	1416.9	192.0	554.2	1488.2	0.1	6.2
16	22.78	4955.9	1507.6	227.8	792.8	188.1	542.8	589.3	0.1	1.6
17	22.75	4956.5	1507.0	227.5	543.0	188.0	542.6	623.4	0.1	0.7
18	16.95	4922.9	1540.6	241.8	1416.9	192.0	554.2	1488.2	0.1	6.2
19	22.75	4956.3	1507.3	227.5	1191.1	188.0	542.7	0	0.1	0
20	16.95	4887.6	1575.9	249.5	1422.9	196.3	566.5	1233.5	0.1	5.2

5.3.3 Sensitivity to Gasoline Prices

In scenarios 6-10, the gasoline price changes between $1.5 and $4.0. Even though the cost values in Table 5.6 change almost linearly with the gasoline prices, the three cost components in Table 5.5 react differently. As gasoline prices increase from $1.5 to $4.0, the gasoline cost decreases from $386.6 to $246.8, the electricity cost increases from $1238.6 to $1418.4 and the battery degradation cost increases from $15.4 to $244.9. The reason is that when the gasoline prices increase, the PHEV owners prefer to travel more on the CD mode. Observe that the decrease in gasoline cost cannot compensate for the electricity and battery cost increases. Therefore, the cost increases as gasoline prices increase.

The CD mode distances in 6^{th} and 7^{th} scenarios in Table 5.5 are much less than the distances in 8^{th}, 9^{th} and 10^{th} scenarios. Observe that there is a break-even price between $2.0 and $2.5. For gasoline costs higher than the break-even price, CD mode driving is more profitable than CS mode driving in almost every trip. Note that this break-even price is specific only for this scenario and would change in different combination of EPs and/or PHEVs.

Table 5.6: Sensitivity of daily average cost and emission to gasoline prices

Scenario #	Gas Price [$]	Cost [$]	CO_2 [kg]	NO_x [kg]
6	1.5	1640.6	3155.9	4.2
7	2.0	1764.7	2857.5	4.3
8	2.5	1815.1	2058.4	6.3
9	3.0	1850.7	2042.4	6.4
10	4.0	1910.0	2038.5	6.4

5.3.4 Sensitivity to Battery Prices

In scenarios 11-14, we analyze the effect of the battery price change (Table 5.7). In the 11^{th} scenario, the battery prices for each PHEV type are as presented in

Table 5.1. In the 12th and 13th scenarios, we assume a price reduction of \$1000 and \$2000 for each PHEV battery, respectively. In the 14th scenario, we simply do not consider the battery prices to see how the results are affected.

Table 5.7: Sensitivity of daily average cost and emission to battery prices

Scenario #	Battery Price Change [$]	Cost [$]	CO_2 [kg]	NO_x [kg]
11	0 (as is)	1850.7	2042.6	6.4
12	-1000	1781.6	2041.0	6.4
13	-2000	1711.4	2042.2	6.4
14	No battery cost	1586.0	2221.0	7.1

In the 12th and 13th scenarios, we benefit \$69.1 and \$139.3 battery degradation cost reduction with respect to the 11th scenario, which amounts to \$9.7 and \$19.6 monthly cost reduction per PHEV. Note that the trip distances on CD and CS modes in 13th and 14th scenarios are exactly the same in Table 5.5. Therefore one would expect that the electricity generation costs need to be the same, since the electricity requirements for both CD mode traveling and residential loads are the same. But the electricity costs are not the same as seen in Table 5.5. The reason is that, the battery has no cost in the 14th scenario. Therefore discharging occurs more and this creates cost savings.

5.3.5 Sensitivity to Energy Prices

In the 15th, 16th and 17th scenarios, we consider different EP prices. 15th scenario uses the pricing data presented in Table 5.2. 16th and 17th scenarios assume half and one third of these prices for each EP (excluding the grid), respectively. Results in Table 5.8 show that the VPP obtains the energy for cheaper with decreasing prices, as expected. Note that the 15th and 16thscenarios have almost identical CD mileages in Table 5.5. Thus, similar levels of electricity are generated in both scenarios. However, the emission values differ significantly. The reason is that when the prices decrease, more renewable EPs are used to generate the electricity, and the emissions reduce accordingly.

Table 5.8: Sensitivity of daily average cost and emission to DER prices

Scenario #	DER Price Change [$]	Cost [$]	CO_2 [kg]	NO_x [kg]
15	$\times$ 1	1850.7	2042.4	6.4
16	$\times$ 1/2	1208.8	1132.1	1.7
17	$\times$ 1/3	958.5	1166.0	0.8

5.3.6 Sensitivity to Generation Capacity

In this analysis, we consider doubling the EP capacities that are presented in Table 5.2. In the 19^{th} scenario, capacity expansion results in more DERs being used to generate the required energy. Thus the cost as well as emissions reduce accordingly. When there is enough capacity of renewable EPs to satisfy the demand load, the emission due to generation decreases to insignificant amounts, virtually zero as it is in the 19^{th} scenario (see Table 5.5).

Table 5.9: Sensitivity of daily average cost and emission to DER total capacity

Scenario #	DER Capacity Change [$]	Cost [$]	CO_2 [kg]	NO_x [kg]
18	$\times$ 1	1850.7	2042.4	6.4
19	$\times$ 2	1606.6	542.6	1.1

5.3.7 Sensitivity to Hourly Energy Availability

Though in our illustrative example, we took generation limits as time-invariant, in reality, photovoltaics and wind turbines are technologies which by nature have limitations throughout the day. In the 20^{th} scenario, the wind follows a forecasted distribution within the day and photovoltaics are available depending on the sun angle over the horizon. We have obtained the distribution of production by photovoltaics and wind turbines from CAISO Renewables Watch [241]. The photovoltaics generate electricity from 7 a.m. until 7 p.m. peaking at noon and the average generation is 25 kWh. The wind generate energy throughout the day peaking at midnight and the average generation is 50 kWh. Solving the energy management model for 30 days, the average daily cost is \$ 1868.62, the average CO_2 and NO_x emissions are 1931.33 kg and 5.84 kg, respectively. With current settings, the cost increases from the VPP scenario with V2G capability (5^{th} scenario) by \$25.75 and average CO_2 and NO_x emissions decrease by 111.07 kg and 0.46 kg, respectively. The increase in cost is due to the fact that wind turbines generate less electricity in peak times and energy is provided from more expensive resources instead. On the other hand, the discharging occurs more in peak times in order to compensate for the energy production reduction by wind turbines. This, in turn, reduce the emissions, since discharging leads to less energy being generated.

5.4 Summary

In this chapter, we consider a group of people forming a VPP in a PHEV-penetrated electricity network in order to reduce total electricity spendings through economies of scale. We assume that the VPP obtains energy from several renewable energy resources. To compare the cases with and without VPP and/or PHEVs, we first developed a new model that schedules the dispatch of EPs and the charging and discharging of PHEV batteries. Solving the model for several different settings, we obtained insightful results.

First and the foremost, this chapter highlights the cost and emission benefits of VPP formation and PHEV penetration into the network. Additionally, sensitivity of these benefits to different changes in the system is analyzed. The results show that the benefits of VPP formation can flourish if energy generation costs of renewable energy resources decrease or the capacities of the contracted EPs increase. For the scenarios considered in this paper, an average of 29.5% cost reduction and 79% CO_2 and 83% NO_x emission reductions are attained as shared benefits of consumers in PHEV-penetrated networks. The benefits of VPP formation are even more significant when PHEV battery costs decrease and uncertainty in gasoline prices persists. Results are illustrative of opportunities that VPP formation can provide for the community.

In addition, we show that charging and discharging do not simultaneously occur in the solutions and hence the binary variables that are traditionally included in energy management models can be excluded.

There are several challenges that the electricity market needs to tackle in the near future including volatile prices, threats of supply shortages and capacity expansion requirements of the regular electricity grid with increasing population. In the meantime, there are some real world applications of VPPs emerging all around the world [143], which could be a fundamental solution to these challenges. Together with the cost and emission benefits presented in this study, we expect that the upward trend towards VPPs will continue, especially with the introduction of new technologies such as Smart Grid.

As possible future research areas, the uncertainties associated with the whole system can be taken into account for more robust schedules. Also we assumed no pricing between the consumers and the VPP. Even though we have shown the cost reduction of VPP formation, how to share this cost reduction fairly among the parties can further be investigated.

Chapter 6

Conclusions

Uncertainty associated with gasoline prices and environmental impacts of fossil fuels have led to alternative forms of energy to be used in transportation sector. One of the most predominant forms of alternative energy has been the electricity. Therefore, the electrified transportation appeal to more people worldwide. Besides using electricity as an energy resource similar to EVs, PHEVs also eliminate the range-anxiety of the drivers in long-distance trips. Therefore, they have attracted significant attention in the market. With increasing number of PHEVs on the road, there has been new challenges to be faced both by the drivers and by the governments and/or investors. In this thesis effort, we investigated those challenges that arise with the introduction of PHEVs into the transportation system.

The practical importance of the problems associated with the electrified transportation, accompanied by computational complexity in solving them, have made these problems attractive in areas of recent research. In this context, we have identified two new problems pertinent to long-distance usage of PHEVs: 'finding the minimum cost path for PHEVs' and 'hybrid charging station location' and introduced solution approaches to the literature. Our results show that by establishing an adequate level of the intercity charging station infrastructure, well-studied benefits of PHEVs in urban regions can be extended to long-distance trips. In the following part, we show some directions that current research might be extended.

In the minimum cost path problem, we considered finding optimal paths for PHEVs considering the total cost of transportation without putting any limit on the environmental impacts. However, one of the major reasons people are more drawn to electrified transportation is the environmental concerns. Therefore, some drivers might consider the level of carbon emission when driving. Minimizing the total emission might be the objective of the transportation for them, or it could simply be a constraint with an upper bound per mile. Another factor that might be taken into account is the time. In this respect, one needs to consider the speed of the vehicle, the speed limits on the roads, the slope of the roads etc. This not only affects the problem at hand from the timing perspective, but also the comsumption of the energy might create additional complications. Because the consumption rate of electricity is different than that of gasoline, taking them into account will bring in non-linearities to the routing problem.

We assumed that the prices are known with certainty before solving the minimum cost path problem. However, especially the electricity prices vary significantly during peak-hours. Therefore pricing at charging stations might be only approximations when we consider long-distance transportation. Research might be directed towards hedging against inherent uncertainties in this routing problem.

We only consider one way when planning a trip. The return trip can also be taken into account. In this regard, relaxing the assumption that the vehicle is fully charged at the origin and destination nodes might be required.

Further research in this green-transportation research topic can be directed towards vehicle routing problems taking a mixed fleet of vehicles with CVs, PHEVs and EVs into account. This emerging topic of electrified transportation has a wide range of applicability to existing transportation problems. In this context, use of

PHEVs in future transportation fleets might be investigated by considering the hub location and the vehicle routing problems simultaneously.

A sub-objective of our study is to compare different technologies by considering long-distance transportation costs. This comparison could be part of a larger research incentive to investigate the lifetime economics of PHEVs versus CVs. For this purpose, initial purchase prices and urban region transportation costs need to be further taken into account.

We have identified that the drivers' tolerance towards additional stops or additional mileage could affect the level of electricity usage and transportation costs. Therefore new research need to be directed towards exploring the drivers' behavior which could show differences in different parts of the world.

Looking at the charging station location problem, additional factors can still be taken into account such as capacities. Possible congestions at these stations and varying electricity prices in time are additional complications for the location problem. Furthermore, the investment decisions and the associated funds for the charging stations do not usually arrive at one point in time, but rather, these decisions are spread over a time horizon. Therefore multi-period nature of the charging station location problem is a possible future research area. The uncertain nature of release of funds can also be taken into account as a future research topic. In a similar fashion, uncertainty of the demand might be considered in the charging station location problem. In the minimum cost path problem, we also assumed that the electricity and gasoline prices are fixed and known with certainty. This assumption can be relaxed in future studies, because these prices are subject to change in time.

For the energy management in virtual power plants and microgrids, we considered minimizing the total cost to satisfy a given demand. However the cost sharing problem among participants is another critical problem that needs to be addressed. The system must be designed so as to promote the people to participate in the microgrid incentive. One idea could be to use game-theoretic approaches to share the cost among participants.

From the solution perspective, our approach in solving the large-scale hybrid charging station problem might be implemented to different flow capturing problems such as flow-evading facility location problem, another newly introduced problem to the literature. Also a path-segment formulation can be implemented for the minimum cost path problem.

Bibliography

[1] U.S. Department of Energy. Alternative fuel vehicles in use, 2014. URL `www.afdc.energy.gov/data/10300`. accessed May 22, 2015.

[2] Aaron Windecker and Adam Ruder. Fuel economy, cost, and greenhouse gas results for alternative fuel vehicles in 2011. *Transportation Research Part D: Transport and Environment*, 23(0):34 – 40, 2013.

[3] Gianfranco Pistoia. *Electric and hybrid vehicles: Power sources, models, sustainability, infrastructure and the market*. Access Online via Elsevier, 2010.

[4] Jonn Axsen and Kenneth S Kurani. Anticipating plug-in hybrid vehicle energy impacts in california: Constructing consumer-informed recharge profiles. *Transportation Research Part D: Transport and Environment*, 15(4): 212–219, 2010.

[5] Jonn Axsen, Andy Burke, and Kenneth S Kurani. Batteries for plug-in hybrid electric vehicles (phevs): goals and the state of technology circa 2008, 2008.

[6] Tony Markel and Keith Wipke. Modeling grid-connected hybrid electric vehicles using advisor. In *Applications and Advances, 2001. The Sixteenth Annual Battery Conference on*, pages 23–29. IEEE, 2001.

[7] Elizabeth Traut, Chris Hendrickson, Erica Klampfl, Yimin Liu, and Jeremy J Michalek. Optimal design and allocation of electrified vehicles and dedicated

charging infrastructure for minimum greenhouse gas emissions. In *TRB Annual Meeting*, 2011.

[8] Fang He, Di Wu, Yafeng Yin, and Yongpei Guan. Optimal deployment of public charging stations for plug-in hybrid electric vehicles. *Transportation Research Part B: Methodological*, 47(0):87 – 101, 2013.

[9] U.S. Department of Energy. Plug-in hybrid electric vehicle charging infrastructure review, 2008. avt.inel.gov/pdf/phev/phevInfrastructureReport08.pdf.

[10] ED Tate, Michael O Harpster, and Peter J Savagian. The electrification of the automobile: from conventional hybrid, to plug-in hybrids, to extended-range electric vehicles. Technical report, SAE Technical Paper, 2008.

[11] U.S. Congress. Energy policy act of 2005. *Public Law*, 109(58):42, 2005.

[12] U.S. Department of Energy. Benefits and considerations of electricity as a vehicle fuel, 2015. URL `www.afdc.energy.gov/fuels/electricity_benefits.html`. accessed May 22, 2015.

[13] Hongrui Ma, Felix Balthasar, Nigel Tait, Xavier Riera-Palou, and Andrew Harrison. A new comparison between the life cycle greenhouse gas emissions of battery electric vehicles and internal combustion vehicles. *Energy Policy*, 44(0):160 – 173, 2012.

[14] Page Kyle and Son H. Kim. Long-term implications of alternative light-duty vehicle technologies for global greenhouse gas emissions and primary energy demands. *Energy Policy*, 39(5):3012 – 3024, 2011.

[15] U.S. Department of Transportation. National household travel survey, 2010. URL `nhts.ornl.gov/det/Extraction3.aspx`. Accessed Feb 16, 2014.

[16] Thomas S. Turrentine and Kenneth S. Kurani. Car buyers and fuel economy? *Energy Policy*, 35(2):1213 – 1223, 2007.

[17] Angel A. Juan, Jarrod Goentzel, and Tolga Bektaş. Routing fleets with multiple driving ranges: Is it possible to use greener fleet configurations? *Applied Soft Computing*, 21(0):84 – 94, 2014.

[18] Nakul Sathaye. The optimal design and cost implications of electric vehicle taxi systems. *Transportation Research Part B: Methodological*, 67(0):264 – 283, 2014.

[19] R Parish and W Pitkanen. Demand assessment of first-mover hybrid and electric truck fleets. *CALSTART. URL www. calstart. org/Libraries/Publications/Demand_ Assessment_of_First-Mover_Hybrid_and_Electric_Truck_Fleets. sflb. ashx*, 8(6):2014, 2012.

[20] Brian A. Davis and Miguel A. Figliozzi. A methodology to evaluate the competitiveness of electric delivery trucks. *Transportation Research Part E: Logistics and Transportation Review*, 49(1):8 – 23, 2013. ISSN 1366-5545.

[21] U.S. Department of Energy. Plug-in electric vehicle handbook for fleet managers, 2012. www.afdc.energy.gov/pdfs/pev_handbook.pdf.

[22] Navigant Research. Selecting electric vehicles for fleets, 2013. www.navigantresearch.com/wp-assets/uploads/2013/02/RB-SEVF-13-Executive-Summary.pdf.

[23] Smith Electric Vehicles. Smith electric vehicles, 2015. www.smithelectric.com/smith-vehicles/.

[24] Odyne Systems. Odyne, plug-in hybrid systems for medium- and heavy-duty trucks, 2015. www.smithelectric.com/smith-vehicles/.

[25] Business Wire. Greenkraft inc. and efficient drivetrains, inc. jointly receive grant from california energy commission to develop cng-phev class-4 truck, 2014. www.businesswire.com/news/home/20141027006268/en/Greenkraft-Efficient-Drivetrains-Jointly-Receive-Grant-California#.VOuud3yUfHR.

[26] Quantum Fuel Systems. Quantum announces first delivery of plug-in hybrid electric f-150 pick up truck to florida power & light, 2012. www.qtww.com/press-releases?view=104.

[27] Bloomberg. Vias lutz eyes annual sales of 50,000 plug-in pickups, 2015. www.bloomberg.com/news/articles/2015-01-15/vias-lutz-eyes-annual-sales-of-50000-plugin-pickups.

[28] Volvo. Volvo fe hybrid, 2015. www.volvotrucks.com/trucks/uk-market/en-gb/trucks/volvo-fe-hybrid/Pages/volvo-fe-hybrid.aspx.

[29] United Kingdom Government. Plug-in van grant, 2012. URL `www.gov.uk/government/publications/plug-in-van-grant`. Accessed March 10, 2015.

[30] Clean Transport and Technology Limited. Uk tax incentives for electric vehicles, 2015. URL `www.clean-transport.co.uk/electric-vehicle-tax-incentives`. Accessed March 10, 2015.

[31] Mitsubishi Cars. Outlander PHEV, 2015. URL `mitsubishi-cars.co.uk/outlander/explore-phev.aspx`. Accessed Mar 01, 2015.

[32] Ravi Bapna, Lakshman S Thakur, and Suresh K Nair. Infrastructure development for conversion to environmentally friendly fuel. *European Journal of Operational Research*, 142(3):480–496, 2002.

[33] Marc W Melaina. Initiating hydrogen infrastructures: preliminary analysis of a sufficient number of initial hydrogen stations in the U.S. *International Journal of Hydrogen Energy*, 28(7):743–755, 2003.

[34] Michael Kuby and Seow Lim. The flow-refueling location problem for alternative-fuel vehicles. *Socio-Economic Planning Sciences*, 39(2):125 – 145, 2005.

[35] Joseph Romm. The car and fuel of the future. *Energy Policy*, 34(17):2609–2614, 2006.

[36] Marc Melaina and Joel Bremson. Refueling availability for alternative fuel vehicle markets: sufficient urban station coverage. *Energy Policy*, 36(8): 3233–3241, 2008.

[37] Tolga Bektaş and Gilbert Laporte. The pollution-routing problem. *Transportation Research Part B: Methodological*, 45(8):1232 – 1250, 2011.

[38] Emrah Demir, Tolga Bektaş, and Gilbert Laporte. An adaptive large neighborhood search heuristic for the pollution-routing problem. *European Journal of Operational Research*, 223(2):346 – 359, 2012.

[39] Emrah Demir, Tolga Bektaş, and Gilbert Laporte. The bi-objective pollution-routing problem. *European Journal of Operational Research*, 232 (3):464 – 478, 2014.

[40] Anna Franceschetti, Dorothe Honhon, Tom Van Woensel, Tolga Bektaş, and Gilbert Laporte. The time-dependent pollution-routing problem. *Transportation Research Part B: Methodological*, 56(0):265 – 293, 2013.

[41] Çağrı Koç, Tolga Bektaş, Ola the, and Gilbert Laporte. The fleet size and mix pollution-routing problem. *Transportation Research Part B: Methodological*, 70(0):239 – 254, 2014.

[42] Raphael Kramer, Anand Subramanian, Thibaut Vidal, and Lucdio dos Anjos F. Cabral. A matheuristic approach for the pollution-routing problem. *European Journal of Operational Research*, 243(2):523 – 539, 2015.

[43] Sevgi Erdoğan and Elise Miller-Hooks. A green vehicle routing problem. *Transportation Research Part E: Logistics and Transportation Review*, 48(1): 100 – 114, 2012. ISSN 1366-5545. Select Papers from the 19th International Symposium on Transportation and Traffic Theory.

[44] Ángel Felipe, M. Teresa Ortuno, Giovanni Righini, and Gregorio Tirado. A heuristic approach for the green vehicle routing problem with multiple technologies and partial recharges. *Transportation Research Part E: Logistics and Transportation Review*, 71(0):111 – 128, 2014. ISSN 1366-5545.

[45] Goran Ćirović, Dragan Pamučar, and Darko Boanić. Green logistic vehicle routing problem: Routing light delivery vehicles in urban areas using a neuro-fuzzy model. *Expert Systems with Applications*, 41(9):4245 – 4258, 2014.

[46] Canhong Lin, K.L. Choy, G.T.S. Ho, S.H. Chung, and H.Y. Lam. Survey of green vehicle routing problem: Past and future trends. *Expert Systems with Applications*, 41(4, Part 1):1118 – 1138, 2014.

[47] Michael Schneider, Andreas Stenger, and Dominik Goeke. The electric vehicle-routing problem with time windows and recharging stations. *Transportation Science*, 48(4):500–520, 2014. doi: 10.1287/trsc.2013.0490.

[48] Okan Arslan, Barış Yıldız, and Oya Ekin Karaşan. Minimum cost path problem for plug-in hybrid electric vehicles. *Transportation Research Part E: Logistics and Transportation Review*, 2015. doi: http://dx.doi.org/10.1016/j.tre.2015.05.011.

[49] Dominik Goeke and Michael Schneider. Routing a mixed fleet of electric and conventional vehicles. *European Journal of Operational Research*, (0):–, 2015. doi: dx.doi.org/10.1016/j.ejor.2015.01.049.

[50] Yenming J. Chen and Jiuh-Biing Sheu. Environmental-regulation pricing strategies for green supply chain management. *Transportation Research Part E: Logistics and Transportation Review*, 45(5):667 – 677, 2009.

[51] Susana G. Azevedo, Helena Carvalho, and V. Cruz Machado. The influence of green practices on supply chain performance: A case study approach. *Transportation Research Part E: Logistics and Transportation Review*, 47 (6):850 – 871, 2011.

[52] Jiuh-Biing Sheu and Yenming J. Chen. Transportation and economies of scale in recycling low-value materials. *Transportation Research Part B: Methodological*, 65(0):65 – 76, 2014.

[53] Angappa Gunasekaran, Nachiappan Subramanian, and Shams Rahman. Green supply chain collaboration and incentives: Current trends and future directions. *Transportation Research Part E: Logistics and Transportation Review*, 74(0):1 – 10, 2015. Green Supply Chain Collaboration and Incentives.

[54] Michael Kuby and Seow Lim. The flow-refueling location problem for alternative-fuel vehicles. *Socio-Economic Planning Sciences*, 39(2):125–145, 2005.

[55] Ying-Wei Wang and Chuah-Chih Lin. Locating road-vehicle refueling stations. *Transportation Research Part E: Logistics and Transportation Review*, 45(5):821 – 829, 2009.

[56] Ying-Wei Wang and Chuan-Ren Wang. Locating passenger vehicle refueling stations. *Transportation Research Part E: Logistics and Transportation Review*, 46(5):791–801, 2010.

[57] Ying-Wei Wang and Chuah-Chih Lin. Locating multiple types of recharging stations for battery-powered electric vehicle transport. *Transportation Research Part E: Logistics and Transportation Review*, 58(0):76 – 87, 2013. ISSN 1366-5545.

[58] Nakul Sathaye and Scott Kelley. An approach for the optimal planning of electric vehicle infrastructure for highway corridors. *Transportation Research Part E: Logistics and Transportation Review*, 59(0):15 – 33, 2013. ISSN 1366-5545.

[59] Xiaomin Xi, Ramteen Sioshansi, and Vincenzo Marano. Simulationoptimization model for location of a public electric vehicle charging infrastructure.

Transportation Research Part D: Transport and Environment, 22(0):60 – 69, 2013.

[60] Shengyin Li and Yongxi Huang. Heuristic approaches for the flow-based set covering problem with deviation paths. *Transportation Research Part E: Logistics and Transportation Review*, 72(0):144 – 158, 2014. ISSN 1366-5545.

[61] Samuel Pelletier, Ola Jabali, and Gilbert Laporte. Goods distribution with electric vehicles: Review and research perspectives. Technical report, Technical Report CIRRELT-2014-44, CIRRELT, Montréal, Canada, 2014.

[62] Nathaniel S. Pearre, Willett Kempton, Randall L. Guensler, and Vetri V. Elango. Electric vehicles: How much range is required for a days driving? *Transportation Research Part C: Emerging Technologies*, 19(6):1171 – 1184, 2011.

[63] Thomas Franke and Josef F. Krems. What drives range preferences in electric vehicle users? *Transport Policy*, 30(0):56 – 62, 2013.

[64] Ramteen Sioshansi. Or forummodeling the impacts of electricity tariffs on plug-in hybrid electric vehicle charging, costs, and emissions. *Operations Research*, 60(3):506–516, 2012.

[65] Christoph Flath, Jens Ilg, Sebastian Gottwalt, Hartmut Schmeck, and Christof Weinhardt. Improving electric vehicle charging coordination through area pricing. *Available at SSRN 2197327*, 2013.

[66] Xiaohui Cui, Hoe Kyoung Kim, Cheng Liu, Shih-Chieh Kao, and Budhendra L. Bhaduri. Simulating the household plug-in hybrid electric vehicle distribution and its electric distribution network impacts. *Transportation Research Part D: Transport and Environment*, 17(7):548 – 554, 2012.

[67] Ramteen Sioshansi and Jacob Miller. Plug-in hybrid electric vehicles can be clean and economical in dirty power systems. *Energy Policy*, 39(10):6151 – 6161, 2011.

[68] Sarah G. Nurre, Russell Bent, Feng Pan, and Thomas C. Sharkey. Managing operations of plug-in hybrid electric vehicle (phev) exchange stations for use with a smart grid. *Energy Policy*, 2013. doi: http://dx.doi.org/10.1016/j.enpol.2013.11.052.

[69] Okan Arslan and Oya Ekin Karaşan. Cost and emission impacts of virtual power plant formation in plug-in hybrid electric vehicle penetrated networks. *Energy*, 60(0):116 – 124, 2013.

[70] Matthias D. Galus, Marek Zima, and Gran Andersson. On integration of plug-in hybrid electric vehicles into existing power system structures. *Energy Policy*, 38(11):6736 – 6745, 2010.

[71] Claire Weiller. Plug-in hybrid electric vehicle impacts on hourly electricity demand in the united states. *Energy Policy*, 39(6):3766 – 3778, 2011.

[72] Jonn Axsen, Kenneth S. Kurani, Ryan McCarthy, and Christopher Yang. Plug-in hybrid vehicle GHG impacts in California: Integrating consumer-informed recharge profiles with an electricity-dispatch model. *Energy Policy*, 39(3):1617 – 1629, 2011.

[73] Paul Albertus, Jeremy Couts, Venkat Srinivasan, and John Newman. II. a combined model for determining capacity usage and battery size for hybrid and plug-in hybrid electric vehicles. *Journal of Power Sources*, 183(2):771 – 782, 2008.

[74] Michela Catenacci, Elena Verdolini, Valentina Bosetti, and Giulia Fiorese. Going electric: Expert survey on the future of battery technologies for electric vehicles. *Energy Policy*, 61(0):403 – 413, 2013.

[75] Bruno Scrosati and Jrgen Garche. Lithium batteries: Status, prospects and future. *Journal of Power Sources*, 195(9):2419 – 2430, 2010.

[76] Craig H Stephan and John Sullivan. Environmental and energy implications of plug-in hybrid-electric vehicles. *Environmental Science & Technology*, 42 (4):1185–1190, 2008.

[77] William J. Smith. Plug-in hybrid electric vehiclesa low-carbon solution for Ireland? *Energy Policy*, 38(3):1485 – 1499, 2010.

[78] Brandon M. Marshall, Jarod C. Kelly, Tae-Kyung Lee, Gregory A. Keoleian, and Zoran Filipi. Environmental assessment of plug-in hybrid electric vehicles using naturalistic drive cycles and vehicle travel patterns: A michigan case study. *Energy Policy*, 58(0):358 – 370, 2013.

[79] Lauren M. Gardner, Melissa Duell, and S. Travis Waller. A framework for evaluating the role of electric vehicles in transportation network infrastructure under travel demand variability. *Transportation Research Part A: Policy and Practice*, 49(0):76 – 90, 2013.

[80] Mobashwir Khan and Kara M. Kockelman. Predicting the market potential of plug-in electric vehicles using multiday GPS data. *Energy Policy*, 46(0): 225 – 233, 2012.

[81] Jonn Axsen and Kenneth S. Kurani. Hybrid, plug-in hybrid, or electric-what do car buyers want? *Energy Policy*, 61(0):532 – 543, 2013.

[82] Margaret J. Eppstein, David K. Grover, Jeffrey S. Marshall, and Donna M. Rizzo. An agent-based model to study market penetration of plug-in hybrid electric vehicles. *Energy Policy*, 39(6):3789 – 3802, 2011.

[83] Thomas F. Golob and Jane Gould. Projecting use of electric vehicles from household vehicle trials. *Transportation Research Part B: Methodological*, 32 (7):441 – 454, 1998.

[84] John K Dagsvik, Tom Wennemo, Dag G Wetterwald, and Rolf Aaberge. Potential demand for alternative fuel vehicles. *Transportation Research Part B: Methodological*, 36(4):361 – 384, 2002.

[85] Stefan L. Mabit and Mogens Fosgerau. Demand for alternative-fuel vehicles when registration taxes are high. *Transportation Research Part D: Transport and Environment*, 16(3):225 – 231, 2011.

[86] Mafalda Mendes Lopes, Filipe Moura, and Luis M. Martinez. A rule-based approach for determining the plausible universe of electric vehicle buyers in the lisbon metropolitan area. *Transportation Research Part A: Policy and Practice*, 59(0):22 – 36, 2014.

[87] Ying-Wei Wang and Chuah-Chih Lin. Locating road-vehicle refueling stations. *Transportation Research Part E: Logistics and Transportation Review*, 45(5):821–829, 2009.

[88] SA MirHassani and R Ebrazi. A flexible reformulation of the refueling station location problem. *Transportation Science*, 2012.

[89] Tetsuo Ichimori, Hiroaki Ishii, and Toshio Nishida. Routing a vehicle with the limitation of fuel. *Journal of the Operations Research Society of Japan*, 24(3):277–281, 1981.

[90] Shieu Hong Lin, Nate Gertsch, and Jennifer R. Russell. A linear-time algorithm for finding optimal vehicle refueling policies. *Operations Research Letters*, 35(3):290 – 296, 2007. ISSN 0167-6377.

[91] Samir Khuller, Azarakhsh Malekian, and Julián Mestre. To fill or not to fill: the gas station problem. In *Algorithms–ESA 2007*, pages 534–545. Springer, 2007.

[92] Shieu-Hong Lin. Finding optimal refueling policies: a dynamic programming approach. *Journal of Computing Sciences in Colleges*, 23(6):272–279, 2008.

[93] Shieu-Hong Lin. Finding optimal refueling policies in transportation networks. In *Algorithmic Aspects in Information and Management*, pages 280–291. Springer, 2008.

[94] Yoshinori Suzuki. A generic model of motor-carrier fuel optimization. *Naval Research Logistics (NRL)*, 55(8):737–746, 2008.

[95] Yoshinori Suzuki. A decision support system of dynamic vehicle refueling. *Decision Support Systems*, 46(2):522–531, 2009.

[96] Yoshinori Suzuki. A decision support system of vehicle routing and refueling for motor carriers with time-sensitive demands. *Decision Support Systems*, 2012.

[97] Jonathan Adler, Pitu B. Mirchandani, Guoliang Xue, and Minjun Xia. The electric vehicle shortest walk problem. *93th TRB Annual Meetings*, 2013.

[98] Nan Jiang and Chi Xie. Computing and analyzing equilibrium network flows of gasoline and electric vehicles. *92nd TRB Annual Meetings*, 2012.

[99] Nan Jiang, Chi Xie, and S Travis Waller. Path-constrained traffic assignment. *Transportation Research Record: Journal of the Transportation Research Board*, 2283(1):25–33, 2012.

[100] Nan Jiang, Chi Xie, Jennifer C Duthie, and S Travis Waller. A network equilibrium analysis on destination, route and parking choices with mixed gasoline and electric vehicular flows. *EURO Journal on Transportation and Logistics*, pages 1–38, 2013.

[101] Shieu-Hong Lin. Vehicle refueling planning for point-to-point delivery by motor carriers. *Proc.2012 IEEE International Conference on Industrial Engineering and Engineering Management*, pages 187–191, 2012.

[102] Andreas Artmeier, Julian Haselmayr, Martin Leucker, and Martin Sachenbacher. The shortest path problem revisited: Optimal routing for electric vehicles. In *KI 2010: Advances in Artificial Intelligence*, pages 309–316. Springer, 2010.

[103] Martin Sachenbacher, Martin Leucker, Andreas Artmeier, and Julian Haselmayr. Efficient energy-optimal routing for electric vehicles. In *Twenty-Fifth AAAI Conference on Artificial Intelligence*, 2011.

[104] Jochen Eisner, Stefan Funke, and Sabine Storandt. Optimal route planning for electric vehicles in large networks. In *Proceedings of the Twenty-Fifth AAAI conference on Artificial Intelligence*, 2011.

[105] Yuichi Kobayashi, Noboru Kiyama, Hirokazu Aoshima, and Masamori Kashiyama. A route search method for electric vehicles in consideration of range and locations of charging stations. In *Intelligent Vehicles Symposium (IV), 2011 IEEE*, pages 920–925. IEEE, 2011.

[106] Umair Farooq Siddiqi, Yoichi Shiraishi, and Sadiq M Sait. Multi-constrained route optimization for electric vehicles (evs) using particle swarm optimization (pso). In *Intelligent Systems Design and Applications (ISDA), 2011 11th International Conference on*, pages 391–396. IEEE, 2011.

[107] Jun Yang and Hao Sun. Battery swap station location-routing problem with capacitated electric vehicles. *Computers & Operations Research*, 55(0):217 – 232, 2015.

[108] Gilbert Laporte and Marta Pascoal. Minimum cost path problems with relays. *Computers & Operations Research*, 38(1):165–173, 2011.

[109] Jacques Desrosiers, François Soumis, and Martin Desrochers. Routing with time windows by column generation. *Networks*, 14(4):545–565, 1984.

[110] Martin Desrochers and Francois Soumis. A column generation approach to the urban transit crew scheduling problem. *Transportation Science*, 23(1): 1–13, 1989.

[111] Guy Desaulniers and Daniel Villeneuve. The shortest path problem with time windows and linear waiting costs. *Transportation Science*, 34(3):312–319, 2000.

[112] Ravindra K Ahuja, James B Orlin, Stefano Pallottino, and Maria Grazia Scutellà. Minimum time and minimum cost-path problems in street networks with periodic traffic lights. *Transportation Science*, 36(3):326–336, 2002.

[113] Enver Doruk Özdemir and Niklas Hartmann. Impact of electric range and fossil fuel price level on the economics of plug-in hybrid vehicles and greenhouse gas abatement costs. *Energy Policy*, 46(0):185 – 192, 2012.

[114] Benedikt Lunz, Zexiong Yan, Jochen Bernhard Gerschler, and Dirk Uwe Sauer. Influence of plug-in hybrid electric vehicle charging strategies on charging and battery degradation costs. *Energy Policy*, 46(0):511 – 519, 2012.

[115] Jeremy Neubauer, Aaron Brooker, and Eric Wood. Sensitivity of plug-in hybrid electric vehicle economics to drive patterns, electric range, energy management, and charge strategies. *Journal of Power Sources*, 236(0):357 – 364, 2013.

[116] Orkun Karabasoglu and Jeremy Michalek. Influence of driving patterns on life cycle cost and emissions of hybrid and plug-in electric vehicle powertrains. *Energy Policy*, 60(0):445 – 461, 2013.

[117] Scott B. Peterson and Jeremy J. Michalek. Cost-effectiveness of plug-in hybrid electric vehicle battery capacity and charging infrastructure investment for reducing U.S. gasoline consumption. *Energy Policy*, 52(0):429 – 438, 2013.

[118] Ching-Shin Norman Shiau, Constantine Samaras, Richard Hauffe, and Jeremy J. Michalek. Impact of battery weight and charging patterns on the economic and environmental benefits of plug-in hybrid vehicles. *Energy Policy*, 37(7):2653 – 2663, 2009.

[119] Jeremy Neubauer, Aaron Brooker, and Eric Wood. Sensitivity of battery electric vehicle economics to drive patterns, vehicle range, and charge strategies. *Journal of Power Sources*, 209(0):269 – 277, 2012.

[120] Jamie Davies and Kenneth S. Kurani. Moving from assumption to observation: Implications for energy and emissions impacts of plug-in hybrid electric vehicles. *Energy Policy*, 62(0):550 – 560, 2013.

[121] Michael Kuby, Lee Lines, Ronald Schultz, Zhixiao Xie, Jong-Geun Kim,

and Seow Lim. Optimization of hydrogen stations in florida using the flow-refueling location model. *International Journal of Hydrogen Energy*, 34(15): 6045 – 6064, 2009.

[122] Michael J. Kuby, Scott B. Kelley, and Joseph Schoenemann. Spatial refueling patterns of alternative-fuel and gasoline vehicle drivers in los angeles. *Transportation Research Part D: Transport and Environment*, 25(0):84 – 92, 2013.

[123] Christopher Upchurch, Michael Kuby, and Seow Lim. A model for location of capacitated alternative-fuel stations. *Geographical Analysis*, 41(1):85–106, 2009.

[124] Jong-Geun Kim and Michael Kuby. The deviation-flow refueling location model for optimizing a network of refueling stations. *International Journal of Hydrogen Energy*, 37(6):5406 – 5420, 2012.

[125] Barış Yıldız, Okan Arslan, and Oya Ekin Karaşan. A branch and price approach for routing and refueling station location model. *European Journal of Operational Research*, (0):–, 2015. ISSN 0377-2217. doi: http://dx.doi.org/10.1016/j.ejor.2015.05.021.

[126] Michael Kuby and Seow Lim. Location of alternative-fuel stations using the flow-refueling location model and dispersion of candidate sites on arcs. *Networks and Spatial Economics*, 7(2):129–152, 2007.

[127] Seow Lim and Michael Kuby. Heuristic algorithms for siting alternative-fuel stations using the flow-refueling location model. *European Journal of Operational Research*, 204(1):51 – 61, 2010.

[128] Jong-Geun Kim and Michael Kuby. A network transformation heuristic approach for the deviation flow refueling location model. *Computers & Operations Research*, 40(4):1122 – 1131, 2013.

[129] Ismail Capar and Michael Kuby. An efficient formulation of the flow refueling location model for alternative-fuel stations. *IIE Transactions*, 44(8):622–636, 2012.

[130] S. A. MirHassani and R. Ebrazi. A flexible reformulation of the refueling station location problem. *Transportation Science*, 47(4):617–628, 2013.

[131] Ismail Capar, Michael Kuby, V. Jorge Leon, and Yu-Jiun Tsai. An arc coverpath-cover formulation and strategic analysis of alternative-fuel station locations. *European Journal of Operational Research*, 227(1):142 – 151, 2013.

[132] Ying-Wei Wang and Chuan-Ren Wang. Locating passenger vehicle refueling stations. *Transportation Research Part E: Logistics and Transportation Review*, 46(5):791 – 801, 2010.

[133] Sung Hoon Chung and Changhyun Kwon. Multi-period planning for electric car charging station locations: A case of korean expressways. *European Journal of Operational Research*, 242(2):677 – 687, 2015. ISSN 0377-2217. doi: http://dx.doi.org/10.1016/j.ejor.2014.10.029.

[134] Patrick Jochem, Carsten Brendel, Melanie Reuter-Oppermann, Wolf Fichtner, and Stefan Nickel. Optimizing the allocation of fast charging infrastructure along the german autobahn. *Journal of Business Economics*, pages 1–23, 2015.

[135] Meysam Hosseini and S.A. MirHassani. Refueling-station location problem under uncertainty. *Transportation Research Part E: Logistics and Transportation Review*, 84:101 – 116, 2015. ISSN 1366-5545. doi: http://dx.doi.org/10.1016/j.tre.2015.10.009.

[136] Ying-Wei Wang and Chuah-Chih Lin. Locating multiple types of recharging stations for battery-powered electric vehicle transport. *Transportation Research Part E: Logistics and Transportation Review*, 58:76–87, 2013.

[137] Ying-Wei Wang. Locating flow-recharging stations at tourist destinations to serve recreational travelers. *International Journal of Sustainable Transportation*, 5(3):153–171, 2011.

[138] Yu (Marco) Nie and Mehrnaz Ghamami. A corridor-centric approach to planning electric vehicle charging infrastructure. *Transportation Research Part B: Methodological*, 57(0):172 – 190, 2013.

[139] Zhenhong Lin and David Greene. Promoting the market for plug-in hybrid and battery electric vehicles: role of recharge availability. *Transportation Research Record: Journal of the Transportation Research Board*, (2252):49–56, 2011.

[140] Center for Sustainable Energy. California air resources board clean vehicle rebate project, rebate statistics, 2015. URL http://energycenter.org/clean-vehicle-rebate-project/rebate-statistics. Retrieved Aug 20, 2015. Data last updated Aug 17, 2015.

[141] Peter Asmus. Microgrids, virtual power plants and our distributed energy future. *The Electricity Journal*, 23(10):72–82, 2010. ISSN 1040-6190.

[142] Xi Fang, Satyajayant Misra, Guoliang Xue, and Dejun Yang. Smart grid - the new and improved power grid: A survey. *IEEE Commun. Surv. Tutor.*, 14(4):944–980, 2011. ISSN 1553-877X.

[143] Lukasz Bartosz Nikonowicz and Jaroslaw Milewski. Virtual power plants general review: structure, application and optimization. *J Power Tech*, 92 (3):135 – 149, 2012.

[144] Hugo Morais, Pèter Kàdàr, Pedro Faria, Zita A. Vale, and H.M. Khodr. Optimal scheduling of a renewable micro-grid in an isolated load area using mixed-integer linear programming. *Renew. Energy*, 35(1):151–156, 2010. ISSN 0960-1481.

[145] H.M. Khodr, N. El Halabi, and M. García-Gracia. Intelligent renewable microgrid scheduling controlled by a virtual power producer: A laboratory experience. *Renew. Energy*, 48:269–275, 2012. ISSN 0960-1481.

[146] Phillip Oliver Kriett and Matteo Salani. Optimal control of a residential microgrid. *Energy*, 42(1):321–330, 2012. ISSN 0360-5442.

[147] Pavan Kumar Naraharisetti, I.A. Karimi, Abhay Anand, and Dong-Yup Lee. A linear diversity constraint - application to scheduling in microgrids. *Energy*, 36(7):4235–4243, 2011. ISSN 0360-5442.

[148] Amjad Anvari Moghaddam, Alireza Seifi, Taher Niknam, and Mohammad Reza Alizadeh Pahlavani. Multi-objective operation management of a renewable MG (micro-grid) with back-up micro-turbine/fuel cell/battery hybrid power source. *Energy*, 36(11):6490–6507, 2011. ISSN 0360-5442.

[149] Ashoke Kumar Basu, S.P. Chowdhury, S. Chowdhury, and S. Paul. Microgrids: Energy management by strategic deployment of DERs - a comprehensive survey. *Renew. Sust. Energ. Rev.*, 15(9):4348–4356, 2011. ISSN 1364-0321.

[150] Gang Xiong, Chen Chen, S. Kishore, and A. Yener. Smart (in-home) power scheduling for demand response on the smart grid. In *Innovative Smart Grid Technologies (ISGT), IEEE PES*, pages 1–7, jan. 2011.

[151] Michael Angelo A. Pedrasa, Ted D. Spooner, and Iain F. MacGill. A novel energy service model and optimal scheduling algorithm for residential distributed energy resources. *Electr. Power. Syst. Res.*, 81(12):2155–2163, 2011. ISSN 0378-7796.

[152] Mohammad Rastegar, Mahmud Fotuhi-Firuzabad, and Farrokh Aminifar. Load commitment in a smart home. *Appl. Energy*, 96:45–54, 2012. ISSN 0306-2619.

[153] Onur Elma and Ugur Savas Selamogullari. A comparative sizing analysis of a renewable energy supplied stand-alone house considering both demand side and source side dynamics. *Appl. Energy*, 96:400–408, 2012. ISSN 0306-2619.

[154] Eugenia D. Mehleri, Haralambos Sarimveis, Nikolaos C. Markatos, and Lazaros G. Papageorgiou. A mathematical programming approach for optimal design of distributed energy systems at the neighbourhood level. *Energy*, 44(1):96 – 104, 2012.

[155] B.B. Alagoz, A. Kaygusuz, and A. Karabiber. A user-mode distributed energy management architecture for smart grid applications. *Energy*, 44(1): 167 – 177, 2012.

[156] Afzal S. Siddiqui and Chris Marnay. Distributed generation investment by a microgrid under uncertainty. *Energy*, 33(12):1729 – 1737, 2008.

[157] Hasan Doagou-Mojarrad, G.B. Gharehpetian, H. Rastegar, and Javad Olamaei. Optimal placement and sizing of {DG} (distributed generation) units in distribution networks by novel hybrid evolutionary algorithm. *Energy*, 54 (0):129 – 138, 2013.

[158] Elizaveta Kuznetsova, Yan-Fu Li, Carlos Ruiz, Enrico Zio, Graham Ault, and Keith Bell. Reinforcement learning for microgrid energy management. *Energy*, (0):–, 2013. doi: http://dx.doi.org/10.1016/j.energy.2013.05.060.

[159] Sumit Mitra, Lige Sun, and Ignacio E. Grossmann. Optimal scheduling of industrial combined heat and power plants under time-sensitive electricity prices. *Energy*, 54(0):194 – 211, 2013.

[160] Wolfgang Kusch, Tim Schmidla, and Ingo Stadler. Consequences for district heating and natural gas grids when aiming towards 100% electricity supply with renewables. *Energy*, 48(1):153 – 159, 2012.

[161] Milo Panto. Stochastic optimal charging of electric-drive vehicles with renewable energy. *Energy*, 36(11):6567 – 6576, 2011. ISSN 0360-5442.

[162] Camila Fernandes, Pablo Frías, and Jess M. Latorre. Impact of vehicle-to-grid on power system operation costs: The Spanish case study. *Appl. Energy*, 96:194–202, 2012. ISSN 0306-2619.

[163] A.Y. Saber and G.K. Venayagamoorthy. Resource scheduling under uncertainty in a smart grid with renewables and plug-in vehicles. *IEEE Syst. J.*, 6(1):103 –109, march 2012. ISSN 1932-8184.

[164] Trine Krogh Kristoffersen, Karsten Capion, and Peter Meibom. Optimal charging of electric drive vehicles in a market environment. *Appl. Energy*, 88(5):1940–1948, 2011. ISSN 0306-2619.

[165] Qi Zhang, Benjamin C. Mclellan, Tetsuo Tezuka, and Keiichi N. Ishihara. A methodology for economic and environmental analysis of electric vehicles with different operational conditions. *Energy*, 2013. doi: http://dx.doi.org/10.1016/j.energy.2013.01.025.

[166] Bruno Soares M.C. Borba, Alexandre Szklo, and Roberto Schaeffer. Plug-in hybrid electric vehicles as a way to maximize the integration of variable renewable energy in power systems: The case of wind generation in northeastern brazil. *Energy*, 37(1):469 – 481, 2012.

[167] Matteo Muratori, Michael J. Moran, Emmanuele Serra, and Giorgio Rizzoni. Highly-resolved modeling of personal transportation energy consumption in the united states. *Energy*, 2013. doi: http://dx.doi.org/10.1016/j.energy.2013.02.055.

[168] Miadreza Shafie-khah, Mohsen Parsa Moghaddam, Mohamad Kazem Sheikh-El-Eslami, and Mehdi Rahmani-Andebili. Modeling of interactions between market regulations and behavior of plug-in electric vehicle aggregators in a virtual power market environment. *Energy*, 40(1):139 – 150, 2012.

[169] Nina Juul. Battery prices and capacity sensitivity: Electric drive vehicles. *Energy*, 47(1):403 – 410, 2012. ¡ce:title¿Asia-Pacific Forum on Renewable Energy 2011¡/ce:title¿.

[170] Juha Kiviluoma and Peter Meibom. Methodology for modelling plug-in electric vehicles in the power system and cost estimates for a system with either smart or dumb electric vehicles. *Energy*, 36(3):1758 – 1767, 2011.

[171] Karsten Hedegaard, Hans Ravn, Nina Juul, and Peter Meibom. Effects of electric vehicles on power systems in northern europe. *Energy*, 48(1):356 – 368, 2012. ISSN 0360-5442.

[172] Zhe Li and Minggao Ouyang. The pricing of charging for electric vehicles in chinadilemma and solution. *Energy*, 36(9):5765 – 5778, 2011.

[173] Martin Densing, Hal Turton, and Georg Buml. Conditions for the successful deployment of electric vehicles a global energy system perspective. *Energy*, 47(1):137 – 149, 2012.

[174] Matthew A. Kromer, Anup Bandivadekar, and Christopher Evans. Long-term greenhouse gas emission and petroleum reduction goals: Evolutionary pathways for the light-duty vehicle sector. *Energy*, 35(1):387 – 397, 2010.

[175] Han Hao, Hewu Wang, and Minggao Ouyang. Fuel conservation and GHG (greenhouse gas) emissions mitigation scenarios for chinas passenger vehicle fleet. *Energy*, 36(11):6520 – 6528, 2011.

[176] William J. Smith. Can EV (electric vehicles) address irelands CO_2 emissions from transport? *Energy*, 35(12):4514 – 4521, 2010.

[177] Ramteen Sioshansi and Paul Denholm. The value of plug-in hybrid electric vehicles as grid resources. *The Energy Journal*, 31(3):1–24, 2010.

[178] Ramteen Sioshansi. Modeling the impacts of electricity tariffs on plug-in hybrid electric vehicle charging, costs, and emissions. *Oper. Res.*, 43(4): 1199–1204, 2012.

[179] Tiago Sousa, Hugo Morais, Joo Soares, and Zita Vale. Day-ahead resource scheduling in smart grids considering vehicle-to-grid and network constraints. *Appl. Energy*, 96:183–193, 2012. ISSN 0306-2619.

[180] Si Chen, Ivana Ljubić, and S Raghavan. The regenerator location problem. *Networks*, 55(3):205–220, 2010.

[181] Olivia J Smith, Natashia Boland, and Hamish Waterer. Solving shortest path problems with a weight constraint and replenishment arcs. *Computers & Operations Research*, 39(5):964–984, 2012.

[182] Barış Yıldız and Oya Ekin Karaşan. Regenerator location problem and survivable extensions: A hub covering location perspective. *Transportation Research Part B: Methodological*, 71(0):32 – 55, 2015. ISSN 0191-2615.

[183] Michael R Garey and David S Johnson. *Computers and intractability*, volume 174. Freeman New York, 1979.

[184] Electric Power Research Institute. Batteries for electric drive vehicles status 2005. Technical report, Electric Power Research Institute, 2005.

[185] Alan Millner. Modeling lithium ion battery degradation in electric vehicles. In *Innovative Technologies for an Efficient and Reliable Electricity Supply (CITRES), 2010 IEEE Conference on*, pages 349–356. IEEE, 2010.

[186] Richard Bellman. Dynamic programming and lagrange multipliers. *Proceedings of the National Academy of Sciences of the United States of America*, 42(10):767, 1956.

[187] U.S. Department of Energy. Fuel economy of the 2013 chevrolet volt, 2013. www.fueleconomy.gov/feg/noframes/32655.shtml.

[188] Feifei Li and George Kollios. Real datasets for spatial databases, 2007. www.cs.utah.edu/ lifeifei/SpatialDataset.htm.

[189] U.S. Census Bureau. Urban, urbanized area, urban cluster, and rural population, 2010 and 2000: United states, 2010. URL `www.census.gov/geo/reference/ua/urban-rural-2010.html`. Accessed May 18, 2014.

[190] Okan Arslan, Barış Yıldız, and Oya Ekin Karaşan. Impacts of battery characteristics, driver preferences and road network features on travel costs of a plug-in hybrid electric vehicle (phev) for long-distance trips. *Energy Policy*, 74(0):168 – 178, 2014. ISSN 0301-4215.

[191] Jeremy Neubauer and Ahmad Pesaran. *A Techno-Economic Analysis of BEV Service Providers Offering Battery Swapping Services*. National Renewable Energy Laboratory, 2013.

[192] Feifei Li, Dihan Cheng, Marios Hadjieleftheriou, George Kollios, and Shang-Hua Teng. On trip planning queries in spatial databases. In *Advances in Spatial and Temporal Databases*, pages 273–290. Springer, 2005.

[193] U.S. Energy Information Administration. Weekly retail gasoline and diesel prices, 2014. URL `http://www.eia.gov/dnav/pet/pet_pri_gnd_dcus_nus_w.htm`. accessed May 18, 2014.

[194] U.S. Energy Information Administration. Average retail prices of electricity, 2014. URL `http://www.eia.gov/totalenergy/data/monthly/pdf/sec9_11.pdf`. accessed May 18, 2014.

[195] Tesla Motors. Superchargers, 2014. http://www.teslamotors.com/supercharger.

[196] Siddiq A Khan and Martin Kushler. Plug-in electric vehicles: Challenges and opportunities, 2013. URL `http://community-wealth.org/files/downloads/report-kahn-kushler.pdf`. accessed May 18, 2014.

[197] Scott B. Peterson, Jay Apt, and J.F. Whitacre. Lithium-ion battery cell degradation resulting from realistic vehicle and vehicle-to-grid utilization. *Journal of Power Sources*, 195(0):2385 – 2392, 2010.

[198] Jeremy Neubauer and Ahmad Pesaran. The ability of battery second use strategies to impact plug-in electric vehicle prices and serve utility energy storage applications. *Journal of Power Sources*, 196(23):10351 – 10358, 2011.

[199] Victoria A Perk, Joseph S DeSalvo, Tara A Rodrigues, Nina M Versoza, and Steven C Bovino. Improving value of travel time savings estimation for more effective transportation project evaluation. 2011.

[200] Michael H Kutner, Christopher J Nachtsheim, John Neter, and William Li. *Applied linear statistical models*, volume 6. McGraw-Hill New York, 2005.

[201] Jonn Axsen and Kenneth S Kurani. The early U.S. market for phevs: Anticipating consumer awareness, recharge potential, design priorities and energy impacts. *Research Report UCD-ITS-RR-08-22*, 2008. Institute of Transportation Studies, University of California, Davis.

[202] Kate Walsh, Cathy A. Enz, and Linda Canina. The impact of gasoline price fluctuations on lodging demand for {U.S.} brand hotels. *International Journal of Hospitality Management*, 23(5):505 – 521, 2004. ISSN 0278-4319. doi: http://dx.doi.org/10.1016/j.ijhm.2004.02.004. 2003 Review Issue.

[203] Claude Weis, Kay Axhausen, Robert Schlich, and René Zbinden. Models of mode choice and mobility tool ownership beyond 2008 fuel prices. *Transportation Research Record: Journal of the Transportation Research Board*, (2157):86–94, 2010.

[204] Jacques F Benders. Partitioning procedures for solving mixed-variables programming problems. *Numerische mathematik*, 4(1):238–252, 1962.

[205] Jean-François Cordeau, François Soumis, and Jacques Desrosiers. A benders decomposition approach for the locomotive and car assignment problem. *Transportation science*, 34(2):133–149, 2000.

[206] Jean-François Cordeau, Goran Stojković, François Soumis, and Jacques Desrosiers. Benders decomposition for simultaneous aircraft routing and crew scheduling. *Transportation science*, 35(4):375–388, 2001.

[207] Peiling Wu, Joseph C Hartman, and George R Wilson. An integrated model and solution approach for fleet sizing with heterogeneous assets. *Transportation Science*, 39(1):87–103, 2005.

[208] Alysson M Costa. A survey on benders decomposition applied to fixed-charge network design problems. *Computers & Operations Research*, 32(6): 1429–1450, 2005.

[209] R.S. de Camargo, G. Miranda Jr., and H.P. Luna. Benders decomposition for the uncapacitated multiple allocation hub location problem. *Computers & Operations Research*, 35(4):1047 – 1064, 2008.

[210] Ivan Contreras, Jean-Franois Cordeau, and Gilbert Laporte. Benders decomposition for large-scale uncapacitated hub location. *Operations Research*, 59 (6):1477–1490, 2011. doi: 10.1287/opre.1110.0965.

[211] Ricardo Saraiva de Camargo, Gilberto de Miranda Jr, and Henrique Pacca L Luna. Benders decomposition for hub location problems with economies of scale. *Transportation Science*, 43(1):86–97, 2009.

[212] Elisangela Martins de Sá, Ricardo Saraiva de Camargo, and Gilberto de Miranda. An improved benders decomposition algorithm for the tree of hubs location problem. *European Journal of Operational Research*, 226(2):185 – 202, 2013.

[213] Gary Froyland, Stephen J Maher, and Cheng-Lung Wu. The recoverable robust tail assignment problem. *Transportation Science*, 48(3):351–372, 2013.

[214] Pirmin Fontaine and Stefan Minner. Benders decomposition for discretecontinuous linear bilevel problems with application to traffic network design. *Transportation Research Part B: Methodological*, 70(0):163 – 172, 2014.

[215] Maryam Khatami, Masoud Mahootchi, and Reza Zanjirani Farahani. Benders decomposition for concurrent redesign of forward and closed-loop supply chain network with demand and return uncertainties. *Transportation Research Part E: Logistics and Transportation Review*, 79(0):1 – 21, 2015.

[216] David Wheatley, Fatma Gzara, and Elizabeth Jewkes. Logic-based benders decomposition for an inventory-location problem with service constraints. *Omega*, 55(0):10 – 23, 2015.

[217] Elisangela Martins de Sá, Ivan Contreras, Jean-François Cordeau, Ricardo Saraiva de Camargo, and Gilberto de Miranda. The hub line location problem. *Transportation Science*, 2015.

[218] Halit Üster and Panitan Kewcharoenwong. Strategic design and analysis of a relay network in truckload transportation. *Transportation Science*, 45(4): 505–523, 2011.

[219] Gianni Codato and Matteo Fischetti. Combinatorial benders' cuts for mixed-integer linear programming. *Operations Research*, 54(4):756–766, 2006.

[220] John R. Birge and Franois V. Louveaux. A multicut algorithm for two-stage stochastic linear programs. *European Journal of Operational Research*, 34 (3):384 – 392, 1988.

[221] Svyatoslav Trukhanov, Lewis Ntaimo, and Andrew Schaefer. Adaptive multicut aggregation for two-stage stochastic linear programs with recourse. *European Journal of Operational Research*, 206(2):395 – 406, 2010.

[222] Chao Lei, Wei-Hua Lin, and Lixin Miao. A multicut l-shaped based algorithm to solve a stochastic programming model for the mobile facility routing and scheduling problem. *European Journal of Operational Research*, 238(3): 699 – 710, 2014.

[223] Fengqi You and Ignacio E Grossmann. Multicut benders decomposition algorithm for process supply chain planning under uncertainty. *Annals of Operations Research*, 210(1):191–211, 2013.

[224] Thomas L Magnanti and Richard T Wong. Accelerating benders decomposition: Algorithmic enhancement and model selection criteria. *Operations research*, 29(3):464–484, 1981.

[225] Nikolaos Papadakos. Practical enhancements to the magnanti–wong method. *Operations Research Letters*, 36(4):444–449, 2008.

[226] M John Hodgson. A flow-capturing location-allocation model. *Geographical Analysis*, 22(3):270–279, 1990.

[227] IBM. Ibm ilog cplex optimization studio, 2013. URL http://www-03.ibm.com/software/products/en/ibmilogcpleoptistud/.

[228] Ramteen Sioshansi and Paul Denholm. Emissions impacts and benefits of plug-in hybrid electric vehicles and vehicle-to-grid services. *Environ. Sci. Technol.*, 43(4):1199–1204, 2009.

[229] Electric Power Research Institute, EPRI. Batteries for electric drive vehicles status 2005, November 2005.

[230] George L Nemhauser and Laurence A Wolsey. *Integer and combinatorial optimization*, volume 18. Wiley New York, 1988.

[231] U.S. Department of Transportation. National household travel survey, February 2011.

[232] Pasific Gas & Electric. Dynamic load profiles, April 2009.

[233] U.S. Department of Energy. Impacts assessment of plug-in hybrid vehicles on electric utilities and regional U.S. power grids, part 1: Technical analysis, 2007.

[234] Argonne National Laboratory. Modeling the performance and cost of lithium-ion batteries for electric-drive vehicles, December 2012.

[235] California Energy Comission. California distributed energy resources guide, 2012.

[236] California Energy Commission. Comperative costs of California central station electricity generation, January 2010.

[237] Pasific Gas & Electric. Residential time-of-use service, July 2008.

[238] U.S. DOE Energy Efficiency and Renewable Energy (EERE). Distributed energy resource basics website, 2013.

[239] U.S. DOE Energy Efficiency and Renewable Energy (EERE). Fuel economy guide, 2013.

[240] U.S. Environmental Protection Agency. Tier 2 vehicle and gasoline sulfur program, December 1999.

[241] California ISO. Daily renewables watch, accessed on 15 Agu 2013. http://content.caiso.com/green/renewrpt/DailyRenewablesWatch.pdf.